

รายงานวิจัยฉบับสมบูรณ์

โครงการ การคำนวณการแกว่งของวัตถุสมมาตรแนวแกนในการใหลแบบ สมมาตรซึ่งมีความหนืดและมีการไถลบนผิวของวัตถุ (Rotatory Oscillations of Axi-symmetric Bodies in a Bounded Axisymmetric Viscous Flow with Slip: Numerical Solutions)

โดย นายพีระพงศ์ ที่ผสกุล



รายงานวิจัยฉบับสมบูรณ์

โครงการ การคำนวณการแกว่งของวัตถุสมมาตรแนวแกนในการไหลแบบ สมมาตรซึ่งมีความหนืดและมีการไถลบนผิวของวัตถุ (Rotatory Oscillations of Axi-symmetric Bodies in a Bounded Axisymmetric Viscous Flow with Slip: Numerical Solutions)

โดย นายพีระพงศ์ ที่ฆสกุล

รายงานวิจัยฉบับสมบูรณ์

โครงการ การคำนวณการแกว่งของวัตถุสมมาตรแนวแกนในการไหลแบบ สมมาตรซึ่งมีความหนืดและมีการไถลบนผิวของวัตถุ (Rotatory Oscillations of Axi-symmetric Bodies in a Bounded Axisymmetric Viscous Flow with Slip: Numerical Solutions)

คณะผู้วิจัย 1. นายพีระพงศ์ ทีมสกุล สังกัด มหาวิทยาลัยธรรมศาสตร์

สนับสนุนโดยสำนักงานกองทุนสนับสนุนการวิจัย

ชุดโครงการทุนวิจัยหลังปริญญาเอก

กิตติกรรมประกาศ

ผู้วิจัยขอขอบคุณสำนักงานกองทุนสนับสนุนการวิจัยที่ให้ทุนสนับสนุนโครงการวิจัยนี้ ขอขอบคุณ Prof. Dr. Sudarshan K. Loyalka แห่งมหาวิทยาลัย Missouri-Columbia ที่ให้คำ ปรึกษาที่มีประโยชน์ต่อโครงการนี้ด้วยดีมาตลอด ขอขอบคุณภาควิชาวิศวกรรมเครื่องกล คณะวิศวกรรมศาสตร์ มหาวิทยาลัยธรรมศาสตร์ที่ให้การสนับสนุนการดำเนินงานของโครงการ วิจัยนี้ในทุกด้านเป็นอย่างดียิ่ง

บทคัดย่อ

รหัสโครงการ: PDF/32/2541

ชื่อโครงการ: การคำนวณการแกว่งของวัตถุสมมาตรแนวแกนในการไหลแบบสมมาตรซึ่งมี

ความหนืดและมีการใถลบนผิวของวัตถุ

ผู้วิจัย: นายพีระพงศ์ ที่ฆสกุล

ภาควิชาวิศวกรรมเครื่องกล คณะวิศวกรรมศาสตร์ มหาวิทยาลัยธรรม

ศาสตร์

Email Address: tperapon@engr.tu.ac.th

ระยะเวลาที่ทำการวิจัย: 1 กรกฎาคม 2541 – 30 มิถุนายน 2543

ปัญหาของการแกว่งของวัตถุสมมาตรแนวแกน (axi-symmetric bodies) ในแนวเชิงมุม รอบแกนของวัตถุซึ่งมีการใหลแบบ viscous incompressible โดยที่ Reynolds number มีค่าต่ำ นั้น มีความสำคัญในการศึกษาด้านพลศาสตร์ของไหล โดยเฉพาะในการวัดความหนืดของของ ใหลโดยใช้ oscillating disk viscometer ซึ่งมีแผ่นจานทรงกระบอก (cylindrical disk) ถูกทำให้ ค่าต่าง ๆ ที่วัดได้จากการทดลอง ประกอบกับค่าของทอร์กหรือแรงบิด (torque) ซึ่ง คำนวณได้จากทฤษฎีสามารถนำมาคำนวณความหนืดของของไหลได้อย่างแม่นยำ การคำนวณ ค่าของทอร์ก โดยวิธีแน่นอน (exact) เป็นสิ่งที่ทำได้ยากโดยเฉพาะสำหรับวัดถุที่มีรูปร่างต่าง จากทรงกลม การคำนวณที่ผ่านมามักใช้การประมาณโดยวิธีต่าง ๆ ในโครงการนี้ เราจะใช้หลัก การของ Green's Function ในการคำนวณหาค่าของทอร์ก ที่เกิดขึ้นบนวัตถุสมมาตรแนวแกน และแกว่งอยู่ในของไหลทั้งที่ไม่มีขอบเขต (unbounded fluid) และมีขอบเขต (bounded environment) และมีการลื่นไถล (slip) ที่บริเวณผิวของวัตถุที่แกว่ง ทั้งนี้เนื่องจากยังไม่มีทฤษฎีใดที่ สามารถคำนวณคำทอร์กออกมาได้อย่างถูกต้องแม่นยำ ค่าที่ได้จากการคำนวณโดยใช้โปรแกรม คอมพิวเดอร์เมื่อเปรียบเทียบกับค่าที่คำนวณได้จากทฤษฎีที่มีอยู่แล้วทั้งที่เป็นคำตอบแน่นอน สำหรับกรณีของวัตถุทรงกลม และคำตอบโดยประมาณในกรณีของวัตถุแผ่นจานทรงกระบอก บาง (thin cylindrical disk) และวัตถุแท่งทรงกระบอกยาว (long cylinder) พบว่ามีความถูกต้อง แม่นยำสูง ดังนั้นค่าที่ได้จากการคำนวณของวัตถุทรงกระบอกทั่วไป (typical cylindrical body) ซึ่งใช้ใน oscillating disk viscometer สามารถนำไปใช้ในการคำนวณความหนืดของของไหลได้ อย่างถูกต้องแม่นยำ นอกจากนี้จากการศึกษาพบว่าการเพิ่มค่าความถี่ของการสั้นทำให้ทอร์กที่ กระทำต่อวัดถุมีค่าสูงขึ้น ส่วนการเพิ่มขึ้นของการลื่นไถลที่บริเวณผิวของวัตถุมีผลทำให้ค่าทอร์ กลดลง

Keywords: Oscillation, Green's function, Slip, Axi-symmetric flow, Unsteady Stokes' equations

Abstract

Project Code: PDF/32/2541

Project Title: Rotatory Oscillations of Axi-symmetric Bodies in a Bounded Axi-

symmetric Viscous Flow with Slip: Numerical Solutions

Investigator: Mr. Perapong Tekasakul

Department of Mechanical Engineering, Faculty of Engineering,

Thammasat University

Email Address: tperapon@engr.tu.ac.th

Project Period: 1 July 1998 – 30 June 2000

Rotatory or rotational oscillations of several axi-symmetric bodies in axisymmetric, viscous, incompressible flows at low Reynolds number have been investigated. One prominent application of the study of oscillating bodies is the oscillating disk viscometer. In this instrument, a thin cylindrical disk suspended by a thin wire executes torsional oscillation in the fluid. The torque on the disk can be predicted theoretically by solving the equation of fluid flow together with appropriate boundary conditions. Viscosity of the surrounding fluid can be obtained from experimental measurements of certain parameters and comparisons of their values with those calculated from the predicted torque. Accuracy of the viscosity, hence, relies heavily on the value of the torque. Exact solutions for torque are existent only for a sphere and limiting cases of cylinders; an infinite disk and an infinite cylinder. In this research, a numerical method based on the Green's function technique is used to calculate the torque on oscillating bodies in both unbounded and bounded fluids and with slip at The numerical method makes possible the accurate calculations of the torque for arbitrary axi-symmetric bodies. Numerical results have been benchmarked against known analytical solutions and are founded to be very accurate. It is found that in all cases, slip reduces torque, and increasingly so with the increasing frequency of On the other hand, the increment of frequency of oscillation increases torque.

Keywords: Oscillation, Green's function, Slip, Axi-symmetric flow, Unsteady Stokes' equations

Executive Summary

Rotatory or rotational oscillations of several axi-symmetric bodies in axi-symmetric, viscous, incompressible flows at low Reynolds number have been investigated. One prominent application of the study of oscillating bodies is the oscillating disk viscometer. Here, a thin cylindrical disk suspended by a thin wire executes torsional oscillation in the fluid. The torque on the disk can be predicted theoretically by solving the equation of fluid flow together with appropriate boundary conditions. Viscosity of the surrounding fluid can be obtained from experimental measurements of certain parameters and comparisons of their values with those calculated from the predicted torque. Accuracy of the viscosity, hence, relies heavily on the value of the torque. Exact solutions for torque are existent only for a sphere and limiting cases of cylinders; an infinite disk and an infinite cylinder.

In this research, a numerical method based on the Green's function technique is used wherein the relevant Helmholtz equation, as obtained from the unsteady Stokes equation, is converted into Fredholm integral equations of the second kind and then reduced to a system of linear algebraic equations. Gaussian quadrature is used to determine local stresses at each nodal point. Total torque on the body is finally obtained by summation of the local stresses. The calculations are performed by Mathematica® program on a Pentium III-450 MHz computer. Mathematica® is selected because of its ease of use and convenient built-in functions. The technique is benchmarked against known analytical solutions, and accurate numerical results for local stress and torque on spheres, prolate spheroids, oblate spheroids and cylinders in an unbounded fluid as a function of the oscillating frequency and the slip coefficients are obtained. Numerical results for torques on a sphere, prolate spheroids, and oblate spheroids in bounded environments of identical geometries with the same aspect ratios are subsequently obtained. The corresponding results for a thin cylindrical disk used in the oscillating disk viscometer can be obtained from the results of the flat oblate spheroid of the same aspect ratios. The accuracy of this approximation is tested for the unbounded case.

It is found that in all cases, slip reduces torque, and increasingly so with the increasing frequency of oscillation. On the other hand, the increment of frequency of oscillation increases torque.

Background

Problems of oscillation of axi-symmetric bodies in axi-symmetric, viscous, incompressible flow at low Reynolds number with and without slip boundary conditions have been widely studied. Two important modes of oscillation involve the translational and rotatory oscillations. In translational oscillation, the body performing oscillation displaces the fluid around the body. On the other hand, the body performing rotatory oscillation does not displace the fluid. The problem of rotatory oscillations is of interest because of its application in oscillating disk viscometers. Here, a finite cylinder in the form of a circular disk is suspended by a thin wire attached at the center of one face and executes torsional oscillation in the fluid being measured. The dimensional torque on the disk due to the fluid, T', is dependent upon the viscosity and can be predicted theoretically by solving the equation of fluid flow together with appropriate boundary conditions. The exact motion of the disk under the influence of the torque can be determined from

$$I\ddot{\alpha}(t) + (L_0 + L)\dot{\alpha}(t) + K_0[\alpha(t) - \alpha_0] = 0$$

where α_0 is the initial angular deflection of the disk, I is the moment of inertia of the disk, L_0 is the damping factor of the suspension wire, $L=T'/\Omega$ is the damping factor of the fluid, and K_0 is a constant. Note that L_0 , L, and K_0 are time-independent. By substituting $L=L_1+iL_2$ and $\alpha=\alpha_0\exp[(-\Delta+i)\omega t]$ into Eq. (48), L_1 and L_2 can be obtained as functions of Δ and τ , where Δ is the damping decrement of the amplitude in the fluid and τ is the period of oscillation in the fluid. By equating L to the torque obtained from the calculation, the viscosity can be determined provided that the damping decrement and the period of oscillation are measured. This

relationship centers around an accurate prediction of the torque, $\hat{T} = T'/(\Omega \mu a^3)$, exerted on the disk by the surrounding fluid during its oscillation. The accuracy of viscosities obtained via this technique also depends upon the accuracy of the associated damping decrement measurements.

When the body dimension is only about an order of magnitude larger than molecular mean free path of the fluid, one must, however, consider fluid slip at the surface. The slip at boundaries occurs when the Knudsen number (Kn) is in the order of 0.1. The Knudsen number is defined as the ratio of molecular mean free path of the medium (λ_g) and the characteristic length of the body (a), i.e. $Kn = \lambda_g/a$. The flow regimes classified by the Knudsen numbers include the free molecular (Kn >> 1), the transition ($Kn \sim 1$), the slip ($Kn \sim 0.1$), and the continuum flow regime (Kn << 1). The molecular mean free path of the gas medium is defined as

$$\lambda_g = \frac{\mu}{p} \left(\frac{2kT}{m} \right)^{1/2}$$

where μ is the viscosity, p is the pressure, k is the Boltzmann's constant, T is the temperature, and m is the mass of the medium. The slip boundary condition at the surface of a body involves both the molecular mean free path and the slip coefficient, c_m , which can be represented with accuracy within 1%, by (Loyalka, 1990)

$$c_{m} = \frac{2-\alpha}{\alpha} \left[(1-\alpha) \frac{\pi^{\sqrt{2}}}{2} + \alpha \zeta(1) \right]$$

where α is the momentum accommodation coefficient, and $\zeta(1)$, corresponding to $\alpha=1$, has a value between 0.9875 and 1.02, depending on the nature of the gaseous intermolecular interaction. If $\zeta(1)$ is replaced by $\sqrt{\pi}/2$, the above equation becomes Maxwell's relation (Maxwell, 1879). The slip becomes of greater significance as the pressure decreases below atmospheric, particularly for the value of $Kn \sim 0.1$.

Exact solutions to the oscillation problem both with and without slip, however, are limited to certain bodies with simple geometries. For a typical cylindrical body which has been regularly used in the oscillating disk viscometer, no exact solutions are existent. Some approximations have been attempted but these approximations lead to significant discrepancies in most cases. A numerical technique is then unavoidably necessary.

Problem Description

The problem for the oscillation with small amplitude where the Reynolds number is very small arises from the same principle that involves the solutions to the unsteady Stokes equations,

$$\lambda^2 \frac{\partial \mathbf{u}}{\partial \tau} = -\nabla p + \nabla^2 \mathbf{u} \tag{1}$$

where $\lambda^2 = \omega a^2/v$ is the dimensionless frequency parameter. Here, a is the characteristic length of the body and ω is the frequency of oscillation.

The Unsteady Stokes' equation for a time-dependent, dimensionless, ϕ component velocity obtained from Eq. (1) can be written as

$$\lambda^2 \frac{\partial \hat{u}_{\bullet}}{\partial \tau} = \left(\frac{\partial^2}{\partial \varpi^2} + \frac{1}{\varpi} \frac{\partial}{\partial \varpi} - \frac{1}{\varpi^2} + \frac{\partial^2}{\partial z^2} \right) \hat{u}_{\bullet}$$
 (2)

The slip boundary conditions at the body surfaces (Fig. 1) are

$$\hat{u}_{\bullet}(\mathbf{r}_{s1}) = \boldsymbol{\varpi}_{s1} \cos(\tau) + \left(c_{m} \lambda_{s}\right)_{1} \hat{\sigma}_{1}(\mathbf{r}_{s1}) \tag{3}$$

$$\hat{u}_{\bullet}(\mathbf{r}_{i2}) = (c_m \lambda_g)_2 \hat{\sigma}_2(\mathbf{r}_{i2}) \tag{4}$$

Here, \hat{u}_{ϕ} is the dimensionless velocity in ϕ -direction, τ is the oscillation period, c_m is the slip coefficient, λ_g is the molecular mean free path of the surrounding gas, and subscripts 1 and 2 indicate the inner and outer bodies, respectively. In this problem,

the length, time, velocity, and pressure are nondimensionalized in terms of a, ω^{-1} , $U = |\Omega|a = \Omega a$, and $\mu U/a$, respectively.

The dimensionless, time-dependent torque on the inner an outer bodies can be evaluated, respectively, from

$$\tilde{T}_{1}(\tau) = -2\pi \int \boldsymbol{\varpi}^{2} \hat{\sigma}_{1}(\zeta, \tau) ds$$
 (5)

$$\hat{T}_{2}(\tau) = -2\pi \int \sigma^{2} \hat{\sigma}_{2}(\zeta, \tau) ds$$
 (6)

where $\hat{\sigma}(\zeta, \tau)$ is the local stress defined from

$$\hat{\sigma}(\zeta,\tau) = \varpi \frac{\partial}{\partial n} \left(\frac{\hat{u}_{\phi}}{\varpi} \right) \tag{7}$$

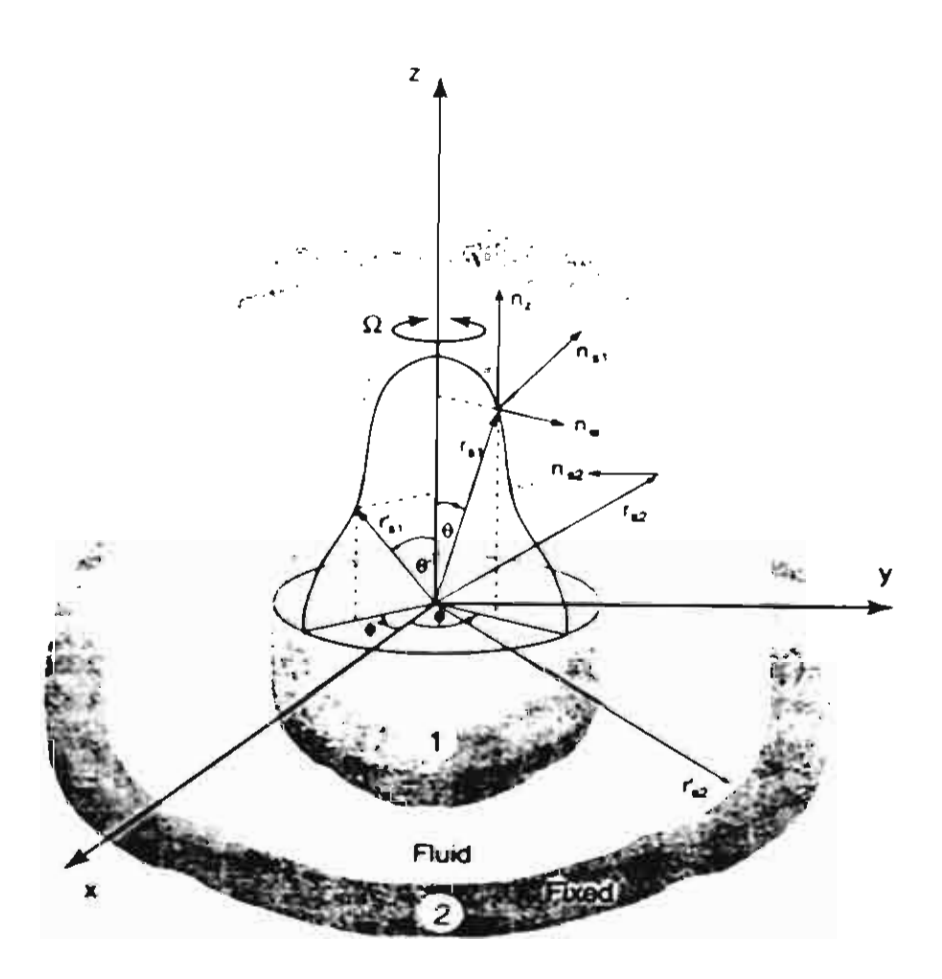


Fig. 1 Coordinate system for the oscillation of an axi-symmetric body inside and coaxial to the identical, larger and fixed body

The dimensionless time-independent torque (T) is obtained by dropping the term, $\exp(i\tau)$, from the time-dependent torque (\hat{T}) .

By mathematical manipulations, Eq. (2) can be written in the form of the Helmholtz equation,

$$\left(\nabla^2 + k^2\right) w = 0 \tag{8}$$

The slip boundary conditions at the surfaces of the bodies the become

$$w(\mathbf{r}_{s1}) = \{ \boldsymbol{\sigma}_{s1} + (c_m \lambda_g)_1 \boldsymbol{\sigma}_1(\mathbf{r}_{s1}) \} \cos(\phi_{s1})$$
 (9)

$$w(\mathbf{r}_{s2}) = \{ (c_m \lambda_g)_2 \sigma_2(\mathbf{r}_{s2}) \} \cos(\phi_{s2})$$
 (10)

Here, we have used $w(\varpi, z, \phi) = u_{\phi}(\varpi, z)\cos(\phi)$, $k^2 = -i\lambda^2 = -i\omega a^2/v$, and

$$\sigma(\zeta) = \varpi \frac{\partial}{\partial n} \left(\frac{u_{\phi}}{\varpi} \right) \tag{11}$$

The Helmholtz equation (8) can be solved by the defined Green's function,

$$(\nabla^2 + k^2)\psi(\mathbf{r}, \mathbf{r}') = -4\pi\delta(\mathbf{r} - \mathbf{r}')$$
(12)

$$\psi(\mathbf{r}, \mathbf{r}') = \frac{\exp(-ik|\mathbf{r} - \mathbf{r}'|)}{|\mathbf{r} - \mathbf{r}'|}$$
(13)

After extensive mathematical manipulations and applying the singularity subtraction technique, the Helmholtz equation becomes (See details in Appendix A)

$$\left[g_{11}(\zeta_{1})-2\pi(c_{m}\lambda_{g})_{1}\right]\sigma_{1}(\zeta_{1})+\int L_{11}\left(\zeta_{1},\zeta_{1}'\right)\left[\sigma_{1}\left(\zeta_{1}'\right)-\sigma_{1}(\zeta_{1})\right]d\zeta_{1}' +\int L_{12}\left(\zeta_{1},\zeta_{2}'\right)\sigma_{2}\left(\zeta_{2}'\right)d\zeta_{2}' =-k^{2}\Psi(\zeta_{1})$$
(14)

and

$$[g_{22}(\zeta_2) - 2\pi(c_m \lambda_g)_2]\sigma_2(\zeta_2) + \int L_{22}(\zeta_2, \zeta_2') \left[\sigma_2(\zeta_2') - \sigma_2(\zeta_2)\right] d\zeta_2'$$

$$+ \int L_{21}(\zeta_2, \zeta_1')\sigma_1(\zeta_1') d\zeta_1' = 0$$
(15)

where

$$g_{11}(\zeta_1) = \int L_{11}(\zeta_1, \zeta_1') d\zeta_1'$$
(16)

$$g_{22}(\zeta_{2}) = \int L_{22}(\zeta_{2}, \zeta_{2}') d\zeta_{2}'$$
 (17)

The integral equations (14) and (15) are converted to a system of linear algebraic equations by the use of Gaussian quadratures together with collocation at each nodal point of the quadrature. The stress, $\sigma(\zeta)$, is determined at the nodal points of the quadrature. The torques on the inner and outer bodies can then be determined from the stresses using Eqs. (5) and (6), respectively.

Previous Research Work

The first study undertaken of an oscillating body involved the translational oscillation of a flat plate which was investigated by Stokes (1851) and subsequently by Lord Rayleigh (1911), Landau and Lifshitz (1959), Schlichting (1979), Kanwal (1955 and 1964), William (1966), Lawrence and Weinbaum (1986, 1988), Pozrikidis (1989a and 1989b), Loewenberg (1993a, 1993b, 1994a and 1994b), Davis (1993), Lovalenti and Brady (1993a and 1993b), and Zhang and Stone (1998).

The rotatory oscillation of an axi-symmetric body was discussed by Lamb (1932). He developed the Helmholtz equation resulting from the unsteady Stokes equations for a sphere executing a rotatory oscillation about an axis passing through its center while bounded by another concentric hollow sphere. Kanwal (1955) studied the rotatory oscillation of several axi-symmetric bodies including a sphere, a prolate spheroid, and a thin cylindrical disk using the Stokes stream function. Landau and Lifshitz (1959) described the rotatory oscillation of a free thin circular disk about its axis by solving for the angular velocity and torque that are applicable in the high

frequency limit ($\lambda >> 1$) whereas Kanwal (1970) obtained the asymptotic torque on a free thin circular disk and a thin cylindrical disk bounded by a cylinder of large radius in the low frequency limit ($\lambda << 1$). Kanwal (1955) used the Stokes stream function to obtain the motions of fluids due to rotatory oscillations of several different free axisymmetric bodies. Further, Hocquart (1976) obtained a series solution for the torque on a spheroid oscillating in an axi-symmetric flow by solving the unsteady Stokes equation assuming a constant pressure. Kestin and Persen (1956) studied torsional oscillation for several bodies, both in an unbounded fluid and in bounded environments, i.e. an infinite disk between two fixed plates, an infinite cylinder inside another cylinder, and a sphere inside another sphere. The simplified Navier-Stokes equation with constant pressure for a slow moving fluid and the equation of body motion, neglecting wire damping, were solved in cylindrical coordinates using the Laplace transform technique. Shah (1971) obtained slip solutions for some simple geometries in Laplace transform domain.

MacWood (1938a, 1938b) obtained an approximate solution for a thin cylindrical disk with slip by use of edge correction where some accuracy was lost. Mariens and van Paemel (1956) analyzed a disk oscillating in an unbounded fluid without slip with inclusion of edge effects. Kestin and Wang (1957) showed that the results of Mariens and van Paemel (1956), though providing a significant improvement over preceding theories, retained a noticeable margin of error. They formulated a correction theory by solving the equations for the fluid flow and the disk motion using Laplace transforms in the manner described by Kestin and Persen (1956). Edge correction factor for a disk was introduced.

Zhang and Stone (1998) have provided a range of useful solutions for bodies in several modes of rotation. These authors reported results for local stresses and

torques on the bodies. The recent numerical work by Tekasakul *et al.* (1998) on rotatory oscillations of arbitrary axi-symmetric bodies in an unbounded fluid in a continuum regime using a Green's function technique is a major step towards the improvement of previous solutions. Torques on a sphere, a prolate spheroid, an oblate spheroid, a thin circular disk, a long cylinder, and a finite cylinder were calculated. The accuracy of the technique was verified against some known analytical solutions. Their work provides an excellent numerical method for solving oscillation problems associated with complicated axi-symmetric systems. Previous investigations on rotatory oscillations are summarized in Table 1.

Table 1. A summary of previous (analytical) works for rotatory oscillations of axi-

symmetric bodies.

Investigators	Body (ies) considered	Flow regime	Nature of solution (torque)
Lamb (1932)	a sphere	continuum	exact
MacWood (1938)	a thin disk	slip	approximate (edge correction)
Kanwal (1955)	a sphere, an infinite circular cylinder, a prolate spheroid, an oblate spheroid, and a thin circular disk	continuum	exact and approximate
Kestin and Persen (1956)	an infinite disk, an infinite cylinder, a sphere, and a stack of infinite disks an infinite disk between two fixed plates, an infinite cylinder inside another cylinder, and a sphere inside another sphere	continuum	exact (Laplace transform)
Mariens and van Paemel (1956)	a thin disk	continuum	approximate (edge correction)
Kestin and Wang (1957)	a thin disk a finite disk with a narrow spacing	continuum	approximate (edge correction)
Landau and Lifshitz (1959)	an infinite circular disk	continuum	exact high frequency limit
Kanwal (1970)	a free thin circular disk a thin cylindrical disk bounded by a cylinder of large radius	continuum	exact Low frequency limit
Shah (1971)	a sphere, an infinite disk and an infinite cylinder an infinite cylinder inside another cylinder, and a sphere inside another sphere	slip	exact (Laplace transform)
Clark <i>et al.</i> (1977)	a thin disk	continuum	approximate (edge correction)
Tekasakul et al. (1998)	a sphere, a prolate spheroid, an oblate spheroid, a thin cylindrical disk, an infinite circular cylinder, and a finite cylinder	continuum	Numerical
Zhang and Stone (1998)	a cylindrical disk, nearly spherical particles	continuum	Numerical

New Developments from This Research

New developments from this research can be summarized as follows:

- 1. Complete numerical procedure for rotatory oscillations of axi-symmetric bodies in axi-symmetric, viscous, incompressible flows at low Reynolds number in bounded environments with slip boundary conditions has been developed (See Appendix A). The numerical technique was fully benchmarked with know analytical solutions and was found to be very accurate. Accuracy of the technique can be enhanced by increasing the number of Gaussian quadrature points on the bodies but computational time would be longer as well. Appropriate number of the Gaussian quadrature points needed for calculations has been displayed for all cases.
- 2. Analytical solution for a sphere oscillating in an unbounded fluid with a slip boundary condition was derived from the no-slip solution. This was used as one of the analytical solutions for benchmarking stated in the previous section.
- 3. Numerical results for torques on a sphere, prolate spheroids, oblate spheroids, and cylinders in an unbounded fluid were obtained. See the manuscripts in Appendices B and C for details.
- 4. Numerical results for torques on a sphere, spheroids in bounded environments of identical geometries with the same aspect ratios were obtained. The corresponding results for a thin cylindrical disk used in the oscillating disk viscometer can be obtained from the results of the flat oblate spheroid of the same aspect ratios. The accuracy of this approximation is tested for the unbounded case. See results in Appendix D. Numerical results for typical cylinders are now under development.
- 5. Approximate solutions for evaporation from nearly spherical particles using techniques that were used in the problem of oscillations were developed. See the manuscript in Appendix E.

Suggestion for Future Research

Results of this research have shown great effectiveness of the numerical method that is based on the Green's function. Any problems arising from the Helmholtz equation with similar boundary conditions can be solved by this method. Problems of evaporation and neutron diffusion are a few examples of possible applications. Continuation of the problem of oscillations of typical cylinders is necessary as well. This is ongoing with significant progress towards the final results. Problem with more complex boundary conditions including oscillating outer body is also of interest, and although more complicated, its solution is also possible.

Conclusion

The problem of rotatory oscillations of axi-symmetric bodies in axisymmetric, viscous, incompressible flows at low Reynolds number in bounded environments with slip boundary conditions has been studied. A possible application of this study is the oscillating disk viscometer. Accuracy of the torque on the disk predicted theoretically is vital to accuracy of the viscosity of the surrounding fluid to be measured by the viscometer. Exact solutions for torque are existent only for a sphere and limiting cases of cylinders; an infinite disk and an infinite cylinder. Several approximations were attempted to determine torques on oscillating disks but these approximations are either limited to a range of oscillating frequency or inaccurate. An accurate numerical method is then unavoidably necessary. In this research, numerical method based on the Green's function was used. The Helmholtz equation was converted to Fredholm integral equations of the second kind and then reduced to a system of linear algebraic equations. Gaussian quadrature was used to determine local stresses at each nodal point. Total torque on the body was finally obtained by summation of the local stresses. The numerical results have been benchmarked against

known analytical solutions and are founded to be very accurate. It is found that in all cases, the increment of frequency of oscillation increases torque. The presence of slip, however, reduces torque, and increasingly so with the increasing frequency of oscillation.

References

- M. Abramowitz and I. A. Stegun, *Handbook of Mathematical Functions* (Dover, New York, NY, 1972), pp. 752-757.
- J. Clark, J. Kestin, and V. L. Shah, "Effect of long-range intermolecular forces on the drag of an oscillating disk and on the viscosity of gases," Physica A 89, 539 (1977).
- A. M. J. Davis, "A hydrodynamic model of the oscillating screen viscometer," Phys. Fluids A 5, 2095 (1993).
- J. Happel and H. Brenner, Low Reynolds Number Hydrodynamics (Prentice-Hall, Englewood Cliffs, NJ, 1965).
- R. Hocquart, "Regime instantane d'un liquide dans lequel un ellipsoid de revolution tourne autour de son axe," C. R. Acad. Sc. Paris 283, 1119 (1976).
- G. B. Jeffrey, "On the steady rotation of a solid of revolution in a viscous fluid," Proc. Lond. Math. Soc. 14, 327 (1915).
- R. P. Kanwal, "Rotatory and longitudinal oscillations of axi-symmetric bodies in a viscous fluid," Quart. J. Mech. Appl. Math. 8, 146 (1955).
- R. P. Kanwal, "Drag on an axially symmetric body vibrating slowly along its axis in a viscous fluid," J. Fluid Mech. 19, 631 (1964).
- R. P. Kanwal, "Note on slow rotation or rotary oscillation of axisymmetric bodies in hydrodynamics and magnetohydrodynamics," J. Fluid Mech. 41, 721 (1970).
- J. Kestin and L. N. Persen, "Slow oscillations of bodies of revolution in a viscous fluid," Proc. International Congress of Applied Mechanics 9, 326 (1956).
- J. Kestin and H. E. Wang, "Corrections for the oscillating disk viscometer," J. Appl. Mech. 24, 197 (1957).
- H. Lamb, *Hydrodynamics*, 6th ed. (Cambridge U.P., Cambridge, England, 1932), pp. 642-644.
- L. D. Landau and E. M. Lifshitz, *Fluid Mechanics* (Pergamon Press, Oxford, England, 1959), translated from Russian by J. B. Sykes and W. H. Reid.
- C. J. Lawrence and S. Weinbaum, "The force on an axisymmetric body in linearized, time-dependent motion: A new memory term," J. Fluid Mech. 171, 209 (1986).

- C. J. Lawrence and S. Weinbaum, "The unsteady force on a body at low Reynolds number; the axisymmetric motion of a spheroid," J. Fluid Mech. 189, 463 (1988).
- P. M. Lovalenti and J. F. Brady, "The hydrodynamic force on a rigid particle undergoing arbitrary time-dependent motion at small Reynolds number," J. Fluid Mech. 256, 561 (1993a).
- P. M. Lovalenti and J. F. Brady, "The force on a sphere in a uniform flow with small-amplitude oscillations at finite Reynolds number," J. Fluid Mech. 256, 607 (1993b).
- M. Loewenberg, "Stokes resistance, added mass, and Basset force for arbitrarily oriented, finite-length cylinders," Phys. Fluids A 5, 765 (1993a).
- M. Loewenberg, "The unsteady Stokes resistance of arbitrarily oriented, finite-length cylinders," Phys. Fluids A 5, 3004 (1993b).
- M. Loewenberg, "Asymmetric, oscillatory motion of a finite-length cylinder: The macroscopic effect of particle edges," Phys. Fluids A 6, 1095 (1994a).
- M. Loewenberg, "Axisymmetric unsteady Stokes flow past an oscillating finite-length cylinder," J. Fluid Mech. 265, 265 (1994b).
- S. K. Loyalka, "Slip and jump coefficients for rarefied gas flows: Variational results for Lennard-Jones and n(r)-6 potential," Physica A 163, 813 (1990).
- S. K. Loyalka and J. L. Griffin, "Condensation on nonspherical aerosol particles: Numerical solutions in the continuum regime," Nucl. Sci. Engr. 114, 135 (1993).
- S. K. Loyalka and J. L. Griffin, "Rotation of non-spherical axi-symmetric particles in the slip regime," J. Aerosol Sci. 25, 509 (1994).
- S. K. Loyalka, "Theory of the spinning rotor gauge in the slip regime," JVST A 14, 2940 (1996a).
- S. K. Loyalka, "Rotation of a closed torus in the slip regime," Ann. Nucl. Energy 23, 371 (1996b).
- G. E. MacWood, "The theory of the measurement of viscosity and slip of fluids by the oscillating disc method," Physica 5, 374 (1938a).
- G. E. MacWood, "The theory of the measurement of viscosity and slip of fluids by the oscillating disc method, part II," Physica 5, 763 (1938b).
- P. Mariens and O. van Paemel, "Theory and experimental verification of the oscillating disk method for viscosity measurements in fluids," Appl. Sci. Res. A 5, 411 (1956).
- O. E. Meyer, "Ü ber die bestimmung der inneren reibung nach Coulomb's verfaren," Ann. Phys. 32, 642 (1887).

- C. Pozrikidis, "A study of linearized oscillatory flow past particles by the boundary-integral method," J. Fluid Mech. 202, 17 (1989a).
- C. Pozrikidis, "A singularity method for unsteady linearized flow," Phys. Fluids A 1, 1508 (1989b).
- Lord Rayleigh, "On the motion of solid body through viscous liquid," Phil. Mag. 21, 697 (1911).
- H. Schlichting, *Boundary-Layer Theory*, 7th ed. (McGraw-Hill, New York, NY, 1979), translated from German to English by J. Kestin, pp. 93-94.
- V. L. Shah, "Theory of the oscillating viscometer for slip flow," J. Appl. Mech. 38, 659 (1971).
- C. Snow, Hypergeometric and Legendre Functions with Special Applications to the Integral Equations of Potential Theory (National Bureau of Standards, Appl. Math. Series 19, 1951).
- G. G. Stokes, "On the effect of the internal friction of fluids on the motion of pendulums," Cambr. Phil. Trans. IX, 8 (1851).
- P. Tekasakul, J. A. Bentz, R. V. Tompson, and S. K. Loyalka, "The spinning rotor gauge: Measurements of viscosity, velocity slip coefficients, and tangential momentum accommodation coefficients," JVST A 14, 2946 (1996).
- P. Tekasakul, R.V. Tompson, and S.K. Loyalka, "Rotatory Oscillations of Arbitrary Axi-symmetric Bodies in An Axi-symmetric Viscous Flow: Numerical Solutions," Phys. Fluids, 10(11), 2797-2818 (1998).
- P. Tekasakul, R.V. Tompson, and S.K. Loyalka, "Evaporation from a Nonspherical Aerosol Particle Situated in an Absorbing Gas," J. Aerosol Sci., 30(2), 139-156 (1999).
- P. Tekasakul, R.V. Tompson, and S.K. Loyalka, "A Numerical Study of Two Coaxial Axi-Symmetric Particles Undergoing Steady Equal Rotation in the Slip Regime," Z. Angew. Math. Phys. (ZAMP), 50(3), 387 403 (1999).
- W. E. William, "A note on slow vibrations in a viscous fluid," J. Fluid Mech. 25, 589 (1966).
- W. Zhang and H. A. Stone, "Oscillatory motions of circular disks and near spheres in viscous flows," to appear in J. Fluid Mech. (1998).

Output

- 1. P. Tekasakul and S.K. Loyalka, "Rotatory Oscillations of Axi-Symmetric Bodies in an Axi-Symmetric Viscous Flow with Slip: Numerical Solutions for Sphere and Spheroids," submitted to Journal of Fluids Engineering.
- 2. P. Tekasakul and S.K. Loyalka, "Rotatory Oscillations of Axi-Symmetric Bodies in an Axi-Symmetric Viscous Flow with Slip: in preparation.
- 3. P. Tekasakul and S.K. Loyalka, "Rotatory Oscillations of Axi-Symmetric Bodies in A Bounded Axi-Symmetric Viscous Flow with Slip: Numerical Solutions for Sphere and Spheroids," in preparation.
- 4. P. Tekasakul and S.K. Loyalka, "Evaporation from Non-Spherical Particles: The Equivalent-Volume and Inscribed Sphere Approximations for Nearly Spherical Particles," accepted for a Poster Presentation at the American Association for Aerosol Research AAAR 2000 Nineteenth Annual Conference, St. Louis, Missouri, U.S.A. on November 9, 2000.

Appendix A

Problem Description and Numerical Procedure

Rotatory Oscillations of Axi-symmetric Bodies in a Bounded Axi-symmetric Viscous Flow with Slip: Numerical Solutions

I. STATEMENT OF THE PROBLEM

The Unsteady Stokes' equation for a time-dependent, dimensionless, ϕ -component velocity is

$$\lambda^2 \frac{\partial \hat{u}_{\phi}}{\partial \tau} = \left(\frac{\partial^2}{\partial \varpi^2} + \frac{1}{\varpi} \frac{\partial}{\partial \varpi} - \frac{1}{\varpi^2} + \frac{\partial^2}{\partial z^2} \right) \hat{u}_{\phi} \tag{1}$$

Boundary conditions with slips are

$$\hat{u}_{\phi}(\mathbf{r}_{s1}) = \varpi_s \exp(i\tau) + \left(c_m \lambda_g\right)_1 \hat{\sigma}_1(\mathbf{r}_{s1})$$
(2)

$$\hat{u}_{\phi}(\mathbf{r}_{s2}) = (c_m \lambda_s)_2 \hat{\sigma}_2(\mathbf{r}_{s2}) \tag{3}$$

where subscripts 1 and 2 represent the inner (oscillating) and the outer (stationary) bodies, respectively.

The dimensionless, time-dependent, torque is

$$\mathbf{T} = -\int_{S} (\mathbf{r}_{s} \times \mathbf{P}) \cdot d\mathbf{S} = -\int_{S} (\mathbf{r}_{s} \times \mathbf{P}_{n}) \, dS$$
 (4)

or in scalar form:

$$\hat{T}_{1}(\tau) = -2\pi \int_{c} \varpi_{1}^{2} \, \hat{\sigma}_{1}(\zeta, \tau) \, \mathrm{d}s \tag{5}$$

$$\hat{T}_2(\tau) = -2\pi \int_{\mathcal{L}} \varpi_2^2 \ \hat{\sigma}_2(\zeta, \tau) \, \mathrm{d} s \tag{6}$$

where $\hat{\sigma}(\zeta, \tau)$ is the time-dependent, dimensionless local stress:

$$\hat{\sigma}(\zeta, \tau) = \varpi \frac{\partial}{\partial n} \left(\frac{\hat{u}_{\phi}}{\varpi} \right) \tag{7}$$

and $\hat{T} = T'/\Omega \mu a^3$ is the time-dependent, dimensionless torque. The time-independent torque (T) is obtained by dropping the term, $\exp(i\tau)$, from the time-dependent torque (\hat{T}) and the time-dependent local stress (σ) is obtained by dropping the term, $\exp(i\tau)$, from the time-dependent local stress $\hat{\sigma}(\zeta,\tau) = \sigma(\zeta) \exp(i\tau)$.

Assume

$$\hat{u}_{\phi}(\varpi, z, \tau) = \exp(i\tau) u_{\phi}(\varpi, z) \tag{8}$$

Substitution of the above ansatz into Eq. (1) yields

$$\left[\left(\frac{\partial^2}{\partial \varpi^2} + \frac{1}{\varpi} \frac{\partial}{\partial \varpi} - \frac{1}{\varpi^2} + \frac{\partial^2}{\partial z^2} \right) + k^2 \right] u_{\phi} = 0$$
 (9)

where $k^2 = -i\lambda^2 = -i\omega a^2/v$ is the dimensionless complex-valued frequency parameter.

Applying the Jeffrey transformation

$$w(\varpi, z, \phi) = u_{\sigma}(\varpi, z) \cos(\phi) \tag{10}$$

we have

$$\nabla^{2}w = \left(\frac{\partial^{2}}{\partial \varpi^{2}} + \frac{1}{\varpi}\frac{\partial}{\partial \varpi} + \frac{1}{\varpi^{2}}\frac{\partial^{2}}{\partial \phi^{2}} + \frac{\partial^{2}}{\partial z^{2}}\right)u_{\phi}\cos(\phi)$$

$$= \left(\frac{\partial^{2}}{\partial \varpi^{2}} + \frac{1}{\varpi}\frac{\partial}{\partial \varpi} - \frac{1}{\varpi^{2}} + \frac{\partial^{2}}{\partial z^{2}}\right)u_{\phi}\cos(\phi) \tag{11}$$

which then leads to the Helmholtz equation

$$\left(\nabla^2 + k^2\right) w = 0 \tag{12}$$

while the boundary conditions become

$$w(\mathbf{r}_{s1}) = \left[\boldsymbol{\varpi}_{s1} + \left(c_{m}\lambda_{g}\right)_{1}\boldsymbol{\sigma}_{1}(\mathbf{r}_{s1})\right]\cos(\phi_{s1})$$
 (13)

$$w(\mathbf{r}_{s2}) = \left[\left(c_m \lambda_s \right)_2 \sigma_2(\mathbf{r}_{s2}) \right] \cos(\phi_{s2})$$
 (14)

where

$$\sigma(\zeta) = \varpi \frac{\partial}{\partial n} \left(\frac{u_{\phi}}{\varpi} \right) \tag{15}$$

II. NUMERICAL PROCEDURE

Define the Green's function:

$$(\nabla^2 + k^2)\psi(\mathbf{r}, \mathbf{r}') = -4\pi \,\delta(\mathbf{r} - \mathbf{r}') \tag{16}$$

such that

$$\psi(\mathbf{r}, \mathbf{r}') = \frac{\exp(-ik|\mathbf{r} - \mathbf{r}'|)}{|\mathbf{r} - \mathbf{r}'|}$$
(17)

Applying the Green's second identity:

$$-\int \left[\psi(\mathbf{r},\mathbf{r}_{s}')\frac{\partial w(\mathbf{r}_{s}')}{\partial n'}-w(\mathbf{r}_{s}')\frac{\partial \psi(\mathbf{r},\mathbf{r}_{s}')}{\partial n'}\right]d\mathbf{r}_{s}'=4\pi\int w(\mathbf{r}_{s}')\delta(\mathbf{r}-\mathbf{r}_{s}')d\mathbf{r}_{s}'$$
(18)

we have, for $\mathbf{r} \to \mathbf{r}_{11}$ (inner body surface):

$$-\int_{\mathbf{I}} \left[\psi(\mathbf{r}_{s1}, \mathbf{r}'_{s1}) \frac{\partial w(\mathbf{r}'_{s1})}{\partial n'_{s1}} - w(\mathbf{r}'_{s1}) \frac{\partial \psi(\mathbf{r}_{s1}, \mathbf{r}'_{s1})}{\partial n'_{s1}} \right] d\mathbf{r}'_{s1}$$

$$-\int_{2} \left[\psi(\mathbf{r}_{s1}, \mathbf{r}'_{s2}) \frac{\partial w(\mathbf{r}'_{s2})}{\partial n'_{s2}} - w(\mathbf{r}'_{s2}) \frac{\partial \psi(\mathbf{r}_{s1}, \mathbf{r}'_{s2})}{\partial n'_{s2}} \right] d\mathbf{r}'_{s2} = 2\pi w(\mathbf{r}_{s1})$$
(19)

and, for $r \rightarrow r_{,2}$ (outer body surface):

$$-\int_{\mathbf{I}} \left[\psi(\mathbf{r}_{s2}, \mathbf{r}'_{s1}) \frac{\partial w(\mathbf{r}'_{s1})}{\partial n'_{s1}} - w(\mathbf{r}'_{s1}) \frac{\partial \psi(\mathbf{r}_{s2}, \mathbf{r}'_{s1})}{\partial n'_{s1}} \right] d\mathbf{r}'_{s1}$$

$$-\int_{\mathbf{I}} \left[\psi(\mathbf{r}_{s2}, \mathbf{r}'_{s2}) \frac{\partial w(\mathbf{r}'_{s2})}{\partial n'_{s2}} - w(\mathbf{r}'_{s2}) \frac{\partial \psi(\mathbf{r}_{s2}, \mathbf{r}'_{s2})}{\partial n'_{s2}} \right] d\mathbf{r}'_{s2} = 2\pi w(\mathbf{r}_{s2})$$
(20)

Consider

$$\frac{\partial w(\mathbf{r}_{si})}{\partial n_{si}} = \frac{\partial}{\partial n_{si}} \left[u_{\phi}(\mathbf{r}_{si}) \cos(\phi_{si}) \right]
= \frac{\partial}{\partial n_{si}} \left[\frac{u_{\phi}(\mathbf{r}_{si})}{\varpi_{si}} \varpi_{si} \cos(\phi_{si}) \right]
= \varpi_{si} \cos(\phi_{si}) \frac{\partial}{\partial n_{si}} \left[\frac{u_{\phi}(\mathbf{r}_{si})}{\varpi_{si}} \right] + \frac{u_{\phi}(\mathbf{r}_{si})}{\varpi_{si}} \frac{\partial}{\partial n_{si}} \left[\varpi_{si} \cos(\phi_{si}) \right]
= \cos(\phi_{si}) \sigma(\mathbf{r}_{si}) + \frac{u_{\phi}(\mathbf{r}_{si})}{\varpi_{si}} \frac{\partial}{\partial n_{si}} \left[\varpi_{si} \cos(\phi_{si}) \right]$$
(21)

For i = 1 (inner body), we have

$$\frac{\partial w(\mathbf{r}_{s1})}{\partial n_{s1}} = \cos(\phi_{s1})\sigma_{1}(\mathbf{r}_{s1}) + \frac{u_{\phi}(\mathbf{r}_{s1})}{\varpi_{s1}} \frac{\partial}{\partial n_{s1}} \left[\varpi_{s1}\cos(\phi_{s1})\right]$$

$$= \cos(\phi_{s1})\sigma_{1}(\mathbf{r}_{s1}) + \left[\frac{\varpi_{s1} + (c_{m}\lambda_{s})_{1}\sigma_{1}(\mathbf{r}_{s1})}{\varpi_{s1}}\right] \frac{\partial}{\partial n_{s1}} \left[\varpi_{s1}\cos(\phi_{s1})\right]$$

$$= \cos(\phi_{s1})\sigma_{1}(\mathbf{r}_{s1}) + \left[1 + \frac{(c_{m}\lambda_{s})_{1}\sigma_{1}(\mathbf{r}_{s1})}{\varpi_{s1}}\right] \frac{\partial}{\partial n_{s1}} \left[\varpi_{s1}\cos(\phi_{s1})\right]$$
(22)

For i = 2 (inner body), we have

$$\frac{\partial w(\mathbf{r}_{s2})}{\partial n_{s2}} = \cos(\phi_{s2})\sigma_2(\mathbf{r}_{s2}) + \left[\frac{(c_m \lambda_s)_2 \sigma_2(\mathbf{r}_{s2})}{\varpi_{s2}}\right] \frac{\partial}{\partial n_{s2}} \left[\varpi_{s2} \cos(\phi_{s2})\right]$$
(23)

Substituting Eqs. (22) and (23) into Eqs. (19) and (20), respectively, with use of the boundary conditions (13) and (14), we obtain

$$-\int_{\mathbf{I}} \left\| \psi(\mathbf{r}_{s1}, \mathbf{r}'_{s1}) \left\{ \cos(\phi'_{s1}) \sigma_{1}(\mathbf{r}'_{s1}) + \left[1 + \frac{(c_{m} \lambda_{g})_{1} \sigma_{1}(\mathbf{r}'_{s1})}{\varpi'_{s1}} \right] \frac{\partial}{\partial n'_{s1}} \left[\varpi'_{s1} \cos(\phi'_{s1}) \right] \right\}$$

$$-\left[\varpi'_{s1} + (c_{m} \lambda_{g})_{1} \sigma_{1}(\mathbf{r}'_{s1}) \right] \cos(\phi'_{s1}) \frac{\partial \psi(\mathbf{r}_{s1}, \mathbf{r}'_{s1})}{\partial n'_{s1}} \right\| d\mathbf{r}'_{s1}$$

$$-\int_{2} \left\| \psi(\mathbf{r}_{s1}, \mathbf{r}'_{s2}) \left\{ \cos(\phi'_{s2}) \sigma_{2}(\mathbf{r}'_{s2}) + \left[\frac{(c_{m} \lambda_{g})_{2} \sigma_{2}(\mathbf{r}'_{s2})}{\varpi'_{s2}} \right] \frac{\partial}{\partial n'_{s2}} \left[\varpi'_{s2} \cos(\phi'_{s2}) \right] \right\}$$

$$-\left[(c_{m} \lambda_{g})_{2} \sigma_{2}(\mathbf{r}'_{s2}) \right] \cos(\phi'_{s2}) \frac{\partial \psi(\mathbf{r}_{s1}, \mathbf{r}'_{s2})}{\partial n'_{s2}} \right\| d\mathbf{r}'_{s2}$$

$$= 2\pi \left[\varpi_{s1} + (c_{m} \lambda_{g})_{1} \sigma_{1}(\mathbf{r}_{s1}) \right] \cos(\phi_{s1})$$

$$(24)$$

and

$$-\int_{\mathbf{I}} \left\| \psi(\mathbf{r}_{s2}, \mathbf{r}'_{s1}) \left\{ \cos(\phi'_{s1}) \sigma_{1}(\mathbf{r}'_{s1}) + \left[1 + \frac{(c_{m} \lambda_{g})_{1} \sigma_{1}(\mathbf{r}'_{s1})}{\varpi'_{s1}} \right] \frac{\partial}{\partial n'_{s1}} \left[\varpi'_{s1} \cos(\phi'_{s1}) \right] \right\}$$

$$-\left[\varpi'_{s1} + (c_{m} \lambda_{g})_{1} \sigma_{1}(\mathbf{r}'_{s1}) \right] \cos(\phi'_{s1}) \frac{\partial \psi(\mathbf{r}_{s2}, \mathbf{r}'_{s1})}{\partial n'_{s1}} \left\| d\mathbf{r}'_{s1} \right\|$$

$$-\int_{2} \left\| \psi(\mathbf{r}_{s2}, \mathbf{r}'_{s2}) \left\{ \cos(\phi'_{s2}) \sigma_{2}(\mathbf{r}'_{s2}) + \left[\frac{(c_{m} \lambda_{g})_{2} \sigma_{2}(\mathbf{r}'_{s2})}{\varpi'_{s2}} \right] \frac{\partial}{\partial n'_{s2}} \left[\varpi'_{s2} \cos(\phi'_{s2}) \right] \right\}$$

$$-\left[(c_{m} \lambda_{g})_{2} \sigma_{2}(\mathbf{r}'_{s2}) \right] \cos(\phi'_{s2}) \frac{\partial \psi(\mathbf{r}_{s2}, \mathbf{r}'_{s2})}{\partial n'_{s2}} \left\| d\mathbf{r}'_{s2} \right\|$$

$$= 2\pi \left[(c_{m} \lambda_{g})_{2} \sigma_{2}(\mathbf{r}_{s2}) \right] \cos(\phi_{s2})$$

$$= 2\pi \left[(c_{m} \lambda_{g})_{2} \sigma_{2}(\mathbf{r}_{s2}) \right] \cos(\phi_{s2})$$

$$(25)$$

Equation (24) and (25) can be rearranged to

$$-\int_{\mathbf{I}} \left\| \psi(\mathbf{r}_{s1}, \mathbf{r}'_{s1}) \left\{ \cos(\phi'_{s1}) \sigma_{1}(\mathbf{r}'_{s1}) + \left[\frac{(c_{m} \lambda_{g})_{1} \sigma_{1}(\mathbf{r}'_{s1})}{\varpi'_{s1}} \right] \frac{\partial}{\partial n'_{s1}} \left[\varpi'_{s1} \cos(\phi'_{s1}) \right] \right\}$$

$$-\left[(c_{m} \lambda_{g})_{1} \sigma_{1}(\mathbf{r}'_{s1}) \right] \cos(\phi'_{s1}) \frac{\partial \psi(\mathbf{r}_{s1}, \mathbf{r}'_{s1})}{\partial n'_{s1}} \left\| d\mathbf{r}'_{s1} \right\|$$

$$-\int_{2} \left\| \psi(\mathbf{r}_{s1}, \mathbf{r}'_{s2}) \left\{ \cos(\phi'_{s2}) \sigma_{2}(\mathbf{r}'_{s2}) + \left[\frac{(c_{m} \lambda_{g})_{2} \sigma_{2}(\mathbf{r}'_{s2})}{\varpi'_{s2}} \right] \frac{\partial}{\partial n'_{s2}} \left[\varpi'_{s2} \cos(\phi'_{s2}) \right] \right\}$$

$$-\left[(c_{m} \lambda_{g})_{2} \sigma_{2}(\mathbf{r}'_{s2}) \right] \cos(\phi'_{s2}) \frac{\partial \psi(\mathbf{r}_{s1}, \mathbf{r}'_{s2})}{\partial n'_{s2}} \left\| d\mathbf{r}'_{s2} \right\|$$

$$-\int_{1} \left[\psi(\mathbf{r}_{s1}, \mathbf{r}'_{s1}) \frac{\partial}{\partial n'_{s1}} \left[\varpi'_{s1} \cos(\phi'_{s1}) \right] - \varpi'_{s1} \cos(\phi'_{s1}) \frac{\partial \psi(\mathbf{r}_{s1}, \mathbf{r}'_{s1})}{\partial n'_{s1}} \right] d\mathbf{r}'_{s1}$$

$$= 2\pi \left[\varpi_{s1} + \left(c_{m} \lambda_{g} \right)_{1} \sigma_{1}(\mathbf{r}_{s1}) \right] \cos(\phi_{s1})$$
(26)

and

$$-\int_{\mathbf{I}} \left\| \psi(\mathbf{r}_{s2}, \mathbf{r}'_{s1}) \left\{ \cos(\phi'_{s1}) \sigma_{\mathbf{I}}(\mathbf{r}'_{s1}) + \left[\frac{\left(c_{m} \lambda_{g}\right)_{\mathbf{I}} \sigma_{\mathbf{I}}(\mathbf{r}'_{s1})}{\varpi'_{s1}} \right] \frac{\partial}{\partial n'_{s1}} \left[\varpi'_{s1} \cos(\phi'_{s1}) \right] \right\}$$

$$-\left[\left(c_{m} \lambda_{g}\right)_{\mathbf{I}} \sigma_{\mathbf{I}}(\mathbf{r}'_{s1}) \right] \cos(\phi'_{s1}) \frac{\partial \psi(\mathbf{r}_{s2}, \mathbf{r}'_{s1})}{\partial n'_{s1}} \left\| d\mathbf{r}'_{s1} \right\|$$

$$-\int_{2} \left\| \psi(\mathbf{r}_{s2}, \mathbf{r}'_{s2}) \left\{ \cos(\phi'_{s2}) \sigma_{2}(\mathbf{r}'_{s2}) + \left[\frac{\left(c_{m} \lambda_{g}\right)_{2} \sigma_{2}(\mathbf{r}'_{s2})}{\varpi'_{s2}} \right] \frac{\partial}{\partial n'_{s2}} \left[\varpi'_{s2} \cos(\phi'_{s2}) \right] \right\}$$

$$-\left[\left(c_{m} \lambda_{g}\right)_{2} \sigma_{2}(\mathbf{r}'_{s2}) \right] \cos(\phi'_{s2}) \frac{\partial \psi(\mathbf{r}_{s2}, \mathbf{r}'_{s2})}{\partial n'_{s2}} \left\| d\mathbf{r}'_{s2} \right\|$$

$$-\int_{\mathbf{I}} \left[\psi(\mathbf{r}_{s2}, \mathbf{r}'_{s1}) \frac{\partial}{\partial n'_{s1}} \left[\varpi'_{s1} \cos(\phi'_{s1}) \right] - \varpi'_{s1} \cos(\phi'_{s1}) \frac{\partial \psi(\mathbf{r}_{s2}, \mathbf{r}'_{s1})}{\partial n'_{s1}} \right] d\mathbf{r}'_{s1}$$

$$= 2\pi \left[\left(c_{m} \lambda_{g}\right)_{2} \sigma_{2}(\mathbf{r}_{s2}) \right] \cos(\phi_{s2})$$

$$(27)$$

According Tekasakul et al. (1998) and Tekasakul et al. (ZAMP, 1999)

$$-\int_{l} \left[\psi(\mathbf{r}_{s1}, \mathbf{r}'_{s1}) \frac{\partial}{\partial n'_{s1}} \left[\varpi'_{s1} \cos(\phi'_{s1}) \right] - \varpi'_{s1} \cos(\phi'_{s1}) \frac{\partial \psi(\mathbf{r}_{s1}, \mathbf{r}'_{s1})}{\partial n'_{s1}} \right] d\mathbf{r}'_{s1}$$

$$= (2\pi \varpi_{s1}) \cos(\phi_{s1}) + k^{2} \int \psi(\mathbf{r}_{s1}, \mathbf{r}'_{s1}) \varpi'_{s1} \cos(\phi'_{s1}) d\mathbf{r}'_{s1}$$
(28)

and

$$-\int_{\mathbf{I}} \left[\psi(\mathbf{r}_{s2}, \mathbf{r}'_{s1}) \frac{\partial}{\partial n'_{s1}} \left[\varpi'_{s1} \cos(\phi'_{s1}) \right] - \varpi'_{s1} \cos(\phi'_{s1}) \frac{\partial \psi(\mathbf{r}_{s2}, \mathbf{r}'_{s1})}{\partial n'_{s1}} \right] d\mathbf{r}'_{s1} = 0$$
 (29)

Then Eqs. (26) and (27) become

$$-\int_{1} \left\| \psi(\mathbf{r}_{s1}, \mathbf{r}'_{s1}) \left\{ \cos(\phi'_{s1}) \sigma_{1}(\mathbf{r}'_{s1}) + \left[\frac{(c_{m} \lambda_{g})_{1} \sigma_{1}(\mathbf{r}'_{s1})}{\varpi'_{s1}} \right] \frac{\partial}{\partial n'_{s1}} \left[\varpi'_{s1} \cos(\phi'_{s1}) \right] \right\}$$

$$-\left[(c_{m} \lambda_{g})_{1} \sigma_{1}(\mathbf{r}'_{s1}) \right] \cos(\phi'_{s1}) \frac{\partial \psi(\mathbf{r}_{s1}, \mathbf{r}'_{s1})}{\partial n'_{s1}} \left\| d\mathbf{r}'_{s1} \right\|$$

$$-\int_{2} \left\| \psi(\mathbf{r}_{s1}, \mathbf{r}'_{s2}) \left\{ \cos(\phi'_{s2}) \sigma_{2}(\mathbf{r}'_{s2}) + \left[\frac{(c_{m} \lambda_{g})_{2} \sigma_{2}(\mathbf{r}'_{s2})}{\varpi'_{s2}} \right] \frac{\partial}{\partial n'_{s2}} \left[\varpi'_{s2} \cos(\phi'_{s2}) \right] \right\}$$

$$-\left[(c_{m} \lambda_{g})_{2} \sigma_{2}(\mathbf{r}'_{s2}) \right] \cos(\phi'_{s2}) \frac{\partial \psi(\mathbf{r}_{s1}, \mathbf{r}'_{s2})}{\partial n'_{s2}} \left\| d\mathbf{r}'_{s2} \right\}$$

$$= 2\pi \left[(c_{m} \lambda_{g})_{1} \sigma_{1}(\mathbf{r}_{s1}) \right] \cos(\phi_{s1}) - k^{2} \int \psi(\mathbf{r}_{s1}, \mathbf{r}'_{s1}) \varpi'_{s1} \cos(\phi'_{s1}) d\mathbf{r}'_{s1}$$

$$(30)$$

and

$$-\int_{\mathbf{I}} \left\| \psi(\mathbf{r}_{s2}, \mathbf{r}'_{s1}) \left\{ \cos(\phi'_{s1}) \sigma_{\mathbf{I}}(\mathbf{r}'_{s1}) + \left[\frac{\left(c_{m} \lambda_{g}\right)_{1} \sigma_{\mathbf{I}}(\mathbf{r}'_{s1})}{\varpi'_{s1}} \right] \frac{\partial}{\partial n'_{s1}} \left[\varpi'_{s1} \cos(\phi'_{s1}) \right] \right\}$$

$$-\left[\left(c_{m} \lambda_{g}\right)_{1} \sigma_{\mathbf{I}}(\mathbf{r}'_{s1}) \right] \cos(\phi'_{s1}) \frac{\partial \psi(\mathbf{r}_{s2}, \mathbf{r}'_{s1})}{\partial n'_{s1}} \left\| d\mathbf{r}'_{s1} \right\|$$

$$-\int_{2} \left\| \psi(\mathbf{r}_{s2}, \mathbf{r}'_{s2}) \left\{ \cos(\phi'_{s2}) \sigma_{2}(\mathbf{r}'_{s2}) + \left[\frac{\left(c_{m} \lambda_{g}\right)_{2} \sigma_{2}(\mathbf{r}'_{s2})}{\varpi'_{s2}} \right] \frac{\partial}{\partial n'_{s2}} \left[\varpi'_{s2} \cos(\phi'_{s2}) \right] \right\}$$

$$-\left[\left(c_{m} \lambda_{g}\right)_{2} \sigma_{2}(\mathbf{r}'_{s2}) \right] \cos(\phi'_{s2}) \frac{\partial \psi(\mathbf{r}_{s2}, \mathbf{r}'_{s2})}{\partial n'_{s2}} \left\| d\mathbf{r}'_{s2} \right\|$$

$$= 2\pi \left[\left(c_{m} \lambda_{g}\right)_{2} \sigma_{2}(\mathbf{r}_{s2}) \right] \cos(\phi'_{s2})$$

$$(31)$$

Since,

$$\mathbf{d}\mathbf{r}_{s} = J\,\mathbf{d}\,\zeta\,\mathbf{d}\,\phi$$

then Eqs. (30) and (31) become

$$-\int_{I} \left\{ \psi(\mathbf{r}_{s1}, \mathbf{r}'_{s1}) \cos(\phi_{s1}') \sigma_{I}(\zeta_{1}') \left[1 + \frac{(c_{m}\lambda_{g})_{I}}{\varpi_{s1}'} \frac{\partial \varpi_{s1}'}{\partial n_{s1}'} \right] \right\} J_{s1}' \, \mathrm{d} \phi_{s1}' \, \mathrm{d} \zeta_{1}'$$

$$+ \int_{I} \left\{ \left[(c_{m}\lambda_{g})_{I} \cos(\phi_{s1}') \sigma_{I}(\zeta_{1}') \right] \frac{\partial \psi(\mathbf{r}_{s1}, \mathbf{r}'_{s1})}{\partial n_{s1}'} \right\} J_{s1}' \, \mathrm{d} \phi_{s1}' \, \mathrm{d} \zeta_{1}'$$

$$- \int_{2} \left\{ \psi(\mathbf{r}_{s1}, \mathbf{r}'_{s2}) \cos(\phi_{s2}') \sigma_{I}(\zeta_{2}') \left[1 + \frac{(c_{m}\lambda_{g})_{2}}{\varpi_{s2}'} \frac{\partial \varpi_{s2}'}{\partial n_{s2}'} \right] \right\} J_{s2}' \, \mathrm{d} \phi_{s2}' \, \mathrm{d} \zeta_{2}'$$

$$+ \int_{2} \left\{ \left[(c_{m}\lambda_{g})_{2} \cos(\phi_{s2}') \sigma_{2}(\zeta_{2}') \right] \frac{\partial \psi(\mathbf{r}_{s1}, \mathbf{r}'_{s2})}{\partial n_{s2}'} \right\} J_{s2}' \, \mathrm{d} \phi_{s2}' \, \mathrm{d} \zeta_{2}'$$

$$= 2\pi (c_{m}\lambda_{g})_{1} \sigma_{I}(\mathbf{r}_{s1}) \cos(\phi_{s1}) - k^{2} \int_{I} \psi(\mathbf{r}_{s1}, \mathbf{r}'_{s1}) \, \varpi_{s1}' \cos(\phi_{s1}') J_{s1}' \, \mathrm{d} \phi_{s1}' \, \mathrm{d} \zeta_{1}'$$
(32)

and

$$-\int_{1} \left\{ \psi(\mathbf{r}_{s2}, \mathbf{r}'_{s1}) \cos(\phi'_{s1}) \sigma_{1}(\zeta'_{1}) \left[1 + \frac{\left(c_{m}\lambda_{g}\right)_{1}}{\varpi'_{s1}} \frac{\partial \varpi'_{s1}}{\partial n'_{s1}} \right] \right\} J'_{s1} \, \mathrm{d} \, \phi'_{s1} \, \mathrm{d} \, \zeta'_{1}$$

$$+ \int_{1} \left\{ \left[\left(c_{m}\lambda_{g}\right)_{1} \cos(\phi'_{s1}) \sigma_{1}(\zeta'_{1}) \right] \frac{\partial \psi(\mathbf{r}_{s2}, \mathbf{r}'_{s1})}{\partial n'_{s1}} \right\} J'_{s1} \, \mathrm{d} \, \phi'_{s1} \, \mathrm{d} \, \zeta'_{1}$$

$$- \int_{2} \left\{ \psi(\mathbf{r}_{s2}, \mathbf{r}'_{s2}) \cos(\phi'_{s2}) \sigma_{1}(\zeta'_{2}) \left[1 + \frac{\left(c_{m}\lambda_{g}\right)_{2}}{\varpi'_{s2}} \frac{\partial \varpi'_{s2}}{\partial n'_{s2}} \right] \right\} J'_{s2} \, \mathrm{d} \, \phi'_{s2} \, \mathrm{d} \, \zeta'_{2}$$

$$+ \int_{2} \left\{ \left[\left(c_{m}\lambda_{g}\right)_{2} \cos(\phi'_{s2}) \sigma_{2}(\zeta'_{2}) \right] \frac{\partial \psi(\mathbf{r}_{s2}, \mathbf{r}'_{s2})}{\partial n'_{s2}} \right\} J'_{s2} \, \mathrm{d} \, \phi'_{s2} \, \mathrm{d} \, \zeta'_{2}$$

$$= 2\pi \left(c_{m}\lambda_{g}\right)_{2} \sigma_{2}(\mathbf{r}_{s2}) \cos(\phi_{s2})$$

$$(33)$$

Define

$$f_{j} = 1 + \frac{\left(c_{m}\lambda_{g}\right)_{j}}{\varpi'_{sj}} \frac{\partial \varpi'_{sj}}{\partial n'_{sj}}$$

$$K_{ij} = \frac{J'_{sj}}{\cos \phi_{si}} \left[\int \psi(\mathbf{r}_{si}, \mathbf{r}'_{sj}) \cos(\phi'_{sj}) d\phi'_{sj} \right]$$

$$H_{ij} = \frac{J'_{sj}}{\cos \phi_{si}} \left[\int \frac{\partial \psi(\mathbf{r}_{si}, \mathbf{r}'_{sj})}{\partial n'_{sj}} \cos(\phi'_{sj}) d\phi'_{sj} \right]$$

and

$$\Psi = \frac{1}{\cos \phi_s} \left[\int \psi(\mathbf{r}_s, \mathbf{r}'_s) \varpi'_s \cos(\phi'_s) J'_s d\phi'_s d\zeta' \right]$$

Eqs. (32) and (33) become

 $-\int_{1} f_{1}(\zeta_{1}') K_{11}(\zeta_{1}, \zeta_{1}') \sigma_{1}(\zeta_{1}') d\zeta_{1}' + \int_{1} (c_{m} \lambda_{g})_{1} H_{11}(\zeta_{1}, \zeta_{1}') \sigma_{1}(\zeta_{1}') d\zeta_{1}'$ $-\int_{2} f_{2}(\zeta_{2}') K_{12}(\zeta_{1}, \zeta_{2}') \sigma_{2}(\zeta_{2}') d\zeta_{2}' - \int_{2} (c_{m} \lambda_{g})_{2} H_{12}(\zeta_{1}, \zeta_{2}') \sigma_{2}(\zeta_{2}') d\zeta_{2}'$ $= 2\pi (c_{m} \lambda_{g})_{1} \sigma_{1}(\zeta_{1}) - k^{2} \Psi(\zeta_{1})$ (34)

and

$$-\int_{1} f_{1}(\zeta_{1}') K_{21}(\zeta_{2}, \zeta_{1}') \sigma_{1}(\zeta_{1}') d\zeta_{1}' + \int_{1} (c_{m} \lambda_{g})_{1} H_{21}(\zeta_{2}, \zeta_{1}') \sigma_{1}(\zeta_{1}') d\zeta_{1}'$$

$$-\int_{2} f_{2}(\zeta_{2}') K_{22}(\zeta_{2}, \zeta_{2}') \sigma_{2}(\zeta_{2}') d\zeta_{2}' - \int_{2} (c_{m} \lambda_{g})_{2} H_{22}(\zeta_{2}, \zeta_{2}') \sigma_{2}(\zeta_{2}') d\zeta_{2}'$$

$$= 2\pi (c_{m} \lambda_{g})_{2} \sigma_{2}(\zeta_{2})$$
(35)

or,

$$\iint_{\mathbf{I}} \left[-f_{1}(\zeta_{1}')K_{11}(\zeta_{1},\zeta_{1}') + (c_{m}\lambda_{g})_{\mathbf{I}}H_{11}(\zeta_{1},\zeta_{1}') \right] \sigma_{1}(\zeta_{1}') d\zeta_{1}'
+ \iint_{2} \left[-f_{2}(\zeta_{2}')K_{12}(\zeta_{1},\zeta_{2}') - (c_{m}\lambda_{g})_{2}H_{12}(\zeta_{1},\zeta_{2}') \right] \sigma_{2}(\zeta_{2}') d\zeta_{2}'
= 2\pi(c_{m}\lambda_{g})_{\mathbf{I}}\sigma_{1}(\zeta_{1}) - k^{2}\Psi(\zeta_{1})$$
(36)

and

$$\int_{I} \left[-f_{1}(\zeta_{1}')K_{21}(\zeta_{2},\zeta_{1}') + (c_{m}\lambda_{g})_{I}H_{21}(\zeta_{2},\zeta_{1}') \right] \sigma_{I}(\zeta_{1}') d\zeta_{1}'
+ \int_{2} \left[-f_{2}(\zeta_{2}')K_{22}(\zeta_{2},\zeta_{2}') - (c_{m}\lambda_{g})_{2}H_{22}(\zeta_{2},\zeta_{2}') \right] \sigma_{2}(\zeta_{2}') d\zeta_{2}'
= 2\pi(c_{m}\lambda_{g})_{2}\sigma_{2}(\zeta_{2})$$
(37)

Define

$$L_{11}(\zeta_1, \zeta_1') = -f_1(\zeta_1')K_{11}(\zeta_1, \zeta_1') + (c_m \lambda_g)H_{11}(\zeta_1, \zeta_1')$$
(37a)

$$L_{12}(\zeta_{1},\zeta_{2}') = -f_{2}(\zeta_{2}')K_{12}(\zeta_{1},\zeta_{2}') - (c_{m}\lambda_{g})_{2}H_{12}(\zeta_{1},\zeta_{2}')$$
(37b)

$$L_{21}(\zeta_2, \zeta_1') = -f_1(\zeta_1') K_{21}(\zeta_2, \zeta_1') + (c_m \lambda_g)_1 H_{21}(\zeta_2, \zeta_1')$$
(37c)

$$L_{22}(\zeta_2, \zeta_2') = -f_2(\zeta_2')K_{22}(\zeta_2, \zeta_2') - (c_m \lambda_g), H_{22}(\zeta_2, \zeta_2')$$
(37d)

We thus have

$$\int_{1} \mathcal{L}_{11}(\zeta_{1}, \zeta_{1}') \, \sigma_{1}(\zeta_{1}') \, \mathrm{d}\zeta_{1}' + \int_{2} \mathcal{L}_{12}(\zeta_{1}, \zeta_{2}') \, \sigma_{2}(\zeta_{2}') \, \mathrm{d}\zeta_{2}' - 2\pi (c_{m}\lambda_{g})_{1} \, \sigma_{1}(\zeta_{1}) = -k^{2} \Psi(\zeta_{1})$$
(38)

and

$$\int_{1} L_{21}(\zeta_{2}, \zeta_{1}') \,\sigma_{1}(\zeta_{1}') \,\mathrm{d}\zeta_{1}' + \int_{2} L_{22}(\zeta_{2}, \zeta_{2}') \,\sigma_{2}(\zeta_{2}') \,\mathrm{d}\zeta_{2}' - 2\pi (c_{m}\lambda_{g})_{2} \,\sigma_{2}(\zeta_{2}) = 0 \tag{39}$$

Applying the singularity subtraction technique, we can write

 $\left[g_{11}(\zeta_{1}) - 2\pi(c_{m}\lambda_{g})_{1}\right]\sigma_{1}(\zeta_{1}) + \int L_{11}(\zeta_{1},\zeta_{1}')\left[\sigma_{1}(\zeta_{1}') - \sigma_{1}(\zeta_{1})\right]d\zeta_{1}'$ $+ \int L_{12}(\zeta_{1},\zeta_{2}')\sigma_{2}(\zeta_{2}')d\zeta_{2}' = -k^{2}\Psi(\zeta_{1})$ (40)

and

$$\left[g_{22}(\zeta_{2}) - 2\pi(c_{m}\lambda_{g})_{2}\right]\sigma_{2}(\zeta_{2}) + \int L_{22}(\zeta_{2}, \zeta_{2}')\left[\sigma_{2}(\zeta_{2}') - \sigma_{2}(\zeta_{2})\right]d\zeta_{2}'
+ \int L_{21}(\zeta_{2}, \zeta_{1}')\sigma_{1}(\zeta_{1}')d\zeta_{1}' = 0$$
(41)

where

$$g_{11}(\zeta_1) = \int L_{11}(\zeta_1, \zeta_1') d\zeta_1'$$
(42)

and

$$g_{22}(\zeta_2) = \int L_{22}(\zeta_2, \zeta_2') d\zeta_2'$$
 (43)

The integrals in Eqs. (40) and (41) are thus converted to summations by the use of Gaussian quadratures and Eqs. (40) and (41) are then reduced to systems of linear algebraic equations by applying collocation at the nodal points of the quadrature. The integrals in Eqs. (42) and (43) are determined in the Cauchy principal value sense. The local stress, $\sigma(\zeta)$, is determined at each nodal point and the torque is finally determined from Eqs. (5) and (6).

Appendix B

Manuscript: Rotatory Oscillations of Axi-Symmetric Bodies in an Axi-Symmetric Viscous Flow with Slip: Numerical Solutions for Sphere and Spheroids

Submitted to Journal of Fluids Engineering

VICAL ASSOCIATE EDITORS . Idresses overleal)

application and Systems)RANJAN N DHAUBHADEL (1999 Coporation 87-2009

10 SCHIAVELLO (1999) soll-Dresser Pump Company 359-7610

Measurements JOY BANERJEE (1999) ersity of California, Santa Barbara 893-3456

d Mechanics ERW. BEARMAN (2001) enal College of Science biology and Medicine 171-594-5055

TER BRADSHAW (2000) nford University)-725-0704

TER E. RAAD (2001) uthern Methodist University 4-768-3043

AVID R. WILLIAMS (2000) nois Institute of Technology 2-567-3192

HAIRUL B.M.Q. ZAMAN (2001) **ASA Lewis Research Center** 16-433-5888

omputational Fluid Dynamics JORDON ERLEBACHER (2000) lorida State University 150-645-0308

JRMILA GHIA (2001) Jniversity of Cincinnati 113-556-4612

CHARLES L. MERKLE (2000) University of Tennessee Space Institute 931-393-7426

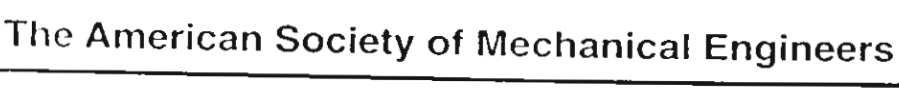
Multiphase Flow JOHN K. EATON (1999) Stanford University 650-723-1971

JOSEPH KATZ (2001) The Johns Hopkins University 410-516-5470

MARTIN SOMMERFELD (1999) Martin-Luther-Universitat Halle-Wittenberg 49 3461-462879

FREDERIC K. WASDEN (2000) Shell E&P Technology Company 281-544-7909

Editorial Office MUHAMMAD R. HAJJ (2001) 540-231-4190



Journal of Fluids Engineering Department of Engineering Science and Mechanics, MC 0219 Virginia Polytechnic Institute and State University Blacksburg, Virginia 24061 Fax: 540-231-4574

Technical Editor (2000) DEMETRI P TELIONIS 540 231-7492 e mail telionis@vt.edu

Executive Secretary (2000) PAT WHITE 540-231-3366 e-mail: whitep@vt.edu

Editorial Assistant (2000) Norman W. Schaeffler 540-951-3858 e-mail: norman.w schaeffler@vt edu

December 9, 1999

Mr. Perapong Tekasakul Faculty of Engineering Department of Mechanical Engineering Thammasat University Klong Luang, Pathum Thani, 12121, Thailand

Dear Mr. Tekasakut:

The manuscript, "Rotatory Oscillations of Axi-Symmetric Bodies in an Axi-Symmetric Viscous Flow with Slip: Numerical Solutions for Sphere and Spheroids," by P. Tekasakul and S. K. Loyalka, has been received and given the Log Number 5310-PER for reference purposes. The Technical Editor has assigned it to Dr. Peter E. Raad (address on reverse), who will oversee the reviewing process. Should you have any questions during the review of this paper, you may contact him directly. We have enclosed information on electronic publishing. You will find there many options worth considering.

The Journal has adopted a set of guidelines on reporting numerical accuracy (see enclosed editorial). The Technical Editor would like you to keep these in mind in case you decide to revise your manuscript. The editors and reviewers will most likely propose to you ways in which you can improve your manuscript on this issue.

Please complete the enclosed green sheet (Form M&P 1903) and return it to this office. You may disregard the questions on this form that are irrelevant, but we will need to have the signatures of all authors which essentially gives ASME formal permission to publish a paper. There is no need to include an abstract. Please note the current estimate on the length of this paper is nine journal pages and therefore subject to the mandatory excess page charges. On this and other relevant issues, please consult "Information for Authors" that appears in each issue of the Journal, as well as the reverse of Form Virginia Polytechnic Institute and State University M&P 1903. By copy of this letter we are requesting Dr. Raad to solicit reviewers for comments on the possible shortening of the paper.

The Technical Forum of the Fluids Engineer

Rotatory oscillations of axi-symmetric bodies in an axi-symmetric viscous flow with slip: Numerical solutions for sphere and spheroids

P. Tekasakul

Assistant Professor

Department of Mechanical Engineering
Faculty of Engineering
Thammasat University, Rangsit Campus
Klong Luang, Pathum Thani 12121, Thailand
(e-mail: tperapon@engr.tu.ac.th)

S. K. Loyalka

Curators' Professor and Director

Particulate Systems Research Center and

Nuclear, Chemical, and Mechanical & Aerospace Engineering Departments

University of Missouri-Columbia

Columbia, MO 65211, USA

(e-mail: loyalkas@missouri.edu)

This article has not been published, either in whole or in part, in a serial, professional journal.

Abstract

Rotatory oscillations of several axi-symmetric bodies in axi-symmetric viscous flows with slip are investigated. A numerical method based on the Green's function technique is used wherein the relevant Helmholtz equation, as obtained from the unsteady Stokes equation, is converted into a surface integral equation. The technique is benchmarked against a known analytical solution, and accurate numerical results for local stress and torque on spheres and spheroids as function of the wave number and the slip coefficients are obtained. It is found that in all cases, slip reduces stress and torque, and increasingly so with the increasing wave number. The method discussed here can be potentially extended to the realistic case of an oscillating disk viscometer.

1 Introduction

There have been several studies of oscillations of axi-symmetric bodies in axi-symmetric, viscous, incompressible flow at low Reynolds number with no-slip boundary conditions. Two important modes of oscillation involved the translational, in which the body performing oscillation displaces the fluid around the body, and rotatory oscillations, in which the body performing oscillation does not displace the fluid. Details of translational oscillation studies can be found in the literature (Kanwal, 1955 and 1964; William, 1966; Lawrence and Weinbaum, 1986 and 1988; Pozrikidis, 1989a and 1989b; Loewenberg, 1993a, 1993b, 1994a and 1994b; Davis, 1993; Lovalenti and Brady, 1993a and 1993b). The problem for the oscillation with small amplitude where the Reynolds number is very small arises from the same principle that involves the solutions to the unsteady Stokes equations (Tekasakul, et al., 1998; and Zhang and Stone, 1998),

$$\lambda^2 \frac{\partial \mathbf{u}}{\partial \tau} = -\nabla p + \nabla^2 \mathbf{u} \quad . \tag{1}$$

where $\lambda^2 = \omega a^2/v$ is the dimensionless frequency parameter. Here, a is the characteristic length of the body and ω is the frequency of oscillation.

Rotatory oscillations of a body in a fluid are of interest in studies of oscillating disk viscometer, Brownian motion, ultrasonics, and electroacoustics. The analytical solutions to the oscillation problem are limited to certain bodies with simple geometries. Some approximations are employed for more complicated bodies in order to facilitate analytical solutions. Recently, Tekasakul, et al. (1998) have solved the problem of several axi-symmetric bodies numerically from the unsteady Stokes equations for noslip boundary conditions, and Zhang and Stone (1998) have provided a range of useful solutions for bodies in several modes of rotation. These authors reported results for local stresses and torques on the bodies. Comparison showed that the accuracy of the numerical method was excellent. When the body dimension is only about an order of magnitude larger than molecular mean free path of the fluid, one must, however, consider fluid slip at the surface. The previous works (Lamb, 1932; Kanwal, 1970; Kestin and Persen, 1956; Mariens and van Paemel, 1956; Kestin and Wang, 1957; Clark, et al., 1977), as it turns out, have emphasized the problem with no-slip boundary conditions with a few exceptions. MacWood (1938a and 1938b) obtained an approximate solution for a thin cylindrical disk with slip by use of edge correction where some accuracy was lost. Shah (1971) obtained slip solutions for some simple geometries in Laplace transform domain.

The slip at boundaries occurs when the Knudsen number (Kn) is in the order of 0.1. The Knudsen number is defined as the ratio of molecular mean free path of the medium (λ_g) and the characteristic length of the body (a), i.e. $Kn = \lambda_g/a$. The flow regimes classified by the Knudsen numbers include the free molecular (Kn >> 1), the transition $(Kn \sim 1)$, the slip $(Kn \sim 0.1)$, and the continuum flow regime (Kn << 1). The molecular mean free path of the gas medium is defined as

$$\lambda_g = \frac{\mu}{p} \left(\frac{2kT}{m} \right)^{1/2}$$

where μ is the dynamic viscosity, p is the pressure, k is the Boltzmann's constant, T is the temperature, and m is the mass of the medium. The slip boundary condition at

the surface of a body involves both the molecular mean free path and the slip coefficient, c_m , which can be represented with accuracy within 1%, by (Loyalka, 1990)

$$c_m = \frac{2 - \alpha}{\alpha} \left[(1 - \alpha) \frac{\pi^{1/2}}{2} + \alpha \zeta(1) \right]$$

where α is the momentum accommodation coefficient, and $\zeta(1)$, corresponding to $\alpha = 1$, has a value between 0.9875 and 1.02, depending on the nature of the gaseous intermolecular interaction. If $\zeta(1)$ is replaced by $\sqrt{\pi}/2$, the above equation becomes Maxwell's relation (Maxwell, 1879). The slip becomes of greater significance as the pressure decreases below atmospheric, particularly for the value of $Kn \sim 0.1$.

In this paper, we investigate calculations of local stresses and, hence, torques on axi-symmetric bodies performing rotatory oscillation in an unbounded fluid medium and in viscous flow with slip boundary condition. The geometries of our interest are sphere, oblate spheroid and prolate spheroid. The numerical technique is based on that used by Tekasakul, et al. (1998).

In the next section, the problem is described. In Sec. 3, analytical solutions for a sphere with constant slip on the surface are obtained from the technique employing the solutions from the no-slip case. In Sec. 4, numerical procedure for this problem is discussed and solution technique is outlined. In Sec. 5, numerical results and available analytical results for local stresses and torques for a sphere, an oblate spheroid and a prolate spheroid are presented. We discuss and conclude the present work in Sec. 6, together with suggestions for possible future work.

2 Statement of the problem

We consider an axi-symmetric body with a characteristic length, a, oscillating with frequency, ω , about its axis of symmetry (defined as the z-direction) in an unbounded gas with kinematic viscosity, $v = \mu/\rho$, slip coefficient, c_m , and molecular mean free path, λ_g , where μ is the dynamic viscosity and ρ is the mass density of the fluid (Fig. 1). The angular velocity of the oscillating body is given by $\Omega \cos(\omega t)$. The Unsteady Stokes' equation for a time-dependent, dimensionless, ϕ -component velocity obtained from Eq. (1) can be written as Tekasakul, et al. (1998)

$$\lambda^2 \frac{\partial \hat{u}_{\phi}}{\partial \tau} = \left(\frac{\partial^2}{\partial \varpi^2} + \frac{1}{\varpi} \frac{\partial}{\partial \varpi} - \frac{1}{\varpi^2} + \frac{\partial^2}{\partial z^2} \right) \hat{u}_{\phi}$$
 (2)

The slip boundary condition at the body surface is

$$\hat{u}_{\phi}(\mathbf{r}_{s}) = \varpi_{s} \cos(\tau) + (c_{m} \lambda_{g}) \hat{\sigma}(\mathbf{r}_{s})$$
(3)

while, far away from the body,

$$\lim_{\mathbf{r} \to \mathbf{r}} \hat{u}_{\phi}(\mathbf{r}) = 0 \tag{4}$$

Here, the length, time, velocity, and pressure are nondimensionalized in terms of a, ω^{-1} , $U = |\Omega| a = \Omega a$, and $\mu U/a$, respectively. For a sphere, the characteristic length, a, is a radius whereas for prolate and oblate spheroids the equatorial radii are used. The solution is assumed to be of the form:

$$\hat{u}_{o}(\varpi, z, \tau) = \exp(i\tau) u_{o}(\varpi, z) . \tag{5}$$

With the Jeffrey transformation (1915):

$$w(\varpi, z, \phi) = u_{\phi}(\varpi, z) \cos(\phi)$$

and following the manipulation of Tekasakul, et al. (1998), we can write the form:

$$\nabla^2 w = \left(\frac{\partial^2}{\partial \varpi^2} + \frac{1}{\varpi} \frac{\partial}{\partial \varpi} - \frac{1}{\varpi^2} + \frac{\partial^2}{\partial z^2}\right) u_{\phi} \cos(\phi) \tag{6}$$

which leads to the Helmholtz equation:

$$\left(\nabla^2 + k^2\right) w = 0 \tag{7}$$

The slip boundary condition at the surface of such a body the becomes

$$w(\mathbf{r}_s) = \left[\varpi_s + (c_m \lambda_g) \sigma(\mathbf{r}_s) \right] \cos(\phi_s)$$
 (8)

and the limiting condition of the fluid far away from the body is

$$\lim_{\mathbf{r} \to \infty} w(\mathbf{r}) = 0 \tag{9}$$

Here $\lambda^2 = \omega a^2/v$ is the dimensionless frequency parameter and $k^2 = -i\lambda^2$ is the dimensionless complex-valued frequency parameter. The dimensionless, time-independent local stress is defined as

$$\sigma(\zeta) = \varpi \frac{\partial}{\partial n} \left(\frac{u_o}{\varpi} \right) \tag{10}$$

while the dimensionless, time-independent torque on the body can be evaluated from

$$T = 2\pi \int_{\mathcal{L}} \overline{\omega}^2 \ \sigma(\zeta) \, \mathrm{d} s \tag{11}$$

Here, ζ is a coordinate specifying a point on the meridian contour of the body for which $-1 \le \zeta \le 1$. Note that the dimensionless, time-independent torque has been nondimesionalized by $\Omega \mu a^3$ and the transient term $\exp(i\tau)$ has been dropped.

3 Analytical solutions for constant slip

The solution of an oscillating sphere in an infinite fluid medium with slip can be obtained from the solution of the oscillation sphere with no-slip. We consider two separate problems, one with no-slip and the other with non-zero constant slip, simultaneously. For the no-slip case, Eqs. (7) to (9) with $c_m \lambda_g = 0$, can be written as

$$Lu_{o1} = 0 ag{12}$$

The no-slip boundary condition at the surface of the sphere becomes

$$u_{\sigma_1} = \sin \theta \tag{13}$$

where θ is the polar angle and far away from the sphere:

$$\lim_{r \to \infty} u_{\phi 1} = 0 \tag{14}$$

For the constant-slip, the problem can be written as

$$Lu_{\alpha 2} = 0 \tag{15}$$

The slip boundary condition at the surface of the sphere is

$$u_{\phi 2} = \sin \theta + c_2 \sin \theta = (1 + c_2) \sin \theta \tag{16}$$

and the limiting condition of the fluid far away from the sphere is

$$u_{\phi 2} = 0 \tag{17}$$

where ϕ_s and c_2 are constants, subscripts 1 and 2 represent the no-slip and constant slip cases, respectively, and the operator L is

$$L = \left(\frac{\partial^2}{\partial \varpi^2} + \frac{1}{\varpi} \frac{\partial}{\partial \varpi} - \frac{1}{\varpi^2} + \frac{\partial^2}{\partial z^2}\right) + k^2$$

Substituting $u_{\phi 2} = (1 + c_2)u_{\phi 1}$ into Eqs (15) to (17), the slip problem becomes the no-slip problem. Therefore the relation

$$u_{o2} = (1 + c_2)u_{o1} \tag{18}$$

is the solution for the slip problem.

From Eq. (8) for the slip case, the constant, c_2 , can be written as

$$c_2 = \frac{\left(c_m \lambda_g\right)}{\sin \theta} \sigma_2 = \frac{\left(c_m \lambda_g\right)}{\sin \theta} \varpi \frac{\partial}{\partial n} \left(\frac{u_{\phi 2}}{\varpi}\right)$$
 (19)

Now in Eq. (18), dividing by ϖ and differentiating with respect to the normal direction and multiplying by ϖ , we get

$$\varpi \frac{\partial}{\partial n} \left(\frac{u_{\phi 2}}{\varpi} \right) = \left(1 + c_2 \right) \varpi \frac{\partial}{\partial n} \left(\frac{u_{\phi 1}}{\varpi} \right) \tag{20}$$

that is,

$$\sigma_2 = \left(1 + \frac{c_m \lambda_g}{\sin \theta} \, \sigma_2\right) \sigma_1 \tag{21}$$

And we get,

$$\sigma_2 = \frac{\sigma_1}{1 - \sigma_1 \left(c_m \lambda_g \right) / \sin \theta} \tag{22}$$

The above equation shows that the stress on the oscillating sphere for the constant-slip case (σ_2) can be determined from the knowledge of the stress for the no-slip case (σ_1)

Since the local stress for the no-slip case is (Lamb, 1932; and Tekasakul, et al., 1998)

$$\sigma_{\text{zero-slip}} = \sigma_1 = -\left[3 - \frac{k^2}{1 + ik}\right] \sin\theta \tag{23}$$

The local stress for the slip case becomes

$$\sigma_{\text{slip}} = \sigma_2 = \frac{-\left[3 - \frac{k^2}{1 + ik}\right] \sin \theta}{1 + \left(c_m \lambda_g\right) \left[3 - \frac{k^2}{1 + ik}\right]}$$
(24)

Torque on the sphere can then be evaluated straightforwardly from

$$T = 2\pi \int_{c}^{\pi} \varpi^{2} \sigma \, ds$$

$$= 2\pi \int_{0}^{\pi} \sin^{2} \theta \left\{ \frac{-\left[3 - \frac{k^{2}}{1 + ik}\right] \sin \theta}{1 + \left(c_{m} \lambda_{s}\right) \left[3 - \frac{k^{2}}{1 + ik}\right]} \right\} d\theta$$

$$= -\frac{8}{3}\pi \frac{3 - \frac{k^{2}}{1 + ik}}{1 + \left(c_{m} \lambda_{s}\right) \left[3 - \frac{k^{2}}{1 + ik}\right]}$$
(25)

These simple forms of relationship do not appear to hold in general for spheroids, for which even the no-slip case leads to complicated eigenfunction expansions. We have thus not reported such results here.

4 Numerical solutions

The numerical method used in the present work is based on the Green's function approach (Tekasakul, et al., 1998; Tekasakul, et al., 1999). The Green's function for this problem is defined by

$$(\nabla^2 + k^2)\psi(\mathbf{r}, \mathbf{r}') = -4\pi \,\delta(\mathbf{r} - \mathbf{r}') \tag{26}$$

such that

$$\psi(\mathbf{r}, \mathbf{r}') = \frac{\exp(-i k |\mathbf{r} - \mathbf{r}'|)}{|\mathbf{r} - \mathbf{r}'|}$$
(27)

Following the procedure of Tekasakul, et al. (1998) [see their Eqs. (23)-(26)], and applying the slip boundary condition, the problem becomes

$$-\int \left(\psi(\mathbf{r}_{s}, \mathbf{r}'_{s}) \left\{ \cos(\phi') \sigma(\mathbf{r}'_{s}) + \left[\frac{(c_{m} \lambda_{g}) \sigma(\mathbf{r}'_{s})}{\varpi'_{s}} \right] \frac{\partial}{\partial n'_{s}} \left[\varpi'_{s} \cos(\phi') \right] \right\}$$

$$-\left[(c_{m} \lambda_{g}) \sigma(\mathbf{r}'_{s}) \right] \cos(\phi') \frac{\partial \psi(\mathbf{r}_{s}, \mathbf{r}'_{s})}{\partial n'_{s}} \right] d\mathbf{r}'_{s}$$

$$= 2\pi \left[\varpi_{s} + (c_{m} \lambda_{g}) \sigma(\mathbf{r}_{s}) \right] \cos(\phi)$$

$$+ \int \left[\psi(\mathbf{r}_{s}, \mathbf{r}'_{s}) \frac{\partial}{\partial n'_{s}} \left[\varpi'_{s} \cos(\phi') \right] - \varpi'_{s} \cos(\phi') \frac{\partial \psi(\mathbf{r}_{s}, \mathbf{r}'_{s})}{\partial n'_{s}} \right] d\mathbf{r}'_{s}$$
(28)

Using Green's second identity and

$$\nabla_{\mathbf{r}'}^2 \varpi_s' \cos(\phi_s') = 0 \tag{29}$$

Equation (28) becomes

$$-\int \left(\psi(\mathbf{r}_{s}, \mathbf{r}'_{s}) \left\{ \cos(\phi'_{s}) \sigma(\mathbf{r}'_{s}) + \left[\frac{(c_{m} \lambda_{g}) \sigma(\mathbf{r}'_{s})}{\varpi'_{s}} \right] \frac{\partial}{\partial n'_{s}} \left[\varpi'_{s} \cos(\phi') \right] \right\}$$

$$-\left[(c_{m} \lambda_{g}) \sigma(\mathbf{r}'_{s}) \right] \cos(\phi') \frac{\partial \psi(\mathbf{r}_{s}, \mathbf{r}'_{s})}{\partial n'_{s}} d\mathbf{r}'_{s}$$

$$= 2\pi \left[(c_{m} \lambda_{g}) \sigma(\mathbf{r}_{s}) \right] \cos(\phi) - k^{2} \int \psi(\mathbf{r}_{s}, \mathbf{r}'_{s}) \varpi'_{s} \cos(\phi') d\mathbf{r}'_{s}$$
(30)

or,

$$-\int \left\{ \psi(\mathbf{r}_{s}, \mathbf{r}'_{s}) \cos(\phi'_{s}) \sigma(\zeta') \left[1 + \frac{\left(c_{m}\lambda_{g}\right)}{\varpi'_{s}} \frac{\partial \varpi'_{s}}{\partial n'_{s}} \right] \right\} J'_{s} d\phi'_{s} d\zeta'$$

$$+ \int \left\{ \left[\left(c_{m}\lambda_{g}\right) \cos(\phi') \sigma_{1}(\zeta') \right] \frac{\partial \psi(\mathbf{r}_{s}, \mathbf{r}'_{s})}{\partial n'_{s}} \right\} J'_{s} d\phi'_{s} d\zeta'$$

$$= 2\pi \left(c_{m}\lambda_{g}\right) \sigma(\mathbf{r}_{s}) \cos(\phi) - k^{2} \int \psi(\mathbf{r}_{s}, \mathbf{r}'_{s}) \varpi'_{s} \cos(\phi'_{s}) J'_{s} d\phi' d\zeta'$$
(31)

since $d\mathbf{r}_s = J d\zeta d\phi$.

We define.

$$f = 1 + \frac{\left(c_{m}\lambda_{g}\right)}{\varpi'_{s}} \frac{\partial \varpi'_{s}}{\partial n'_{s}}$$

$$K = \frac{J'_{s}}{\cos(\phi)} \left[\int \psi(\mathbf{r}_{s}, \mathbf{r}'_{s}) \cos(\phi') d\phi' \right]$$

$$H = \frac{J'_{s}}{\cos\phi_{s}} \left[\int \frac{\partial \psi(\mathbf{r}_{s}, \mathbf{r}'_{s})}{\partial n'_{s}} \cos(\phi') d\phi' \right]$$

and

$$\Psi = \frac{J_s'}{\cos \phi_s} \left[\int \psi(\mathbf{r}_s, \mathbf{r}_s') \varpi_s' \cos(\phi') d\phi' d\zeta' \right]$$

Therefore Eq. (31) can be written as

$$\int L(\zeta, \zeta') \, \sigma(\zeta') \, \mathrm{d} \, \zeta' = -k^2 \Psi(\zeta, \zeta') + 2\pi (c_m \lambda_*) \, \sigma(\zeta) \tag{32}$$

where

$$L(\zeta,\zeta') = -f(\zeta')K(\zeta,\zeta') + (c_m\lambda_s)H(\zeta,\zeta')$$

Equation (32) is a Fredholm integral equation of the second kind. Applying the singularity subtraction technique (Loyalka and Griffin, 1993; Loyalka and Griffin, 1994; Tekasakul, et al., 1998; Tekasakul, et al., 1999), the above equation becomes

$$g(\zeta)\sigma(\zeta) + \int L(\zeta,\zeta') \left[\sigma(\zeta') - \sigma(\zeta)\right] d\zeta' = -k^2 \Psi(\zeta,\zeta') + 2\pi \left(c_m \lambda_g\right) \sigma(\zeta)$$

or

$$\left[g(\zeta) - 2\pi \left(c_m \lambda_g\right)\right] \sigma(\zeta) + \int L(\zeta, \zeta') \left[\sigma(\zeta') - \sigma(\zeta)\right] d\zeta' = -k^2 \Psi(\zeta, \zeta')$$
 (33)

where,

$$g(\zeta) = \int_{-1}^{1} L(\zeta, \zeta') d\zeta'$$
(34)

The integrals in Eq. (33) are converted to summations by the use of Gaussian quadratures. Together with collocation at the nodal points of the quadrature, Eq. (33) then reduces to a system of linear algebraic equations. The stress, $\sigma(\zeta)$, is determined at the nodal points of the quadrature. The total torque can then be determined from the stresses using Eqs. (10) and (11).

4.1 Determination of f

Sphere

For the case of a sphere, we can write

$$z = r\cos\theta$$
$$\boldsymbol{\varpi} = r\sin\theta$$

and

$$\frac{1}{\varpi_s} \frac{\partial \varpi_s}{\partial n_s} = \frac{1}{\varpi_s} \frac{\partial \varpi}{\partial r} \bigg|_{r=1} = 1$$

then

$$f = 1 + \left(c_m \lambda_g\right) \tag{35}$$

Spheroids

For spheroids with the geometries shown in Fig. 2, we have

$$z = c \lambda \zeta$$

$$\boldsymbol{\varpi} = c \left[\left(1 + \lambda^2 \right) \left(1 - \zeta^2 \right) \right]^{1/2}$$

$$c^{2} = \begin{cases} A^{-2} - 1 & \text{Prolate spheroid} \\ 1 - A^{-2} & \text{Oblate spheroid} \end{cases}$$

$$\lambda_{0} = \frac{b}{c} \quad \text{at surface}$$

$$h_{\lambda} = \frac{1}{c} \left(\frac{1 + \lambda^{2}}{\zeta^{2} + \lambda^{2}} \right)^{1/2}$$

and,

$$\frac{1}{\varpi_{s}}\frac{\partial \varpi_{s}}{\partial n_{s}} = \frac{1}{\varpi_{s}}h_{\lambda_{0}}\frac{\partial \varpi}{\partial \lambda}\Big|_{\lambda_{0}} = \frac{\lambda_{0}}{c\left[\left(1 + \lambda_{0}^{2}\right)\left(\zeta^{2} + \lambda_{0}^{2}\right)\right]^{1/2}}$$

Hence;

$$f = 1 + \frac{\left(c_m \lambda_g\right)}{c} \cdot \frac{\lambda_o}{\left[\left(1 + \lambda_o^2\right)\left(\zeta^2 + \lambda_o^2\right)\right]^{1/2}}$$
(36)

4.2 Determination of K

From Tekasakul, et al. (1998), the expression of K can be written as

$$K(\zeta, \zeta') = \frac{J_s'}{\cos(\phi)} \int \psi(\mathbf{r}_s, \mathbf{r}_s') \cos(\phi') d\phi'$$
$$= K_L(\zeta, \zeta') + K_H(\zeta, \zeta')$$
(37)

where,

$$K_{L}(\zeta,\zeta') = \frac{J_{s}'}{\cos(\phi)} \int \frac{\cos(\phi')}{|\mathbf{r}_{s}' - \mathbf{r}_{s}|} d\phi' = \frac{2J_{s}'}{\sqrt{\varpi_{s} \varpi_{s}'}} Q_{1/2}(\gamma)$$
(38)

and

$$K_{H}(\zeta,\zeta') = \frac{J'_{s}}{\cos(\phi)} \int \frac{\exp(-ik|\mathbf{r}'_{s} - \mathbf{r}_{s}|) - 1}{|\mathbf{r}'_{s} - \mathbf{r}_{s}|} \cos(\phi') d\phi'$$

$$= \frac{J'_{s}}{\cos(\phi)} \int_{0}^{2\pi} \frac{\exp(-ik[2\varpi_{s}\varpi'_{s}(\gamma - \cos(\phi - \phi'))]^{1/2}) - 1}{[2\varpi_{s}\varpi'_{s}(\gamma - \cos(\phi - \phi'))]^{1/2}} \cos(\phi') d\phi' \quad (39)$$

Here, $Q_{V2}(\gamma)$ is an Associated Legendre function of fractional order with the argument

$$\gamma = 1 + \frac{\beta}{2\varpi_* \, \varpi'_*}$$

in which

$$\beta = \left(\varpi_s' - \varpi_s\right)^2 + \left(z_s' - z_s\right)^2$$

4.3 Determination of H

The expression of H can be written as

$$H = \frac{J_s'}{\cos(\phi)} \left[\int \frac{\partial \psi(\mathbf{r}_s, \mathbf{r}_s')}{\partial n_s'} \cos(\phi_s') d\phi_s' \right]$$

Since,

$$\psi(\mathbf{r}_s, \mathbf{r}_s') = \frac{\exp(-i\,k\,t)}{t}$$

where $t = |\mathbf{r}_s - \mathbf{r}'_s|$. Therefore,

$$\frac{\partial \psi(\mathbf{r}_{s}, \mathbf{r}'_{s})}{\partial n'_{s}} = (1 + i k t) \exp(-i k t) \frac{\partial}{\partial n'} \left(\frac{1}{t}\right)$$
$$= (1 + i k t) \exp(-i k t) \left(-\frac{(\mathbf{r}'_{s} - \mathbf{r}_{s}) \cdot \mathbf{n}'_{outward}}{|\mathbf{r}_{s} - \mathbf{r}'_{s}|^{3}}\right)$$

For general spheroids (including sphere)

$$H(\zeta,\zeta') = -\frac{1}{\cos(\phi)} \frac{\varpi_s'}{A} \int_0^{2\pi} \left\{ (1+ikt) \exp(-ikt) \left[2\varpi_s \varpi_s' \left(\gamma - \cos(\phi - \phi') \right) \right]^{-3/2} \right\}$$

$$\left[\left[z_s' - z_s \right] \frac{z_s'}{\left[A^{-2} - z_s'^2 \right]^{1/2}} A + \varpi_s' - \varpi_s \cos(\phi - \phi') \right] \cos(\phi') \right\} d\phi'$$

$$(40)$$

4.4 Determination of Ψ

From Tekasakul, et al. (1998), we have

$$\Psi(\zeta)\cos(\phi) = -\frac{4\pi}{k^2} \left(\varpi_s\cos(\phi)\right) - \int_{\substack{\text{inside} \\ \text{body}}} \frac{\exp(-i k |\mathbf{r}' - \mathbf{r}_s|)}{|\mathbf{r}' - \mathbf{r}_s|} \varpi'\cos(\phi') d\mathbf{r}'$$
(41)

Sphere

$$\Psi(\zeta)\cos(\phi) = \frac{2\pi \,\varpi_s \cos(\phi)}{k^2} \left\{ -2 + \left(1 + \frac{i}{k}\right) + \exp(-i\,2\,k) \left(1 - \frac{i}{k}\right) + \frac{i}{k} \left(1 + \frac{3}{k^2}\right) - \frac{\exp(-i\,2\,k)}{k^3} \left(3\,i - 6\,k - 5\,i\,k^2 + 2\,k^3\right) \right\}$$
(42)

Prolate spheroid (see Happel and Brenner, 1965)

$$\Psi(\zeta)\cos(\phi) = \frac{4\pi}{k^{2}} \left[\varpi_{s}\cos(\phi)\right] - \frac{c^{3}}{2} \int_{0}^{\xi_{0}} d\xi' \int_{0}^{\pi} d\eta' \int_{0}^{2\pi} d\phi' \\
\times \left\{ \frac{\exp\left(-ik\left[2\varpi_{s}\varpi'_{s}\left(\gamma - \cos(\phi - \phi')\right)\right]^{1/2}\right)}{\left[2\varpi_{s}\varpi'_{s}\left(\gamma - \cos(\phi - \phi')\right)\right]^{1/2}} \right\} \\
\times \left\{ \varpi'\cos(\phi')\left[\cosh(2\xi') - \cos(2\eta')\right] \sinh(\xi')\sin(\eta') \right\} (43)$$

Oblate spheroid (see Happel and Brenner, 1965)

$$\Psi(\zeta)\cos(\phi) = \frac{-4\pi}{k^{2}} \left[\varpi_{s}\cos(\phi)\right] - \frac{c^{3}}{2} \int_{0}^{\xi_{0}} d\xi' \int_{0}^{\pi} d\eta' \int_{0}^{2\pi} d\phi' \\
\times \left\{ \frac{\exp\left(-ik\left[2\varpi_{s}\varpi'_{s}\left(\gamma - \cos(\phi - \phi')\right)\right]^{1/2}\right)}{\left[2\varpi_{s}\varpi'_{s}\left(\gamma - \cos(\phi - \phi')\right)\right]^{1/2}} \right\} \\
\times \left\{ \varpi'\cos(\phi')\left[\cosh(2\xi') + \cos(2\eta')\right]\cosh(\xi')\sin(\eta') \right\} (44)$$

5 Local stresses and torques

Our main goal in this paper was to study the effect of the slip on the local stress on the surface and torque exerted on an oscillating sphere and spheroids, and to assess the accuracy of a numerical technique. We have benchmarked the accuracy of the method against known solution for a sphere. The results of this benchmarking are reported below and are followed by our results for the prolate and oblate spheroids.

Numerical results for the dimensionless time-independent torque (T) are presented as functions of the multiplication of slip coefficient and molecular mean free path $(c_m \lambda_g)$ for the dimensionless frequency parameter (λ^2) between 0.01 to 100.0. Since $k^2 = -i\lambda^2$, only the positive root of k is used, i.e.:

$$k = +(1-i)\lambda/\sqrt{2} \quad . \tag{45}$$

The time-independent torque is obtained by dropping the term, $\exp(i\tau)$. The real part of torque is a component that varies in phase with body motion while the imaginary part is the out-of-phase component and then does not contribute to energy dissipation (Zhang and Stone, 1998).

5.1 Sphere

Since the analytical solution for an oscillating sphere with slip can be obtained from the no-slip solution, we first benchmark the accuracy of the numerical method against the analytical solutions for a sphere for values of $c_m \lambda_g$ ranging from 0.001 to 0.1 and values of λ^2 ranging from 0.01 to 100.0. In these calculations, 20 point Gaussian quadratures were used for $\lambda^2 \le 10.0$ and 30 point quadratures were used for $\lambda^2 = 100.0$. Both the torques and the local stresses on the sphere are calculated and compared to the corresponding analytical values.

Numerical results for the real and imaginary parts of the torque on a sphere are given in Figs. 3(a) and 3(b), respectively. Analytical values for this sphere that have been determined from Eq. (25) are also included for comparison. In general the agreement is very good. The numerical results differ from the analytical values by a maximum of 4%. In this section, values of λ^2 is displayed instead of k^2 since k^2 is complex. Values of torques increase as the values of λ^2 increase as expected (Tekasakul, et al., 1998). As seen in Figs. 3(a) and 3(b), the values of torques decrease as the slip term $c_m \lambda_g$ becomes greater. The decrease of the real part of torque ranges from 23% for $\lambda^2 = 0.01$ to 41% for $\lambda^2 = 100.0$, while, for the imaginary part, the decrease ranges from 41% for $\lambda^2 = 0.01$ to 76% for $\lambda^2 = 100.0$. It is obvious that the effect of slip is significant for the range considered $(0.001 \le c_m \lambda_g \le 0.1)$ and becomes greater for an oscillation with higher frequency. Numerical results for the real and imaginary parts of the local stress on a sphere for which $\lambda^2 = 1.0$ have been obtained via our numerical technique and are compared with values calculated from Eq. (24) in Figs. 3(c) and 3(d), respectively. The agreement is generally very good with

errors less than 1% over the entire range of ζ except for $c_m \lambda_g = 0.1$ where the error increases to about 5%.

The good agreement between the numerical and analytical values for the case of a sphere demonstrates that the order of quadrature used are appropriate. The errors are quite small for small values of λ^2 and increase noticeably only for the largest values of λ^2 . The errors at large values of λ^2 are due to the relative thinness of the oscillatory viscous boundary layer which requires a higher number of Gaussian quadrature points for accurate modeling.

5.2 Prolate Spheroid

Twenty-point Gaussian quadratures were also used in these calculations. Numerical results for the real and imaginary parts of the torque on a typical prolate spheroid with A=0.5 are given in Figs. 4(a) and 4(b), respectively. Tekasakul, et al. (1998) showed that for the prolate spheroid with the same aspect ratio, value of the torque increases as the value of λ^2 increases. As shown in Figs. 4(a) and 4(b), the value of torque decreases as the slip term $c_m \lambda_g$ becomes greater, as in the case of the sphere. The decrease of the real part of torque ranges from 16% for $\lambda^2=0.01$ to 31% for $\lambda^2=100.0$, while, for the imaginary part, the decrease ranges from 35% for $\lambda^2=0.01$ to 72% for $\lambda^2=100.0$. The effect of slip for a prolate spheroid is similar to the case of a sphere in the previous section for the range considered $(0.001 \le c_m \lambda_g \le 0.1)$. Numerical results for the real and imaginary parts of the local stress on the same prolate spheroid for which $\lambda^2=1.0$ are also shown in Figs. 4(c) and 4(d), respectively. The results are similar to those of a sphere as one should reasonably expect.

5.3 Oblate Spheroid

We used 20-point Gaussian quadratures in the calculation for an oblate spheroid also. Numerical results for the real and imaginary parts of the torque on a typical oblate spheroid with A = 2.0 are given in Figs. 5(a) and 5(b), respectively. As also shown by Tekasakul, et al. (1998), value of the torque increases as the value of λ^2 increases.

The value of torque for the oblate spheroid decreases as the slip term $c_m \lambda_g$ becomes greater, as in the case of the sphere and the prolate spheroid considered previously. The decrease of the real part of torque ranges from 29% for $\lambda^2 = 0.01$ to 44% for $\lambda^2 = 100.0$, while, for the imaginary part, the decrease ranges from 51% for $\lambda^2 = 0.01$ to 76% for $\lambda^2 = 100.0$. The effect of slip for an oblate spheroid is also similar to the case of a sphere and a prolate spheroid in the previous section for the range considered $(0.001 \le c_m \lambda_g \le 0.1)$. Numerical results for the real and imaginary parts of the local stress on the same oblate spheroid for which $\lambda^2 = 1.0$ are shown in Figs. 5(c) and 5(d), respectively. The results are similar to those of a sphere and a prolate spheroid.

6 Discussions and conclusion

We have shown that the numerical technique used in the calculations of torques and local stresses on axi-symmetric bodies undergoing slow rotatory oscillations about their axes of symmetry in unbounded viscous fluids with slip is accurate by benchmarking against exact solution for a sphere. The numerical results for spheres agree well (maximum error less than 4%) with the corresponding analytical values as shown in Figs. 3(a)-3(d). The accuracy of the calculations can be improved for high oscillating frequency (λ^2) by increasing number of Gaussian quadrature points. In the present work, we have used 20-point quadrature throughout for the values of λ^2 as high as 100.0 except for the case of a sphere where the 30-point quadrature was used for the case of $\lambda^2 = 100.0$. In the range of slip we have studied ($0.001 \le c_m \lambda_g \le 0.1$), it is apparent that the increase of slip always lowers the values of torques and the effect is greater for higher value of λ^2 . The reduction of torque due to the presence of slip at the body surface therefore shortens the period of oscillation of the bodies. The effect of slip for a typical prolate spheroid (A = 0.5) and a typical oblate spheroid (A = 2.0) were found to follow the same trend as in the case of a sphere.

This work is a continuing effort in the investigation for the complete solutions for the problem of axi-symmetric bodies undergoing oscillation used previously in calculations of the torque on axi-symmetric bodies undergoing oscillation in an unbounded fluid without slip on the surface of the bodies (Tekasakul, et al., 1998).

One of the most notable applications of rotatory oscillation of an axi-symmetric body, as stated earlier, is the oscillating disk viscometer. We are planning to extend the work of this paper to viscometer in the near future, and this should facilitate the extraction of the velocity slip and tangential momentum accommodation coefficients also from the data in the same manner as has been accomplished by the use of spinning rotor gauge (Loyalka, 1996; Tekasakul, et al., 1996).

Acknowledgments

This research was supported by the Thailand Research Fund (TRF) through grant PDF/32/2541. We are particularly thankful to R. V. Tompson for his critical reading and many helpful comments.

References

Clark, J., Kestin J., and Shah, V. L., 1977, "Effect of long-range intermolecular forces on the drag of an oscillating disk and on the viscosity of gases," *Physica A* Vol. 89, pp. 539-554.

Davis, A. M. J., 1993, "A hydrodynamic model of the oscillating screen viscometer," *Physics of Fluids A*, Vol. 5, pp. 2095-2103.

Happel, J., and Brenner, H., 1965, Low Reynolds Number Hydrodynamics, Prentice Hall, Englewood Cliffs, New Jersey.

Jeffrey, G. B., 1915, "On the steady rotation of a solid of revolution in a viscous fluid," *Proceedings of the London Mathematical Society*, Vol. 14, pp. 327-338.

Kanwal, R. P., 1955, "Rotatory and longitudinal oscillations of axi-symmetric bodies in a viscous fluid," *The Quarterly Journal of Mechanics and Applied Mathematics*, Vol. 8, pp. 146-163.

Kanwal, R. P., 1964, "Drag on an axially symmetric body vibrating slowly along its axis in a viscous fluid," *Journal of Fluid Mechanics*, Vol. 19, pp. 631-636.

Kanwal, R. P., 1970, "Note on slow rotation or rotary oscillation of axisymmetric bodies in hydrodynamics and magnetohydrodynamics," *Journal of Fluid Mechanics*, Vol. 41, pp. 721-726.

Kestin, J., and Persen, L. N., 1956, "Slow oscillations of bodies of revolution in a viscous fluid," *Proceedings of the International Congress of Applied Mechanics*, Vol. 9, pp. 326-338.

Kestin, J., and Wang, H. E., 1957, "Corrections for the oscillating disk viscometer," *Journal of Applied Mechanics*, Vol. 24, pp. 197-206.

Lamb, H., 1932, Hydrodynamics, 6th ed., Dover, New York.

Landau, L. D., and Lifshitz, E. M., 1959, Fluid Mechanics, Pergamon Press, Oxford, England.

Lawrence, C. J., and Weinbaum, S., 1986, "The force on an axisymmetric body in linearized, time-dependent motion: A new memory term," *Journal of Fluid Mechanics*, Vol. 171, pp. 209-218.

Lawrence, C. J., and Weinbaum, S., 1988, "The unsteady force on a body at low Reynolds number; the axisymmetric motion of a spheroid," *Journal of Fluid Mechanics*, Vol. 189, pp. 463-489.

Loewenberg, M., 1993a, "Stokes resistance, added mass, and Basset force for arbitrarily oriented, finite-length cylinders," *Physics of Fluids A*, Vol. 5, pp. 765-767.

Loewenberg, M., 1993b, "The unsteady Stokes resistance of arbitrarily oriented, finite-length cylinders," *Physics of Fluids A*, Vol. 5, pp. 3004-3006.

Loewenberg, M., 1994a, "Asymmetric, oscillatory motion of a finite-length cylinder: The macroscopic effect of particle edges," *Physics of Fluids A*, Vol. 6, pp. 1095-1107.

Loewenberg, M., 1994b, "Axisymmetric unsteady Stokes flow past an oscillating finite-length cylinder," *Journal of Fluid Mechanics*, Vol. 265, pp. 265-288.

Lovalenti, P. M., and Brady, J. F., 1993a, "The hydrodynamic force on a rigid particle undergoing arbitrary time-dependent motion at small Reynolds number," *Journal of Fluid Mechanics*, Vol. 256, pp. 561-605.

Lovalenti, P. M., and Brady, J. F., 1993b, "The force on a sphere in a uniform flow with small-amplitude oscillations at finite Reynolds number," *Journal of Fluid Mechanics*, Vol. 256, pp. 607-614.

Loyalka, S. K., 1990, "Slip and jump coefficients for rarefied gas flows: variational results for Lennard-Jones and n(r)-6 potential," *Physica A*, Vol. 163, pp. 813-821.

Loyalka, S. K., 1996, "Theory of the spinning rotor gauge in the slip regime," Journal of Vacuum Science and Technology A, Vol. 14, pp. 2940-2945.

Loyalka, S. K., and Griffin, J. L., 1993, "Condensation on nonspherical aerosol particles: Numerical solutions in the continuum regime," *Nuclear Science and Engineering*, Vol. 114, pp. 135-140.

Loyalka, S. K., and Griffin, J. L., 1994, "Rotation of non-spherical axisymmetric particles in the slip regime," *Journal of Aerosol Science*, Vol. 25, pp. 509-525.

MacWood, G. E., 1938a, "The theory of the measurement of viscosity and slip of fluids by the oscillating disc method," *Physica*, Vol. 5, pp. 374-383.

MacWood, G. E., 1938b, "The theory of the measurement of viscosity and slip of fluids by the oscillating disc method, part II," *Physica*, Vol. 5, pp. 763-768.

Mariens, P., and van Paemel, O., 1956, "Theory and experimental verification of the oscillating disk method for viscosity measurements in fluids," *Applied Scientific Research A*, Vol. 5, pp. 411-424.

Maxwell, J. C., 1879, "On stresses in rarefied gases arising from inequalities of temperature," *Royal Society-Philosophical Transactions A*, Vol. 170, pp. 231-256.

Pozrikidis, C., 1989a, "A study of linearized oscillatory flow past particles by the boundary-integral method," *Journal of Fluid Mechanics*, Vol. 202, pp. 17-41.

Pozrikidis, C., 1989b, "A singularity method for unsteady linearized flow," *Physics of Fluids A*, Vol. 1, pp. 1508-1520.

Shah, V. L., 1971, "Theory of the oscillating viscometer for slip flow," *Journal of Applied Mechanics*, Vol. 38, pp. 659-664.

Tekasakul, P., Bentz, J. A., Tompson, R. V., and Loyalka, S. K., 1996, "The spinning rotor gauge: Measurements of viscosity, velocity slip coefficients, and tangential momentum accommodation coefficients," *Journal of Vacuum Science and Technology A*, Vol. 14, pp. 2946-2952.

Tekasakul, P., Tompson, R. V., and Loyalka, S. K., 1998, "Rotatory oscillations of arbitrary axi-symmetric bodies in an axi-symmetric viscous flow: Numerical solutions," *Physics of Fluids*, Vol. 10, pp. 2797-2818.

Tekasakul, P., Tompson, R. V., and Loyalka, S. K., 1999, "Evaporation from a nonspherical aerosol particle situated in an absorbing gas," *Journal of Aerosol Science*, Vol. 30, pp. 139-156.

William, W. E., 1966, "A note on slow vibrations in a viscous fluid," *Journal of Fluid Mechanics*, Vol. 25, pp. 589-590.

Zhang, W., and Stone, H. A., 1998, "Oscillatory motions of circular disks and near spheres in viscous flows," *Journal of Fluid Mechanics*, Vol. 367, pp. 329-358.

igure CAPTIONS

- Figure 1. The coordinate system used in the present work for a general axi-symmetric body ascillating in an unbounded fluid with slip.
- Figure 2. The spheroidal geometries that are considered in this work. (a) Prolate spheroidal coordinates. (b) Oblate spheroidal coordinates. In both cases, the aspect ratio is A = a/b.
- Figure 3. A comparison of the numerically determined torques and local stresses on a sphere with the corresponding values determined analytically. Symbols indicate numerical results while various lines indicate corresponding analytical results. (a) The real parts of the torques for $\lambda^2 = 0.01$ to 100.0. (b) The imaginary parts of the torques for $\lambda^2 = 0.01$ to 100.0. (c) The real parts of the local stresses for $\lambda^2 = 1.0$ and $c_m \lambda_g = 0.001, 0.01$, and 0.1. (d) The imaginary parts of the local stresses for $\lambda^2 = 1.0$ and $c_m \lambda_g = 0.001, 0.01$, and 0.1. The number of Gaussian quadrature points used in the numerical calculations was 20. Due to symmetry, only the stress values for the upper half of each body have been shown. Here, ζ is the coordinate that specifies points on the meridian contours of the bodies, and $\lambda^2 = \omega a^2/v$ is the dimensionless frequency parameter.
- Figure 4. Numerical results for torques and local stresses on a prolate spheroid with A = 0.5. (a) The real parts of the torques for $\lambda^2 = 0.01$ to 100.0. (b) The imaginary parts of the torques for $\lambda^2 = 0.01$ to 100.0. (c) The real parts of the local stresses for $\lambda^2 = 1.0$ and $c_m \lambda_s = 0.001$, 0.01, and 0.1. (d) The imaginary parts of the local stresses for $\lambda^2 = 1.0$ and $c_m \lambda_s = 0.001$, 0.01, and 0.1. The number of Gaussian quadrature points used in the numerical calculations was 20.
- Figure 5. Numerical results for torques and local stresses on an oblate spheroid with A = 2.0. (a) The real parts of the torques for $\lambda^2 = 0.01$ to 100.0. (b) The imaginary parts of the torques for $\lambda^2 = 0.01$ to 100.0. (c) The real parts of the local stresses for $\lambda^2 = 1.0$ and

 $c_m \lambda_g = 0.001, 0.01, \text{ and } 0.1.$ (d) The imaginary parts of the local stresses for $\lambda^2 = 1.0$ and $c_m \lambda_g = 0.001, 0.01, \text{ and } 0.1.$ The number of Gaussian quadrature points used in the numerical calculations was 20.

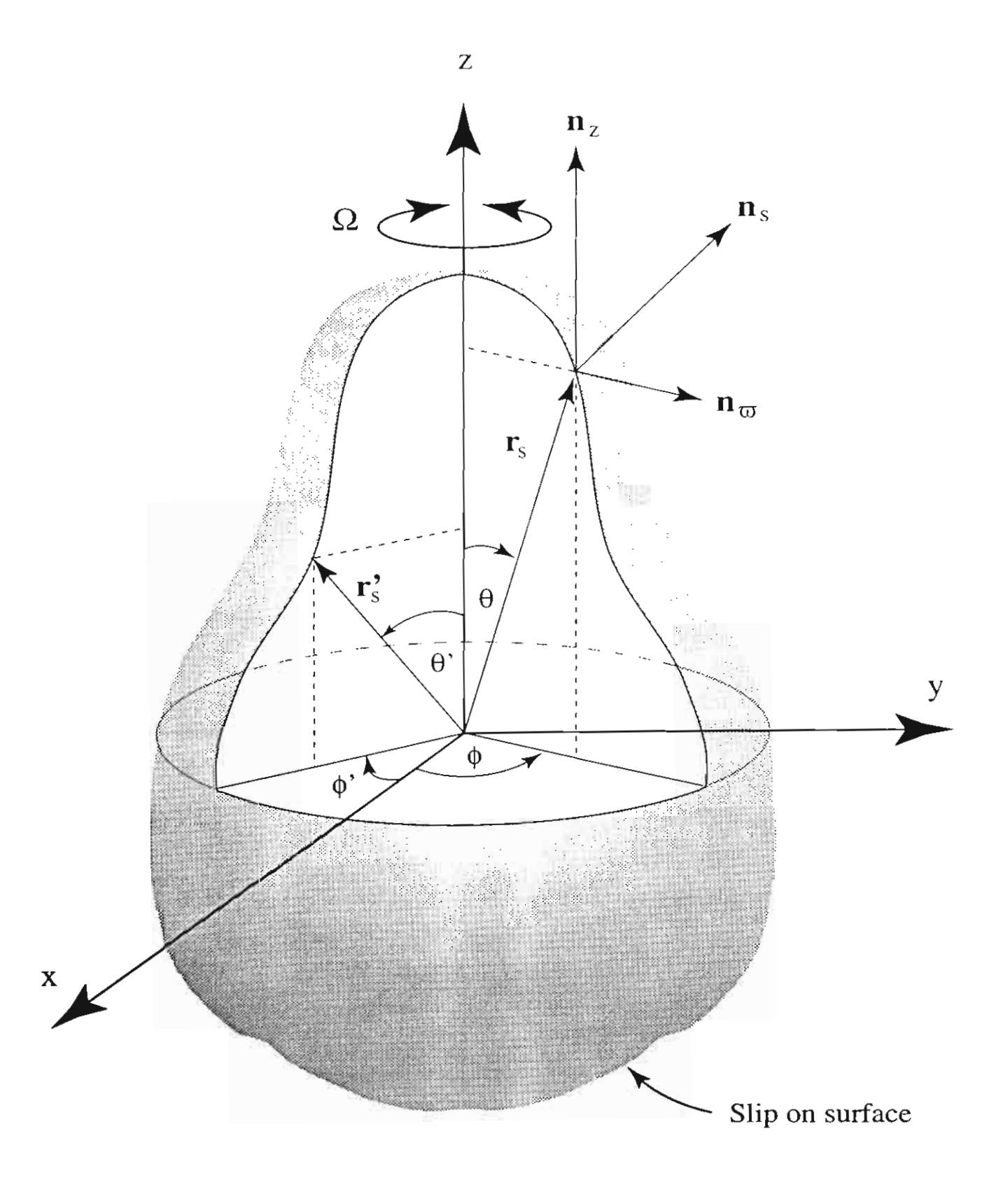


Figure 1. Tekasakul and Loyalka

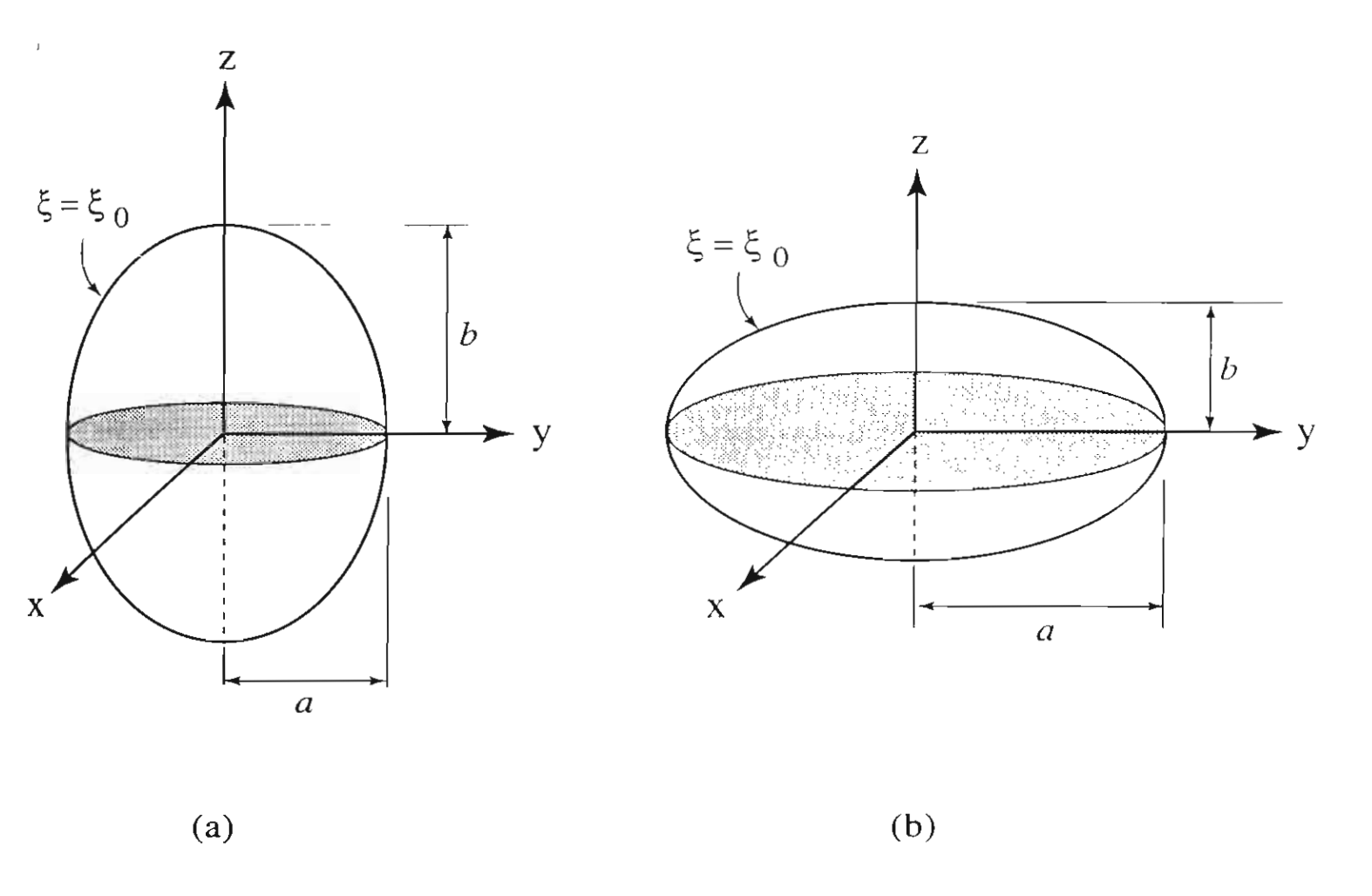


Figure 2. Tekasakul and Loyalka

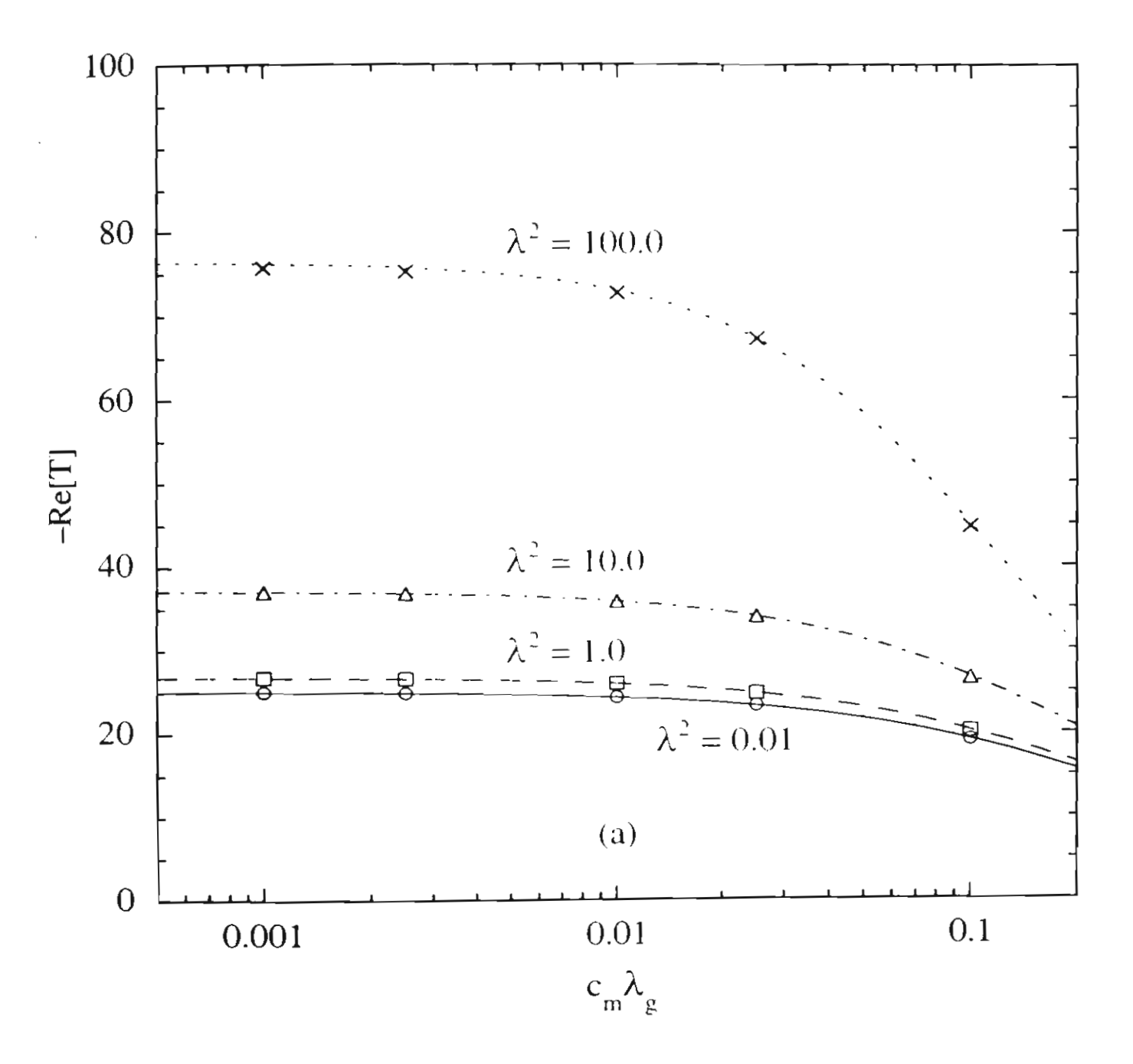


Figure 3(a). Tekasakul and Loyalka

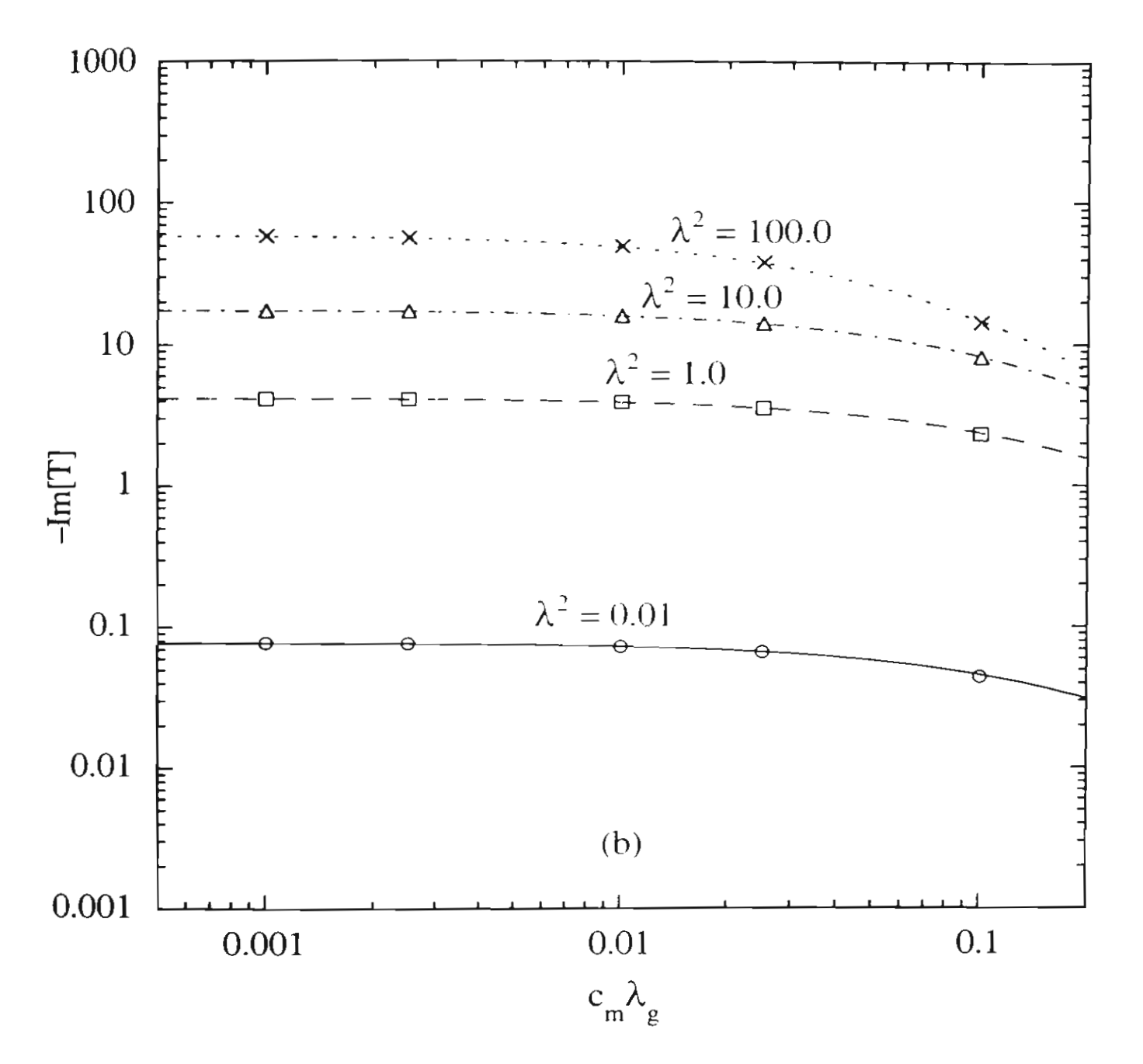


Figure 3(b). Tekasakul and Loyalka

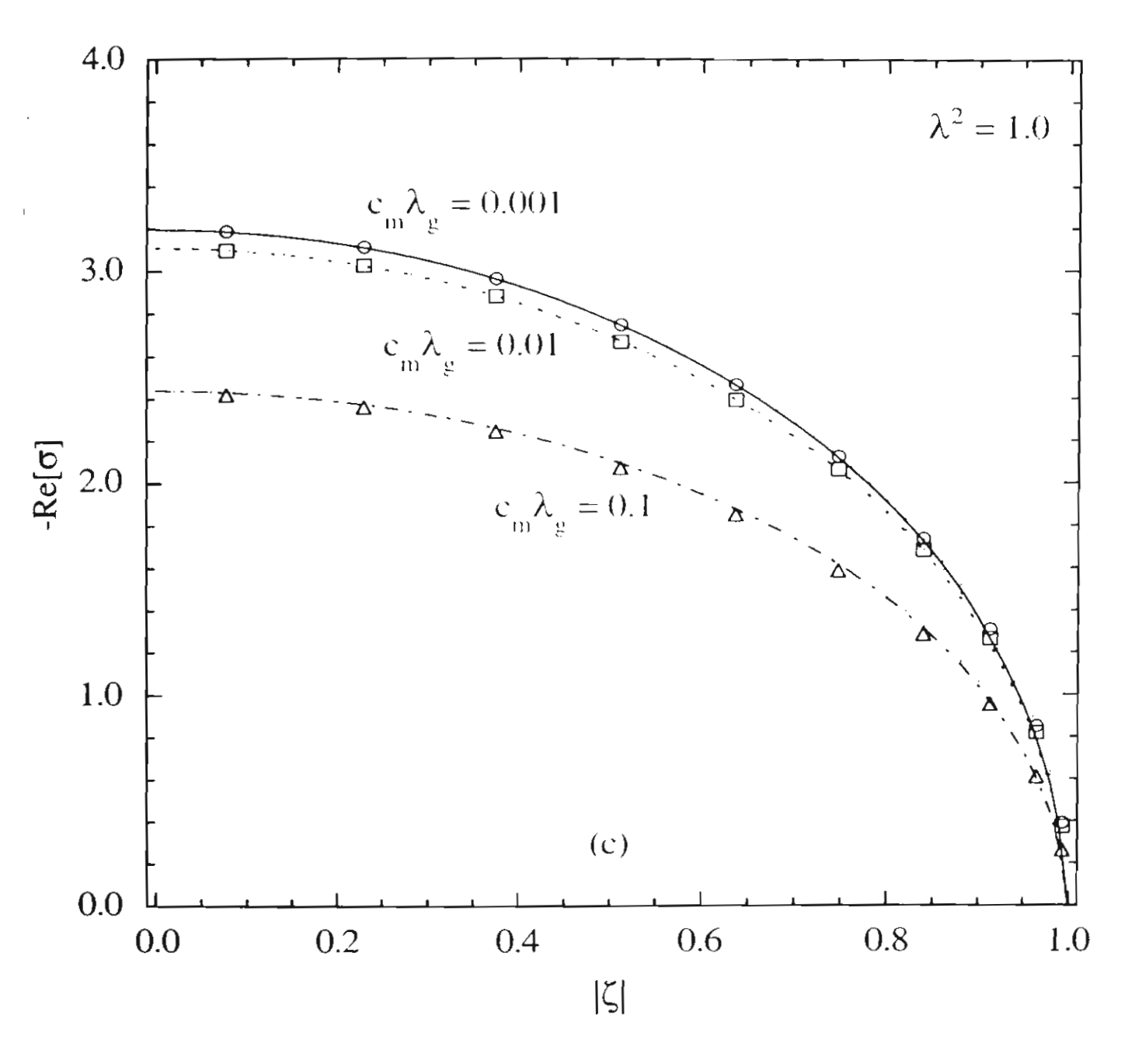


Figure 3(c). Tekasakul and Loyalka

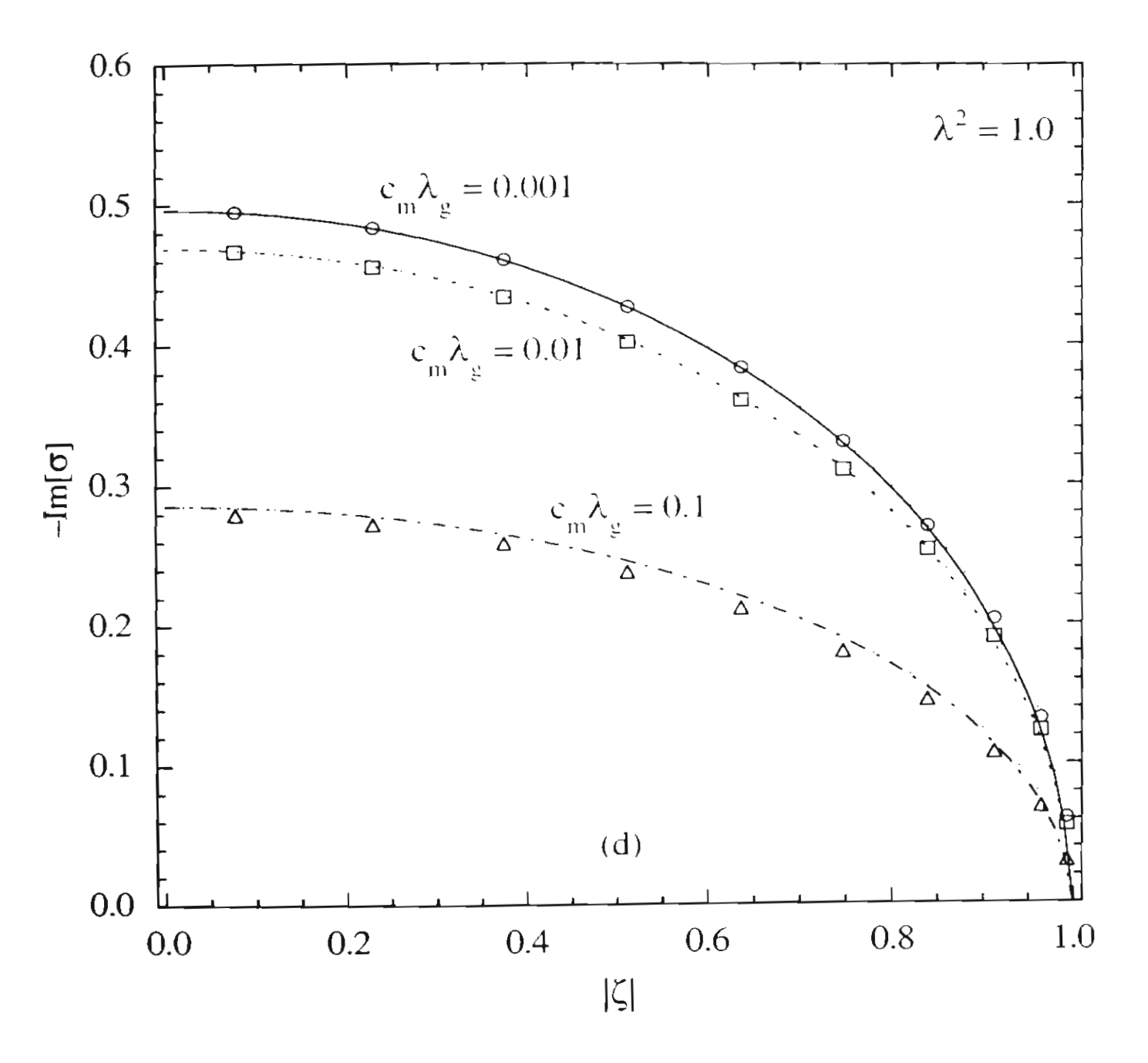


Figure 3(d). Tekasakul and Loyalka

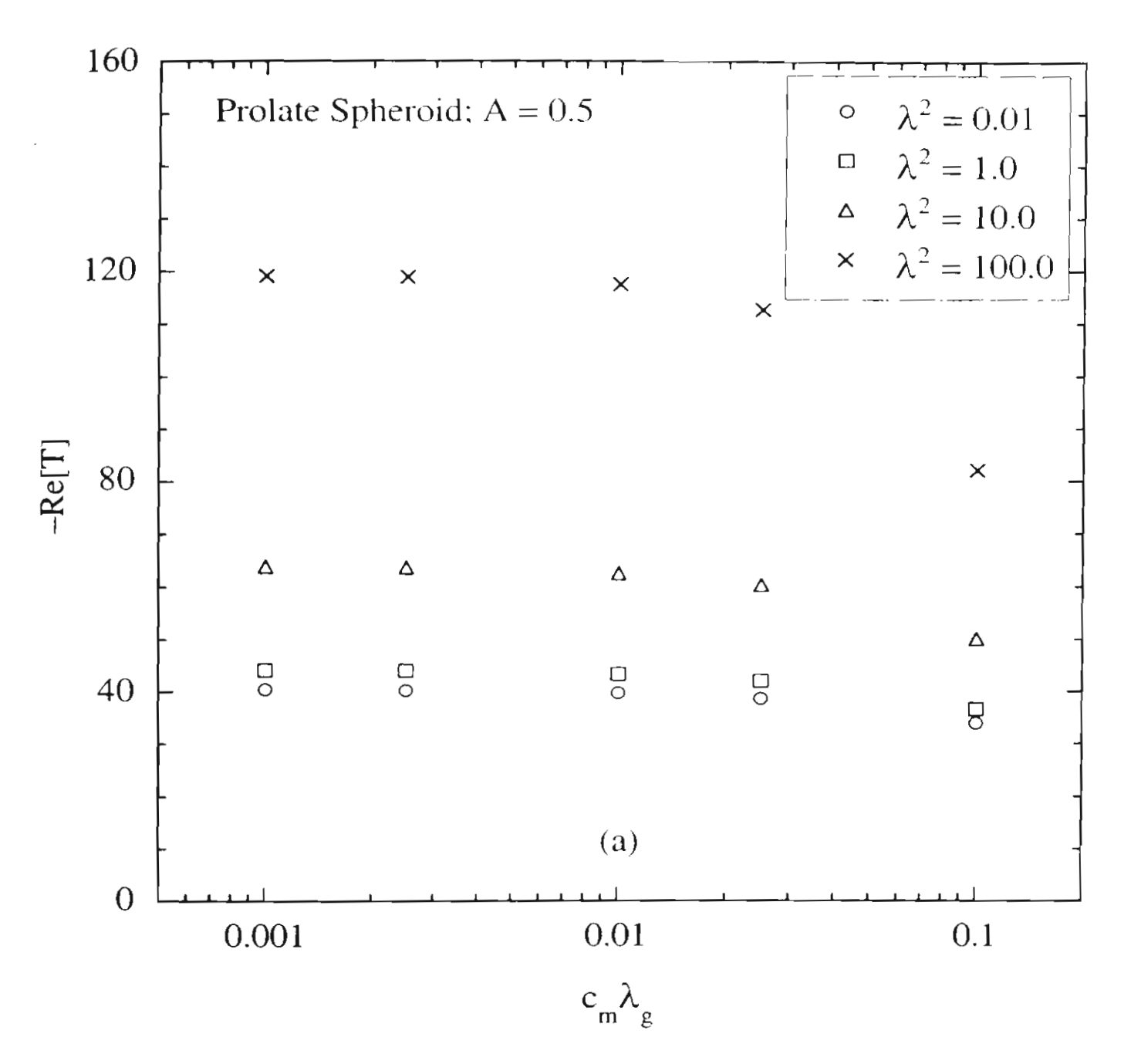


Figure 4(a). Tekasakul and Loyalka

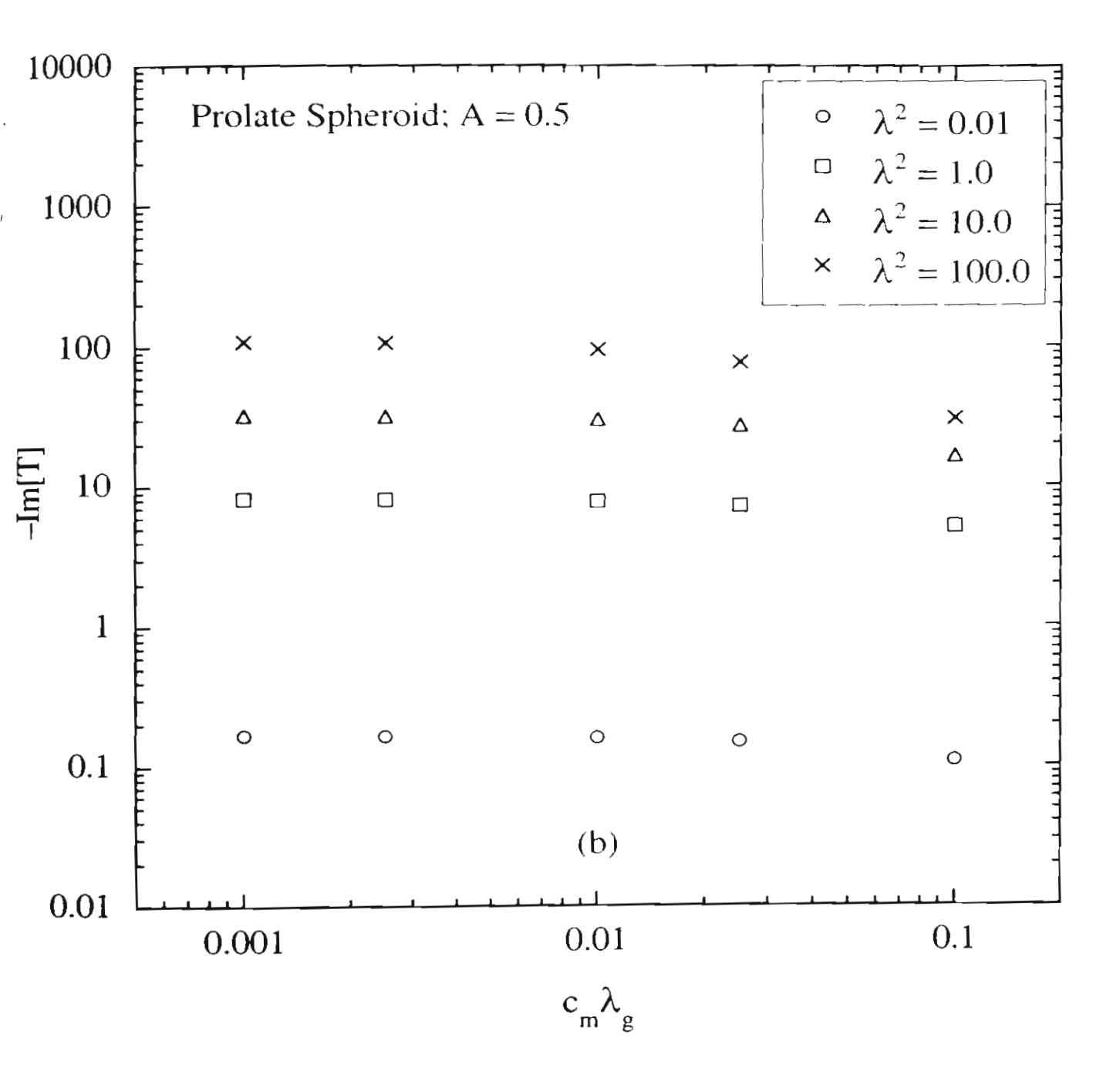


Figure 4(b). Tekasakul and Loyalka

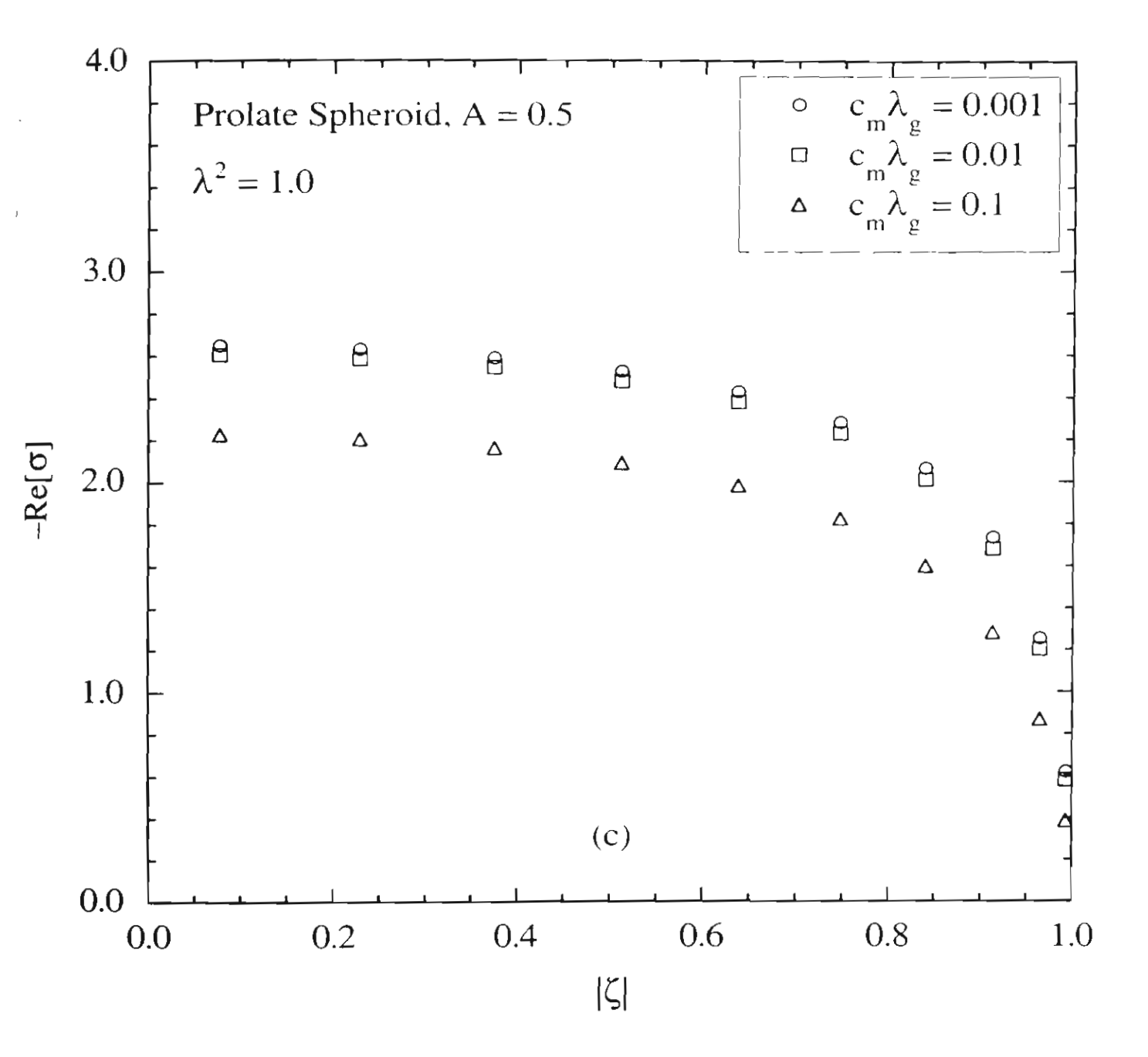


Figure 4(c). Tekasakul and Loyalka

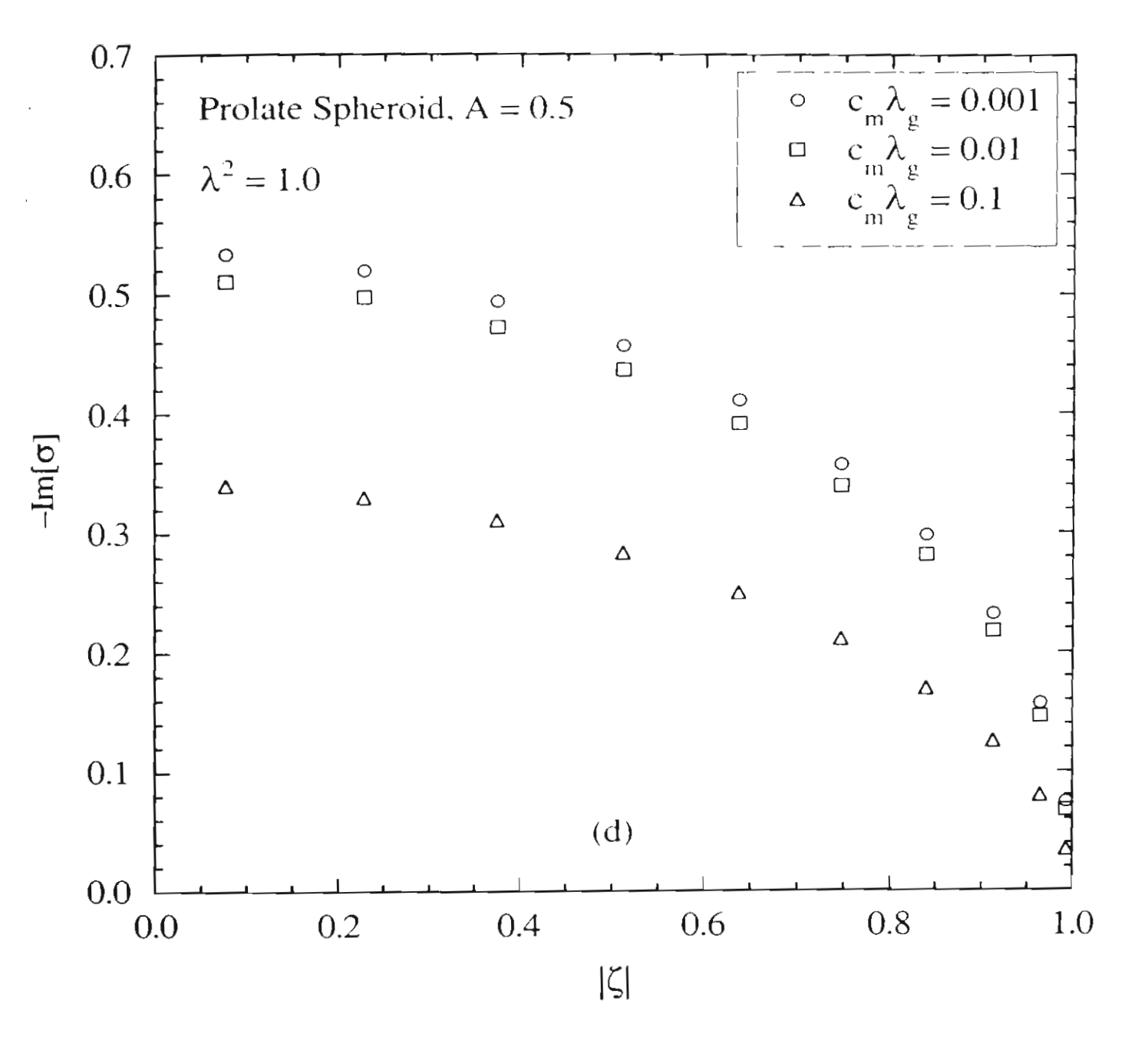


Figure 4(d). Tekasakul and Loyalka

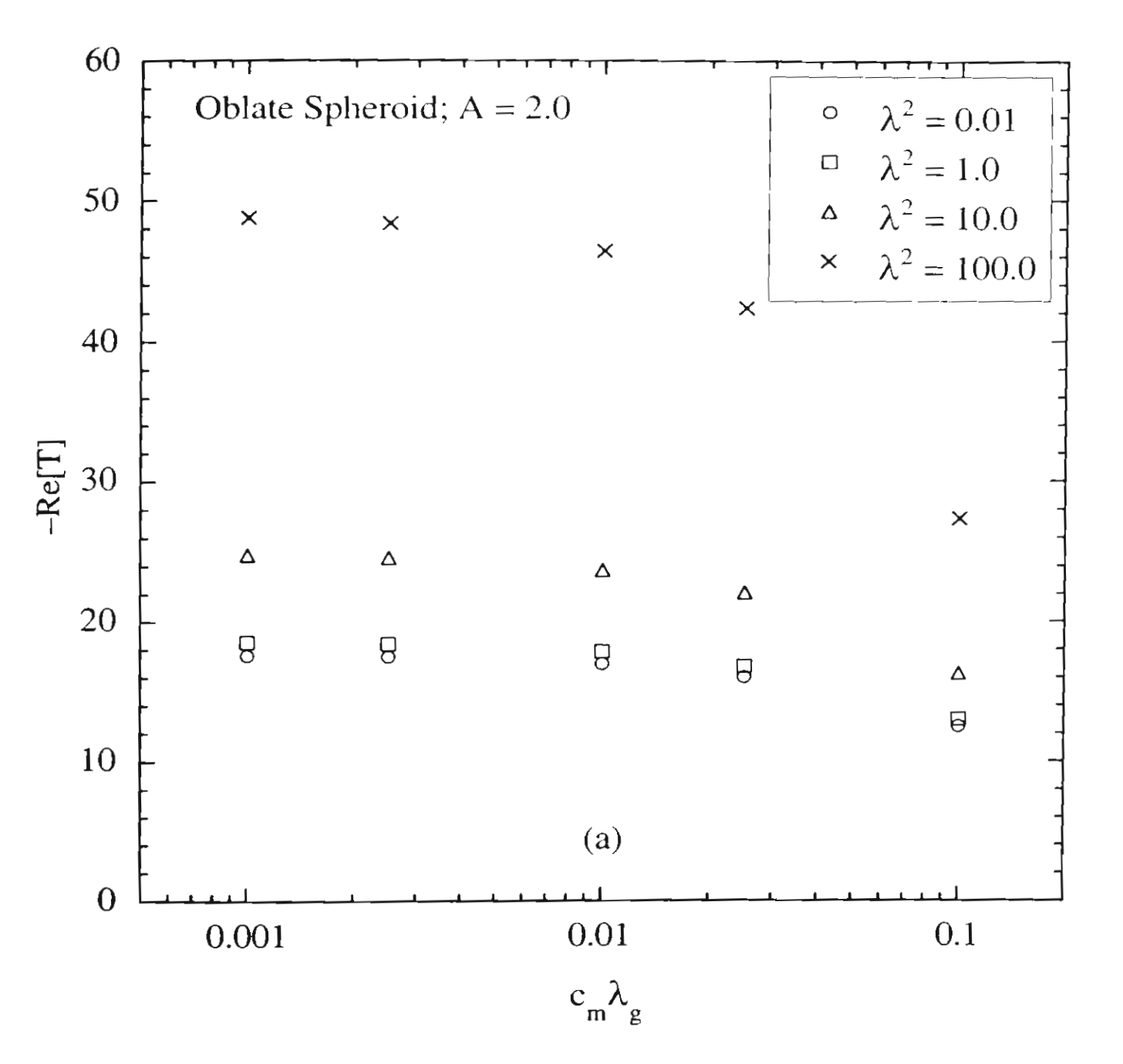


Figure 5(a). Tekasakul and Loyalka

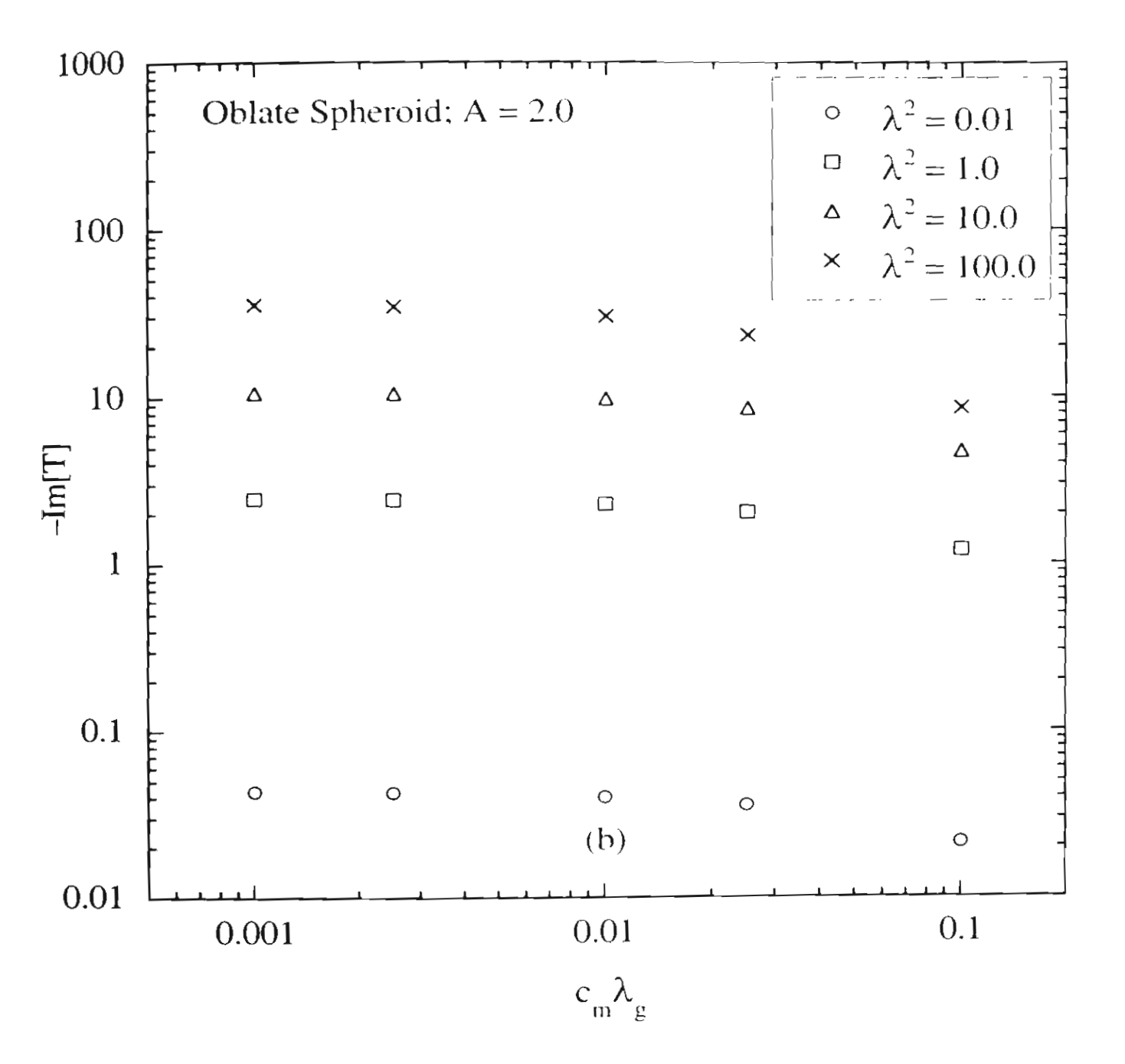


Figure 5(b). Tekasakul and Loyalka

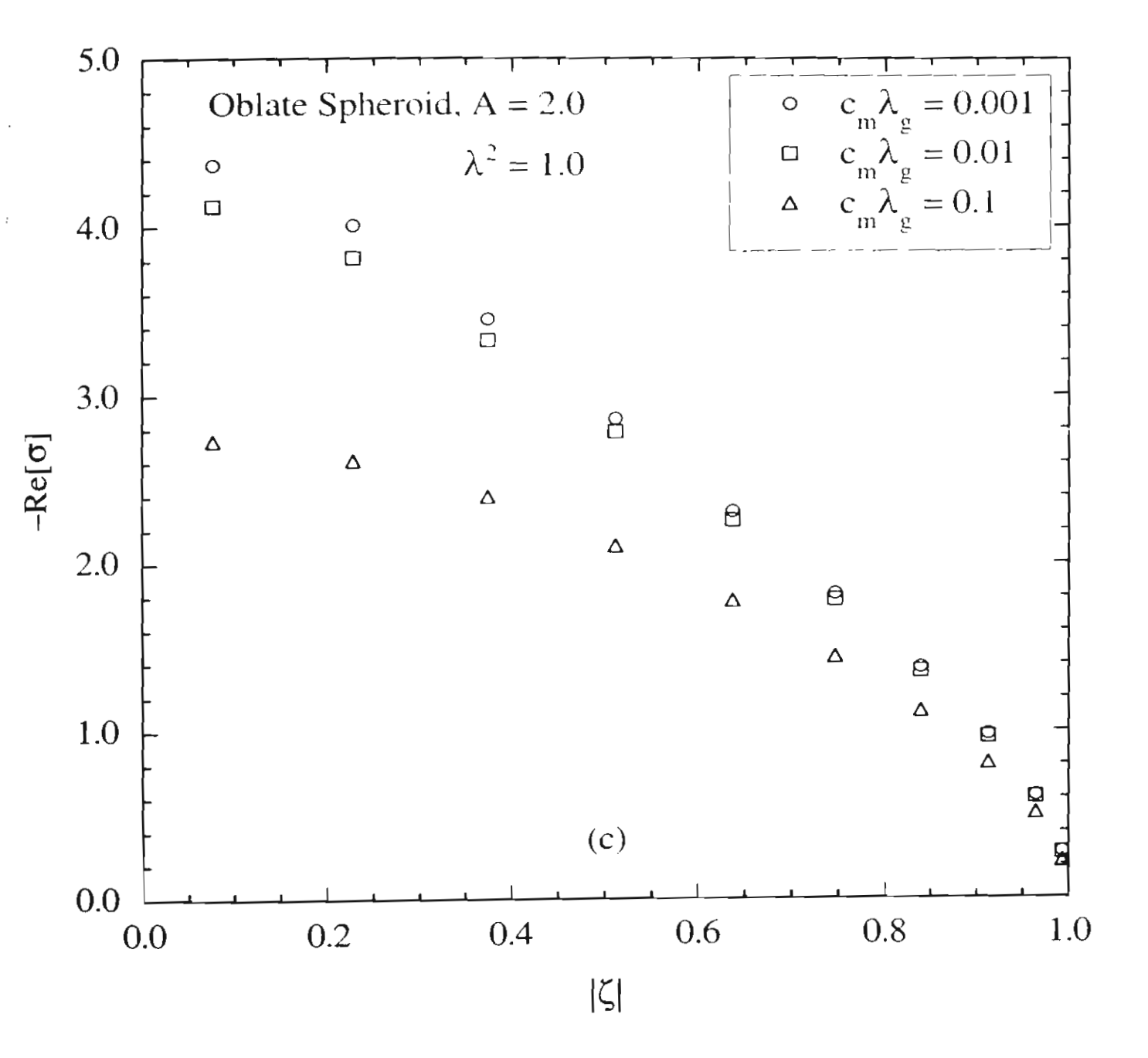


Figure 5(c). Tekasakul and Loyalka

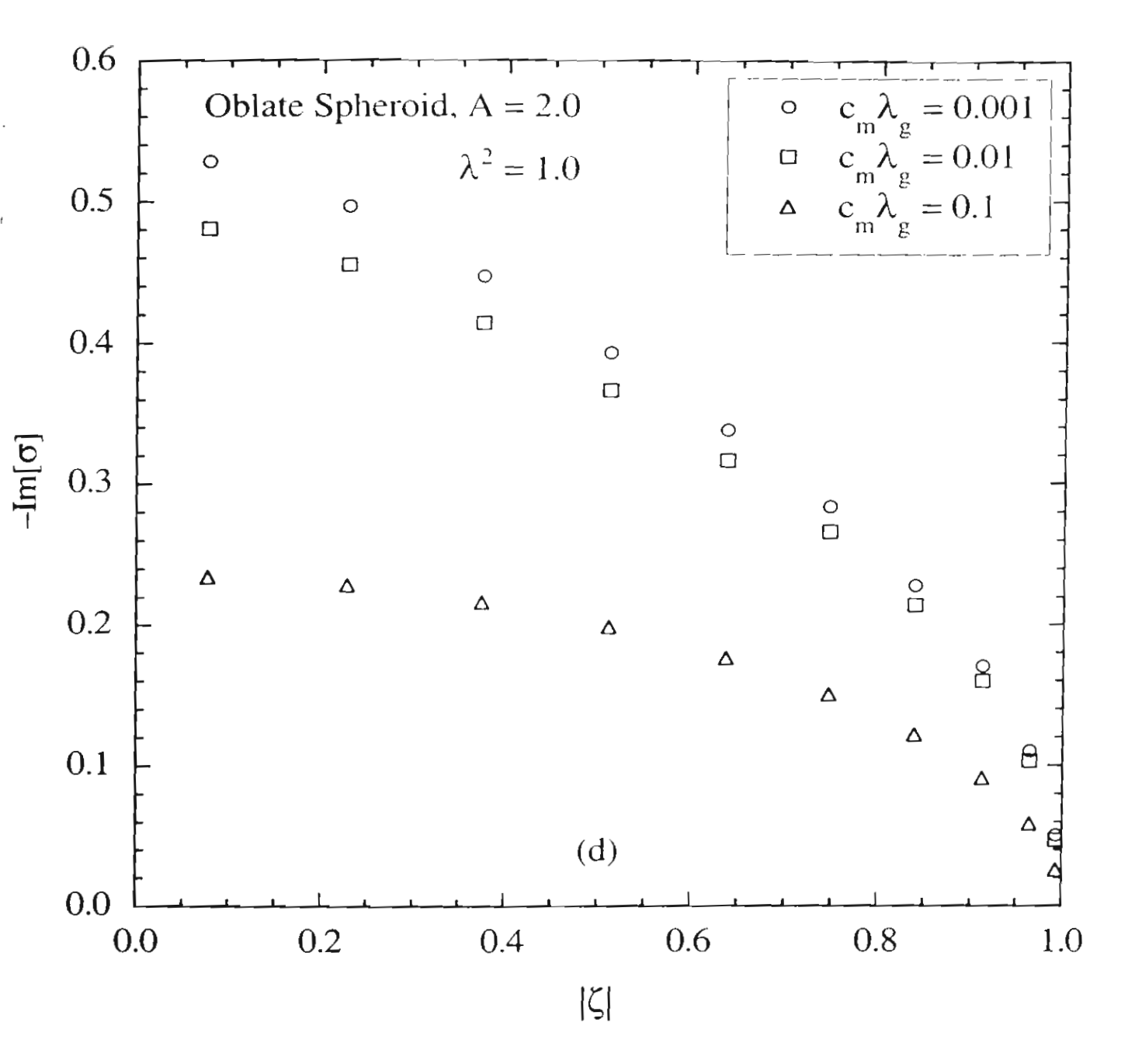


Figure 5(d). Tekasakul and Loyalka

Appendix C

Manuscript: Rotatory Oscillations of Axi-Symmetric Bodies in an Axi-Symmetric Viscous Flow with Slip: Numerical Solutions for Cylinders

Rotatory oscillations of axi-symmetric bodies in an axi-symmetric viscous flow with slip: Numerical solutions for cylinders

P. Tekasakul

Assistant Professor

Department of Mechanical Engineering

Faculty of Engineering

Thammasat University, Rangsit Campus

Klong Luang, Pathum Thani 12121, Thailand

(e-mail: tperapon@engr.tu.ac.th)

S. K. Loyalka

Curators' Professor and Director
Particulate Systems Research Center and
Nuclear, Chemical, and Mechanical & Aerospace Engineering Departments
University of Missouri-Columbia
Columbia, MO 65211, USA
(e-mail: loyalkas@missouri.edu)

Abstract -- Rotatory oscillations of cylindrical bodies in axi-symmetric viscous flows with slip are studied numerically using a technique based on the Green's function. This technique reduces the unsteady Stokes equation into a Helmholtz equation which is then converted to the Fredholm integral equation of the second kind. Gaussian quadratures were used to calculate local stresses at the nodal points and the torque on the body is then determined. Results have shown that no analytical or approximate solutions are sufficiently accurate to predict the torque and this can then result in erroneous evaluation of viscosity of a fluid using typical oscillating disk viscometer. Numerical results from this work should then lead to accurate prediction of viscosity if used with data obtained experimentally by an oscillating disk viscometer.

I. Introduction

The problems of rotatory oscillations of axi-symmetric bodies has been extensively studied. In the previous work (Tekasakul and Loyalka, 2000), oscillations of spheroidal bodies with the presence of slip on the body surfaces was studied. The results show influence of slip to the torques exerted on the bodies. This indicates that the viscosity of a fluid has been affected by the presence of the slip. In this paper, extension to such oscillations on cylindrical bodies will be investigated. The cylindrical disk has been widely used in the oscillating disk viscometer due to geometric simplicity.

The problem for the slow oscillation with small amplitude involves the solutions to the unsteady Stokes equations (Tekasakul, et al., 1998; and Zhang and Stone, 1998),

$$\lambda^2 \frac{\partial \mathbf{u}}{\partial \tau} = -\nabla p + \nabla^2 \mathbf{u} . \tag{1}$$

where $\lambda^2 = \omega a^2/v$ is the dimensionless frequency parameter. Here, a is the characteristic length of the body and ω is the frequency of oscillation.

After mathematical manipulations, the time-dependent, dimensionless, ϕ component velocity obtained from Eq. (1) reduces to the Helmholtz equation
(Tekasakul, et al.,1998):

$$\left(\nabla^2 + k^2\right) w = 0 \tag{2}$$

with the slip boundary condition at the surface,

$$w(\mathbf{r}_s) = \left[\varpi_s + \left(c_m \lambda_g\right) \sigma(\mathbf{r}_s)\right] \cos(\phi_s) \tag{3}$$

and the limiting condition of the fluid far away from the body,

$$\lim_{\mathbf{r} \to \infty} w(\mathbf{r}) = 0 \tag{4}$$

Here, $\lambda^2 = \omega a^2/v$ is the dimensionless frequency parameter, $k^2 = -i\lambda^2$ is the dimensionless complex-valued frequency parameter, and $w(\varpi, z, \phi) = u_{\phi}(\varpi, z) \cos(\phi)$. The dimensionless, time-independent local stress is defined as

$$\sigma(\zeta) = \varpi \frac{\partial}{\partial n} \left(\frac{u_{\bullet}}{\varpi} \right) \tag{5}$$

while the dimensionless, time-independent torque on the body can be evaluated from

$$T = 2\pi \int_{c} \varpi^{2} \, \sigma(\zeta) \, \mathrm{d}s \tag{6}$$

Here, ζ is a coordinate specifying a point on the meridian contour of the body for which $-1 \le \zeta \le 1$. Note that the dimensionless, time-independent torque has been nondimesionalized by $\Omega \mu a^3$ and the transient term $\exp(i\tau)$ has been dropped.

II. Analytical Expressions

Shah (1971) derived expressions for several body shapes including infinite cylindrical disk and infinitely long cylinder in terms of D(s) where s is the Laplace operator. The definition of D(s) is given as

$$D(s) = -\rho \frac{\delta^{5}}{I} s \iint \xi^{2} \frac{\partial \Omega}{\partial n} dS$$
 (7)

where $\delta = (v/\omega_0)^{V^2}$ is the boundary layer thickness, I is the moment of inertia of the body, ξ is the dimensionless radial coordinate (r/δ) , Ω is the dimensionless angular velocity, and S is the body surface area. By replacing s with $-k^2$, and using the definition of (Kestin and Wang, 1957),

$$m = \frac{\pi \rho \delta^5}{I} \xi_0^4$$

expression for torque can be obtained from

$$T = D\left(-k^2\right) \frac{\pi}{mk^2} \tag{8}$$

Note that in this paper, every length dimension is nondimensionalized by the body radius instead of boundary layer thickness as used by Shah (1971).

1. Infinite Cylindrical Disk

Shah (1971) obtained an expression for an infinitely large cylindrical disk oscillating with slip in an infinite fluid as

$$D(s) = \frac{ms^{3/2}}{1 + (c_m \lambda_g)s^{1/2}}$$

By using Eq. (9), we have an expression for torque which is applicable at high frequency:

$$T = -\frac{\pi(ik)}{1 + (c_m \lambda_g)(ik)} \tag{9}$$

Another approximation given by MacWood (1938) for an infinite disk with corrections for exterior fluid to the disk and edge friction is

$$T = -\pi \left\{ \frac{p + (c_m \lambda_g) - (4ik/A)(c_m \lambda_g)p}{1 + (c_m \lambda_g)^2 p^2 + 2(c_m \lambda_g)p} \right\}$$
(10)

where p = 2 + ik and A is the aspect ratio (radius/half-thickness) of the disk.

2. Infinitely Long Cylinder

as

The expression for an infinitely long cylinder was also obtained by Shah (1971)

$$D(s) = \frac{4}{A} m s^{3/2} \left[\frac{K_2(\xi_0 s^{1/2})}{K_1(\xi_0 s^{1/2}) + (c_m \lambda_g) s^{1/2} K_2(\xi_0 s^{1/2})} \right]$$

which can be converted to the torque:

$$T = -\frac{4}{A}\pi(ik)\left[\frac{K_2(ik)}{K_1(ik) + \left(c_m\lambda_g\right)(ik)K_2(ik)}\right]. \tag{11}$$

Equations (9) to (11) will be used to benchmark our numerical results for cylindrical bodies at both geometry extremes.

III. Numerical Procedure

The numerical method used in the present work is based on the Green's function approach (Tekasakul, et al., 1998; Tekasakul, et al., 1999; Tekasakul and Loyalka, 2000). The Green's function for this problem is defined by

$$(\nabla^2 + k^2)\psi(\mathbf{r}, \mathbf{r}') = -4\pi \,\delta(\mathbf{r} - \mathbf{r}')$$
(12)

such that

$$\psi(\mathbf{r}, \mathbf{r}') = \frac{\exp(-ik|\mathbf{r} - \mathbf{r}'|)}{|\mathbf{r} - \mathbf{r}'|}$$
(13)

Following the manipulation of Tekasakul and Loyalka (2000), the problem leads to the Fredholm integral equation of the second kind that contains singularities. Applying the singularity subtraction technique to the equation, it becomes

$$\left[g(\zeta) - 2\pi(c_m \lambda_g)\right]\sigma(\zeta) + \int L(\zeta, \zeta')\left[\sigma(\zeta') - \sigma(\zeta)\right]d\zeta' = -k^2\Psi(\zeta, \zeta') \tag{14}$$

where,

$$g(\zeta) = \int_{-1}^{1} L(\zeta, \zeta') d\zeta'$$
 (15)

$$L(\zeta,\zeta') = -f(\zeta')K(\zeta,\zeta') + (c_m\lambda_s)H(\zeta,\zeta')$$
(16)

The integrals in Eq. (14) are thus converted to summations by the use of Gaussian quadratures and Eq. (33) is then reduced to a system of linear algebraic equations by applying collocation at the nodal points of the quadrature. The local stress, $\sigma(\zeta)$, is determined at each nodal point and the torque is finally determined from Eq. (6).

There are several components in above equations that require simplification for different geometrical bodies.

The parameter f in Eq. (16), for a cylinder, can be determined from

$$f = 1 + \frac{\left(c_{m}\lambda_{g}\right)}{\varpi'_{s}} \frac{\partial \varpi'_{s}}{\partial n'_{s}} \tag{17}$$

Surface of a cylinder can be divided into three separate surfaces; bottom, side and top surfaces. The parameter f for all three cylinder surfaces are then

$$f = \begin{cases} 1 & \text{top surface} \\ 1 + c_m \lambda_g & \text{side surface} \end{cases}$$

$$\begin{cases} 1 & \text{bottom surface} \end{cases}$$
(18)

The expression of K in Eq. (16) was obtained by Tekasakul, et al. (1998):

$$K(\zeta, \zeta') = \frac{J_s'}{\cos(\phi)} \int \psi(\mathbf{r}_s, \mathbf{r}_s') \cos(\phi') d\phi'$$
$$= K_L(\zeta, \zeta') + K_H(\zeta, \zeta')$$
(19)

where,

$$K_L(\zeta,\zeta') = \frac{J_s'}{\cos(\phi)} \int \frac{\cos(\phi')}{|\mathbf{r}_s' - \mathbf{r}_s|} d\phi' = \frac{2J_s'}{\sqrt{\varpi_s \varpi_s'}} Q_{1/2}(\gamma)$$
 (20)

and

$$K_{H}(\zeta,\zeta') = \frac{J_{s}'}{\cos(\phi)} \int \frac{\exp(-ik|\mathbf{r}_{s}'-\mathbf{r}_{s}|) - 1}{|\mathbf{r}_{s}'-\mathbf{r}_{s}|} \cos(\phi') d\phi'$$

$$= \frac{J_{s}'}{\cos(\phi)} \int_{0}^{2\pi} \frac{\exp(-ik[2\varpi_{s}\varpi_{s}'(\gamma - \cos(\phi - \phi'))]^{1/2}) - 1}{[2\varpi_{s}\varpi_{s}'(\gamma - \cos(\phi - \phi'))]^{1/2}} \cos(\phi') d\phi' \quad (21)$$

Here, $Q_{1/2}(\gamma)$ is an Associated Legendre function of fractional order with the argument

$$\gamma = 1 + \frac{\beta}{2\varpi_{\bullet}\varpi'_{\bullet}}$$

in which

$$\beta = (\varpi_s' - \varpi_s)^2 + (z_s' - z_s)^2$$

The expression of H in Eq. (16) can be written as

$$H = \frac{J_s'}{\cos(\phi)} \left[\int \frac{\partial \psi(\mathbf{r}_s, \mathbf{r}_s')}{\partial n_s'} \cos(\phi_s') d\phi_s' \right]$$
(22)

Since,

$$\psi(\mathbf{r}_s, \mathbf{r}_s') = \frac{\exp(-i\,k\,t)}{t}$$

where $t = |\mathbf{r}_s - \mathbf{r}'_s|$. Therefore,

$$\frac{\partial \psi(\mathbf{r}_{s}, \mathbf{r}'_{s})}{\partial n'_{s}} = (1 + ikt) \exp(-ikt) \frac{\partial}{\partial n'} \left(\frac{1}{t}\right)$$

$$= (1 + ikt) \exp(-ikt) \left(-\frac{(\mathbf{r}'_{s} - \mathbf{r}_{s}) \cdot \mathbf{n}'_{outward}}{|\mathbf{r}_{s} - \mathbf{r}'_{s}|^{3}}\right) \tag{23}$$

For a cylinder,

$$H = \frac{\overline{\omega}_{s}'}{\cos(\phi)} \left[\int (1 + ikt) \exp(-ikt) \frac{\partial}{\partial n'} \left(\frac{1}{t} \right) \cos(\phi') d\phi' \right]$$
 (25)

in which

$$\frac{\partial}{\partial n'} \left(\frac{1}{t} \right) = -\frac{\left(\mathbf{r}'_{s} - \mathbf{r}_{s} \right) \cdot \mathbf{n}'_{outward}}{\left| \mathbf{r}_{s} - \mathbf{r}'_{s} \right|^{3}} ,$$

$$= -\left\{ \frac{\left(z'_{s} - z_{s} \right)}{\left[2\varpi_{s}\varpi' \left(\gamma - \cos(\phi - \phi') \right) \right]^{3/2}} ; \text{ bottom surface} \right.$$

$$= -\left\{ \frac{\varpi'_{s} - \varpi_{s} \cos(\phi - \phi')}{\left[2\varpi_{s}\varpi' \left(\gamma - \cos(\phi - \phi') \right) \right]^{3/2}} ; \text{ side surface} \right.$$

$$\frac{\left(z'_{s} - z_{s} \right)}{\left[2\varpi_{s}\varpi' \left(\gamma - \cos(\phi - \phi') \right) \right]^{3/2}} ; \text{ top surface}$$

For a cylinder, an expression for Ψ in Eq. (14) can be calculated from

$$\Psi(\zeta)\cos(\phi) = -\frac{4\pi}{k^2} \left(\varpi_s \cos(\phi)\right) - \int_{\substack{\text{inside} \\ \text{body}}} \frac{\exp(-i k |\mathbf{r}' - \mathbf{r}_s|)}{|\mathbf{r}' - \mathbf{r}_s|} \varpi' \cos(\phi') d\mathbf{r}'$$

$$= -\frac{4\pi}{k^2} \left[\varpi_s \cos(\phi)\right]$$

$$-\int_{-(AR)^{-1}}^{(AR)^{-1}} \frac{2\pi}{0} d\phi' \int_{0}^{1} d\varpi' \frac{\exp(-i k \left[2\varpi_s \varpi'_s (\gamma - \cos(\phi - \phi'))\right]^{1/2})}{\left[2\varpi_s \varpi'_s (\gamma - \cos(\phi - \phi'))\right]^{1/2}} \varpi'^2 \cos(\phi') \quad (26)$$

VI. Torques on cylinders

Torque on a cylinder is of great importance in operation of an oscillating disk viscometer since it can be used to predict the viscosity of the fluid surrounding the disk under periodic oscillation. Accuracy of viscosity measurement lies heavily on the evaluation of the torque. The thin disk is generally used in the oscillating disk

viscometer but torque on the disk were typically approximated and some accuracy was sacrificed. No exact analytical solution for an oscillating disk is obtained for a widerange frequency. Some expressions were derived but with limitation of applications in an extreme frequency and geometries (MacWood, 1938 and Shah, 1971). We thus have used the outlined numerical scheme to calculate exact values of the torques on several cylinders with different aspect ratio, ranging from a thin disk with large aspect ratio to a long cylinder that has a small aspect ratio. In this work, the presence of slip, where the velocity of the fluid adjacent to the surface of the body does not match the velocity of the body itself, has been included.

Results for a reasonably thin disk (A = 200) are shown in Figs. (1) to (3). Numerical results for a thin oblate spheroid with identical aspect ratio and approximate results from MacWood (1938) and Shah (1971) are also shown for comparison. Agreement between the real parts of torque for a disk using the number of Gaussian quadrature, $N_{\text{top}}: N_{\text{side}}: N_{\text{bottom}} = 25:2:25$ and an oblate spheroid using the number of Gaussian quadrature, N = 30 is reasonably well with maximum deviation of about 5% as expected. This was previously confirmed by Tekasakul et al. (1998) for the no-slip case as the solution for a thin disk can be reasonably approximated by the oblate spheroid of the same aspect ratio. The imaginary parts of the torque [Figs. 1(b) - 3(b)] are the out-of-phase component and play no significant role but the results are also shown for comparison and completeness purpose. The values obtained from MacWood's expression agree quite well with the disk results for high frequency limit $(\lambda^2 = 1000.0)$ with error less than 10% as show in Fig. 1a. The high-frequency approximation results obtained from Shah's expression also agree well (10%) with the numerical results at this limit. Both expressions are, however, give poor results at lower frequencies with error as high as 100% [Figs. 2(a) and 3(a)]. The MacWood's expression yields better results but still not sufficiently good. It has been shown that no analytical expression is good for entire range of oscillation frequency. To predict a good value of viscosity by using an oscillating disk viscometer then requires a numerical calculation of the torque exerted on the disk by a fluid. The presence of slip

has lowered the value of the torque and the influence of the slip is increasingly so at a higher oscillation frequency.

Numerical results for a long cylinder (A = 0.02) using $N_{\text{top}}: N_{\text{side}}: N_{\text{bottom}} = 2:30:2$ are shown in Fig. 4 along with values obtained analytically from Shah's expression for $\lambda^2 = 10^{-6}$, 0.1. The values of $\lambda^2 = 0.1$ is considered high frequency since the nondimensionalized length is the radius of the cylinder which is considerably low for a long cylinder compared with the thin disk of comparable size. The agreement is very good (1%) for the real parts of the torque as shown in Fig. 4(a) while the error for imaginary parts is as high as 50%.

Numerical values of the torques on typical finite cylinders are shown in Fig. 5 for A = 2.0 and in Fig. 6 for A = 10.0. In both case, the number of Gaussian quadrature used is $N_{\text{top}}: N_{\text{side}}: N_{\text{bottom}} = 25:15:25$. The influence of slip is the same as in the previous cases of a thin disk and a long cylinder and also the spheroids (Tekasakul and Loyalka, 2000). For the case of a cylinder with A = 2.0, when the slip $\left(c_m \lambda_s\right)$ increases from 0.0 (no slip) to 0.1 the torque (real part) decreases about 23% for $\lambda^2 = 0.01$ and about 40% for $\lambda^2 = 100.0$. The decreases for a cylinder with A = 10.0 are about 28% and 32%, respectively.

Unfortunately, there is no experimental data for an oscillating disk viscometer that can be used for comparison purpose. It has been known that the viscosity is weakly dependent on the pressure. For the case where slip is significant, the pressure must be reasonably low and, from our results, we have shown that the slip has influenced the torque which, in turn, affects the value of the viscosity.

V. Conclusion

Accurate values for torques on various cylindrical bodies were obtained numerically using the Green's function technique to reduce the dimensionality of the problem. Existing analytical expressions are reasonably good only in some cases but are largely erroneous. Both MacWood's and Shah's expressions for a thin disk are applicable only at high frequency ($\lambda^2 \ge 1000.0$) below that the errors are quite large. The results of a flat oblate spheroid agree well with those of the thin disk with identical

aspect ratio, as expected. Shah's expression for a long cylinder, however, yields a fair agreement with numerical results. Numerical results for all cylinders show similar influence of the slip to the torque. That is the torque is reduced by the presence of slip and its influence is larger at a higher frequency. The results for torques on cylindrical bodies can be used together with oscillating disk viscometers to predict more accurate values of viscosity of fluids in the slip flow regime.

This work has completed the problem of axi-symmetric bodies undergoing slow rotatory oscillations about their axes of symmetry in unbounded viscous fluids with slip. Tekasakul, et al. (1998) investigated the problem of axi-symmetric bodies in continuum flow regime while the recent work (Tekasakul, 2000) was to study the problem of spheroidal bodies in slip flow regime. The future work involves the problem in bounded environment, for instance, a sphere oscillating inside a sphere, a spheroid oscillating inside a spheroid, and a cylinder oscillating inside a cylinder, with the outside bodies are generally stationary. The setup of cylinder and cylinder is also used in an oscillating disk viscometer as well as the cylindrical disk in an infinite fluid.

Acknowledgment

This research was carried out with the financial support from the Thailand Research Fund (TRF) through grant PDF/32/2541.

References

Loyalka, S. K., 1990, "Slip and jump coefficients for rarefied gas flows: variational results for Lennard-Jones and n(r)-6 potential," *Physica A*, Vol. 163, pp. 813-821.

Loyalka, S. K., 1996, "Theory of the spinning rotor gauge in the slip regime," Journal of Vacuum Science and Technology A, Vol. 14, pp. 2940-2945.

Loyalka, S. K., and Griffin, J. L., 1994, "Rotation of non-spherical axisymmetric particles in the slip regime," *Journal of Aerosol Science*, Vol. 25, pp. 509-525.

MacWood, G. E., 1938, "The theory of the measurement of viscosity and slip of fluids by the oscillating disc method, part II," *Physica*, Vol. 5, pp. 763-768.

Shah, V. L., 1971, "Theory of the oscillating viscometer for slip flow," *Journal of Applied Mechanics*, Vol. 38, pp. 659-664.

Tekasakul, P., and Loyalka, S. K., 2000, "Rotatory oscillations of axisymmetric bodies in an axi-symmetric viscous flow: Numerical solutions for sphere and spheroids," submitted to *Journal of Fluids Engineering*.

Tekasakul, P., Tompson, R. V., and Loyalka, S. K., 1998, "Rotatory oscillations of arbitrary axi-symmetric bodies in an axi-symmetric viscous flow: Numerical solutions," *Physics of Fluids*, Vol. 10, pp. 2797-2818.

Zhang, W., and Stone, H. A., 1998, "Oscillatory motions of circular disks and near spheres in viscous flows," *Journal of Fluid Mechanics*, Vol. 367, pp. 329-358.

FIGURE CAPTIONS

- Figure 1. A comparison of numerically calculated torques on a thin cylindrical disk and a flat oblate spheroid both with A=200 for $\lambda^2=1000.0$ with the corresponding values determined from Eqs. (9) and (10). (a) The real parts. (b) The imaginary parts. The number of Gaussian quadrature points used in each numerical calculation was $52 (N_{\text{top}}: N_{\text{side}}: N_{\text{bottom}} = 25:2:25)$ for the thin cylindrical disk and 30 for the oblate spheroid. Here, N_{top} , N_{side} , and N_{bottom} represent the number of Gaussian quadrature points on the top, side, and bottom surfaces of the cylindrical disk, respectively. Here, $\lambda^2 = \omega a^2/v$ is the dimensionless frequency parameter.
- Figure 2. A comparison of numerically calculated torques on a thin cylindrical disk and a flat oblate spheroid both with A = 200 for $\lambda^2 = 10.0$ with the corresponding values determined from Eqs. (9) and (10). (a) The real parts. (b) The imaginary parts. The number of Gaussian quadrature points used in each numerical calculation was $52 (N_{top}: N_{side}: N_{bottom} = 25:2:25)$ for the thin cylindrical disk and 30 for the oblate spheroid.
- Figure 3. A comparison of numerically calculated torques on a thin cylindrical disk and a flat oblate spheroid both with A = 200 for $\lambda^2 = 0.1$ with the corresponding values determined from Eqs. (9) and (10). (a) The real parts. (b) The imaginary parts. The number of Gaussian quadrature points used in each numerical calculation was $52 (N_{\text{top}}: N_{\text{side}}: N_{\text{bottom}} = 25:2:25)$ for the thin cylindrical disk and 30 for the oblate spheroid.
- Figure 4. A comparison of numerically calculated torques on a thin cylindrical disk with A = 0.02 for $\lambda^2 = 10^{-6}$ and 0.1 with the corresponding values determined from Eq. (11). (a) The real parts. (b) The imaginary parts. The number of Gaussian quadrature points used in each numerical calculation was 34 (N_{too} : N_{side} : $N_{\text{bottom}} = 2:30:2$).
- Figure 5. Numerical results for torques on a typical finite cylinder with A = 2.0. (a) The real parts. (b) The imaginary parts. The number of Gaussian quadrature points used in each numerical calculation was 65 (N_{top} : N_{side} : $N_{\text{bottom}} = 25:15:25$).

Figure 6. Numerical results for torques on a typical finite cylinder with A = 10.0. (a) The real parts. (b) The imaginary parts. The number of Gaussian quadrature points used in each numerical calculation was 65 (N_{top} : N_{side} : $N_{\text{bottom}} = 25:15:25$).

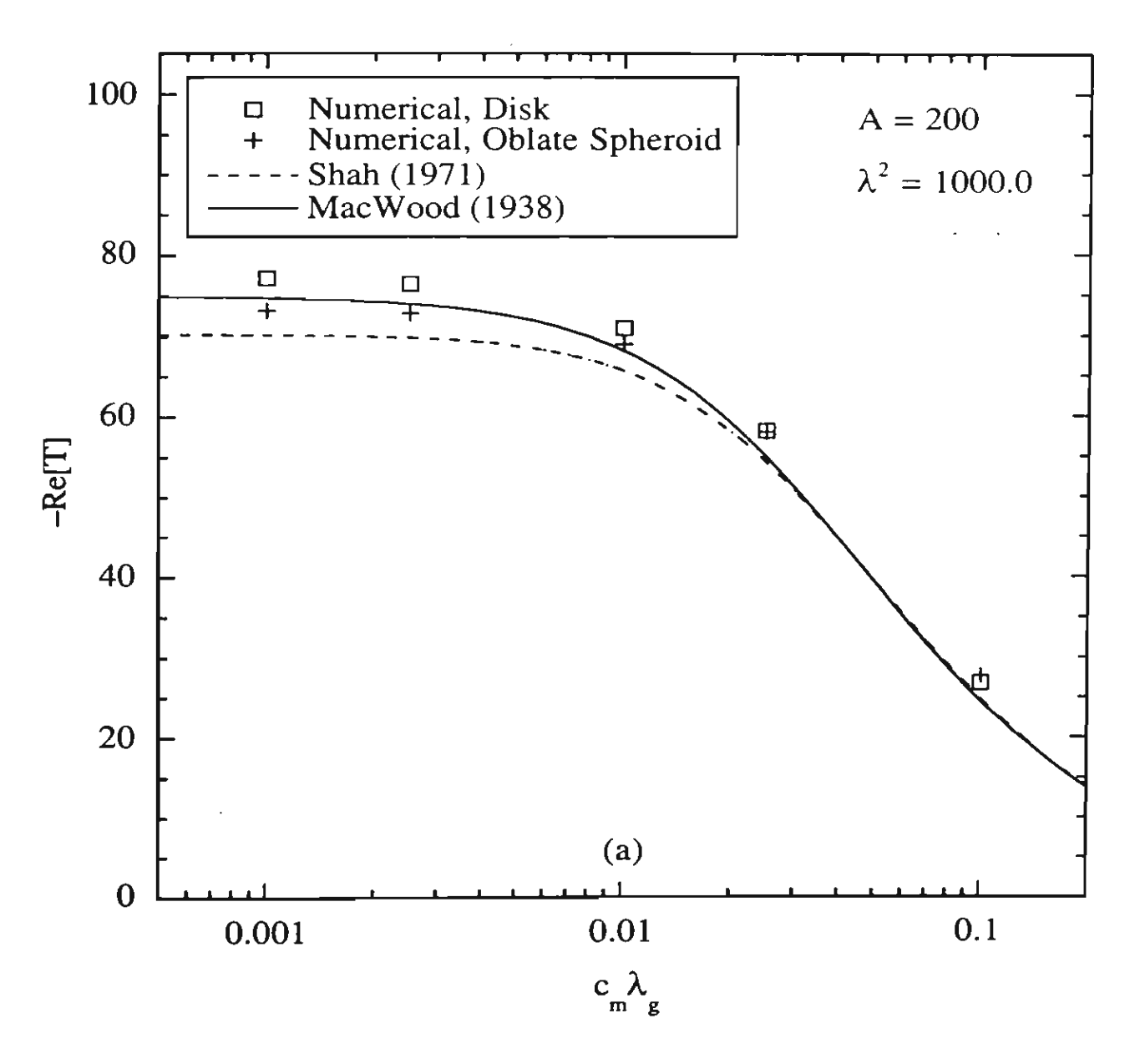


Figure 1(a). Tekasakul and Loyalka

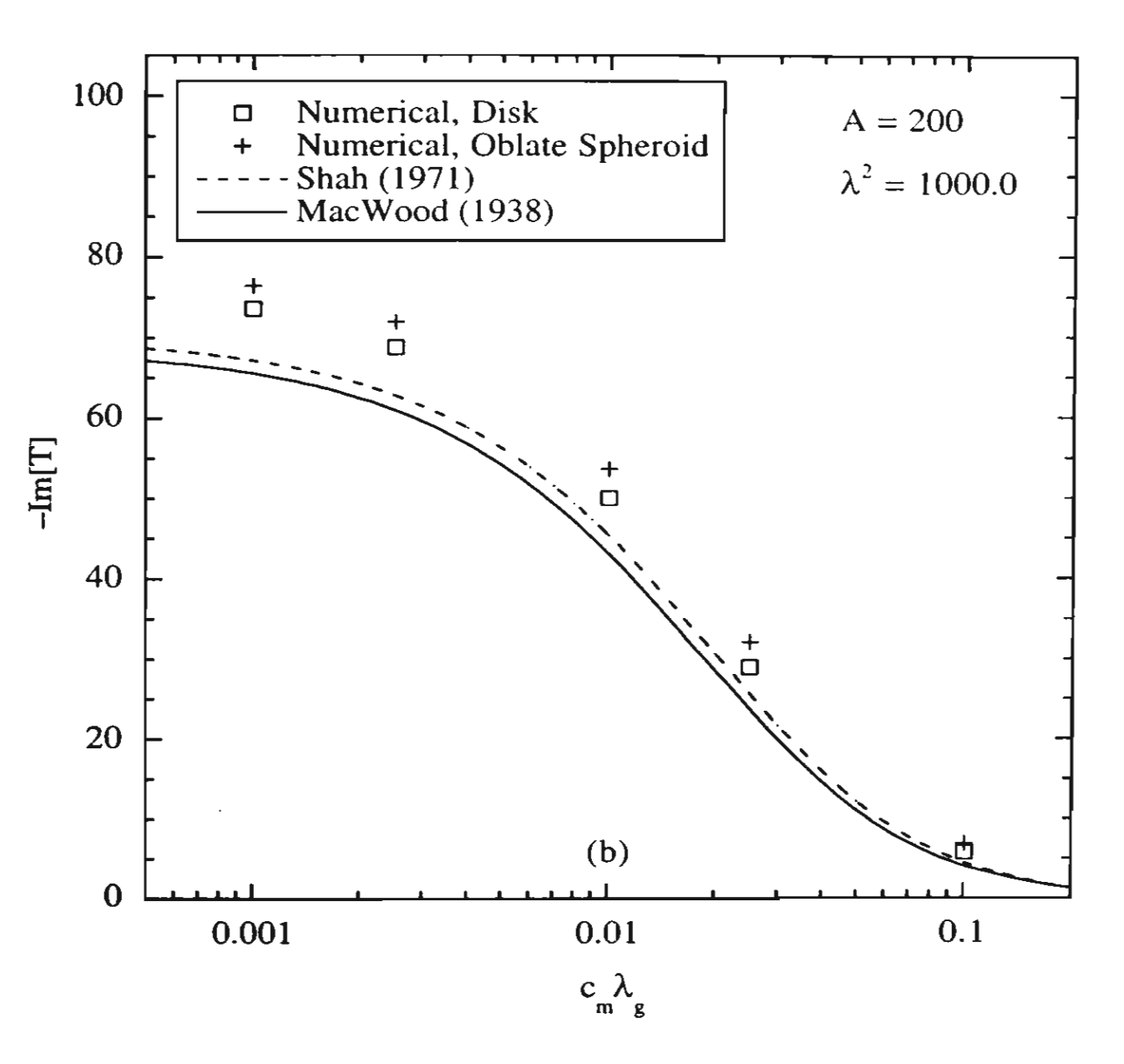


Figure 1(b). Tekasakul and Loyalka

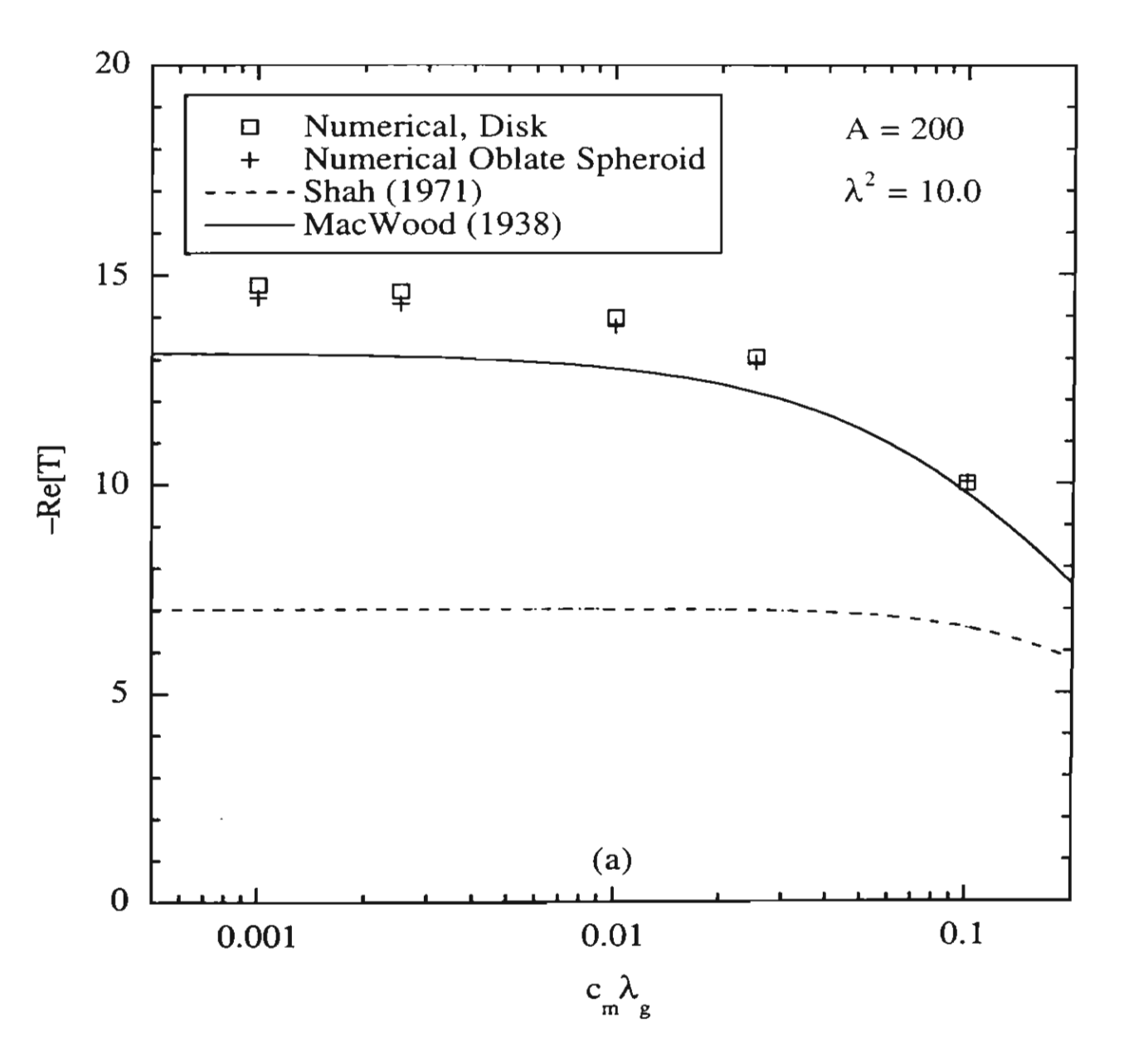


Figure 2(a). Tekasakul and Loyalka

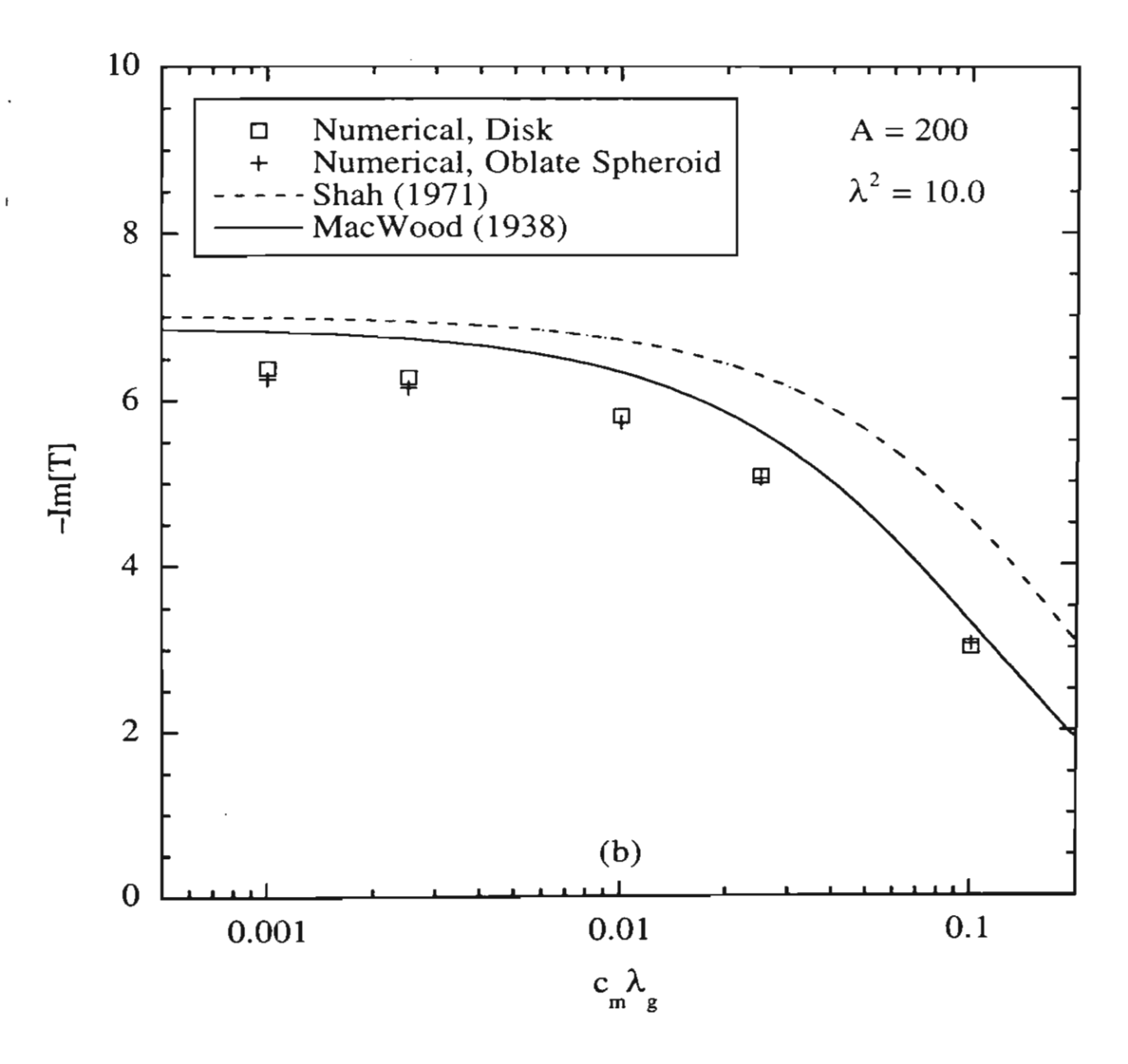


Figure 2(b). Tekasakul and Loyalka

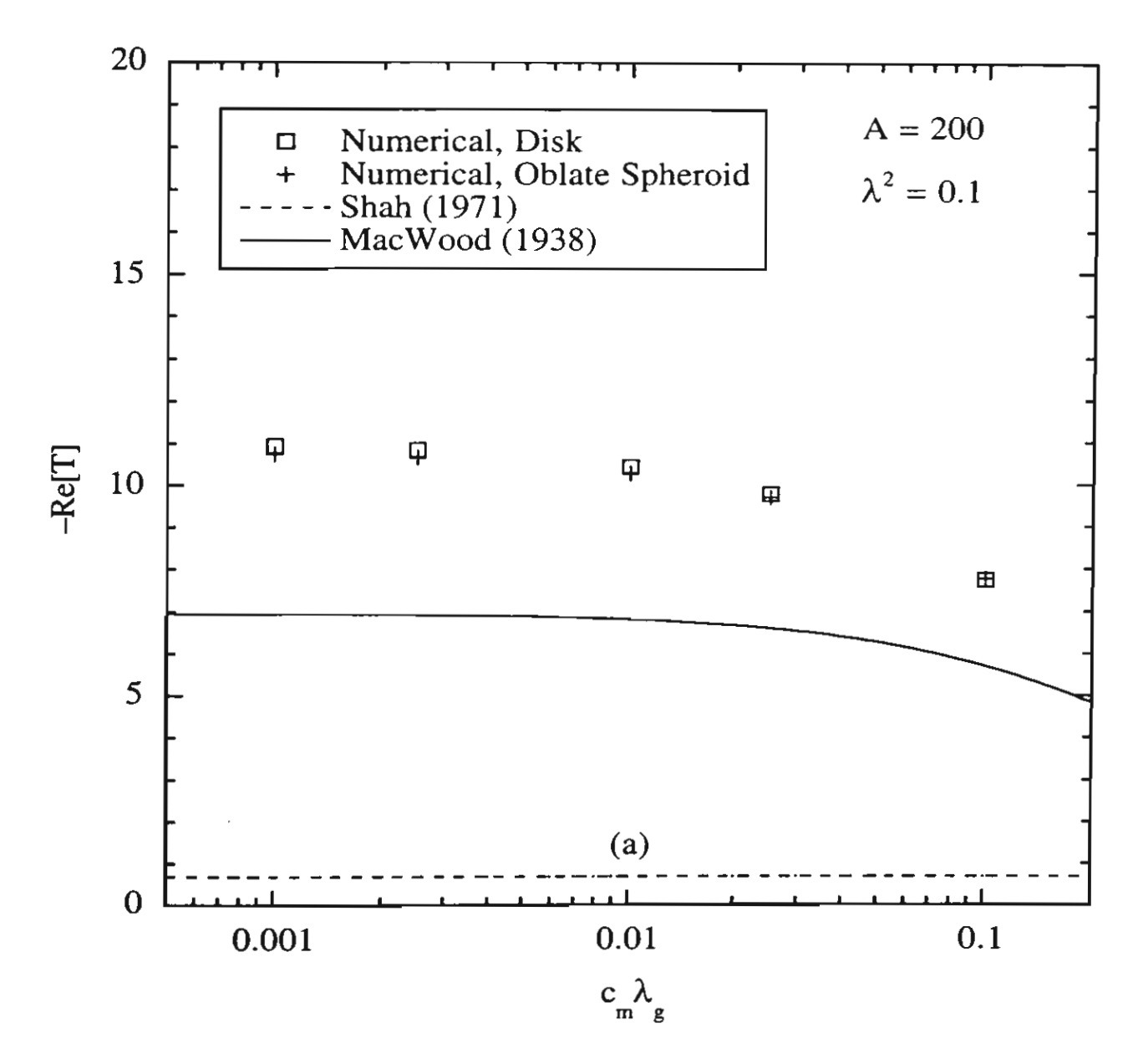


Figure 3(a). Tekasakul and Loyalka

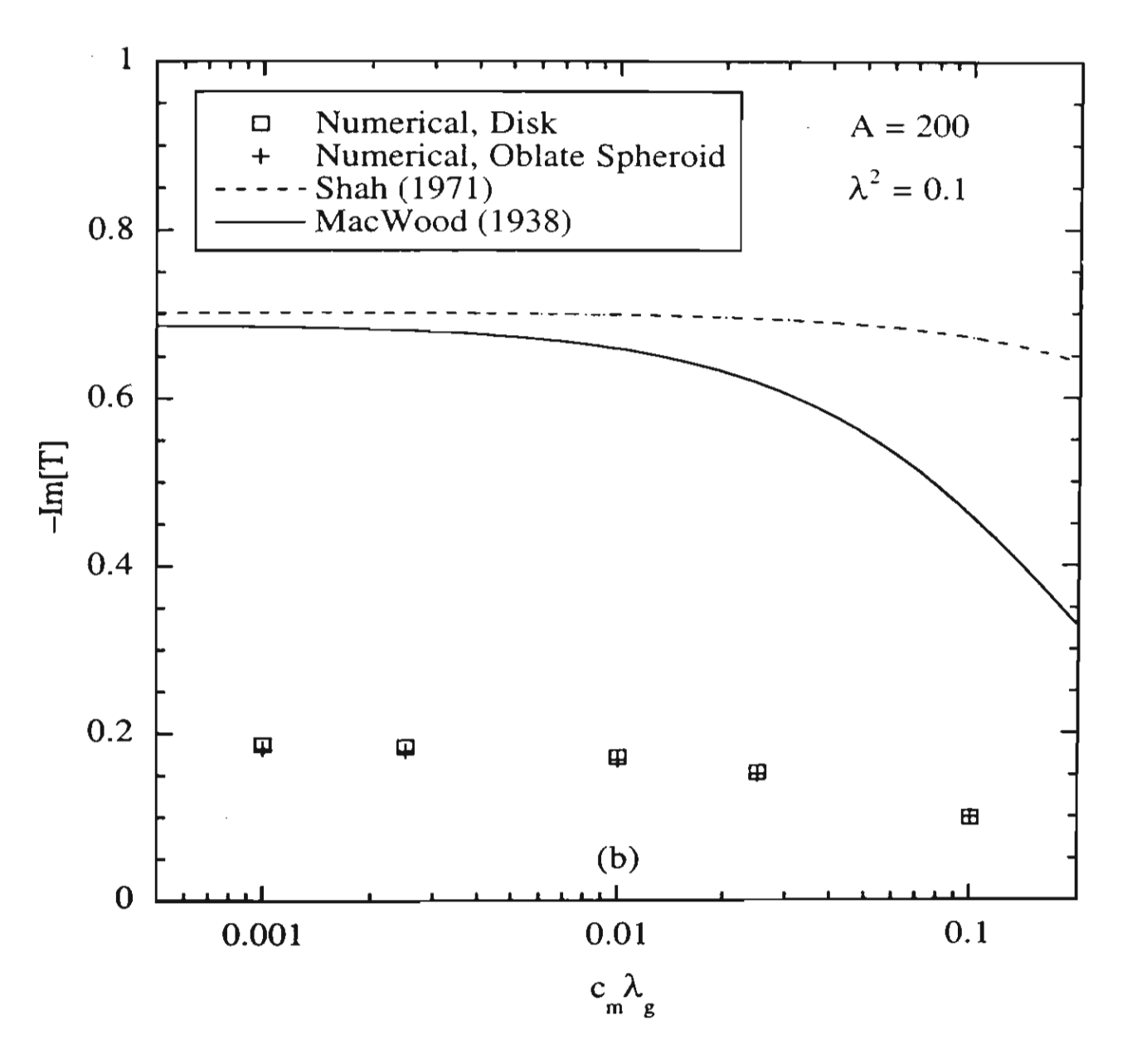


Figure 3(b). Tekasakul and Loyalka

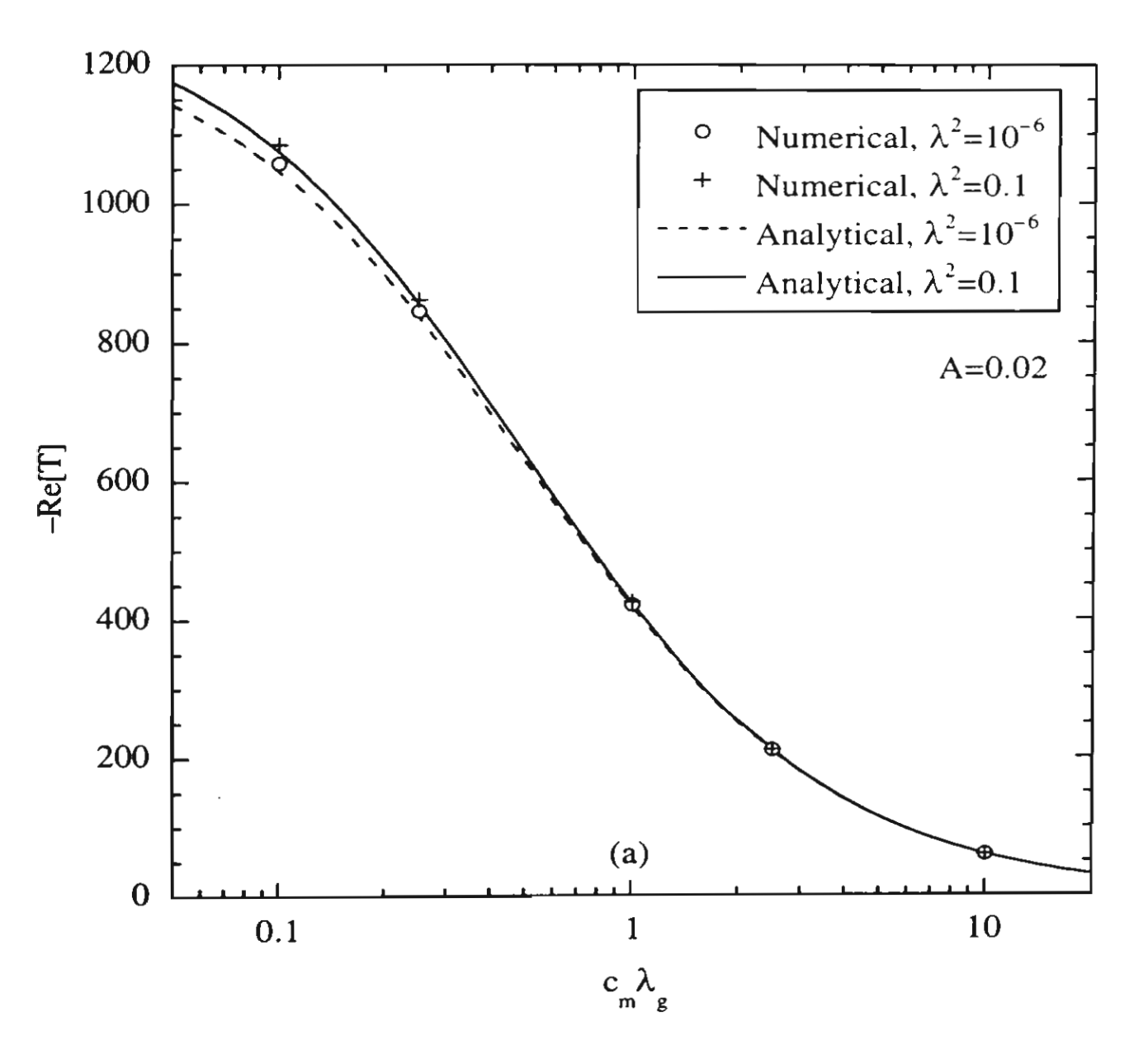


Figure 4(a). Tekasakul and Loyalka

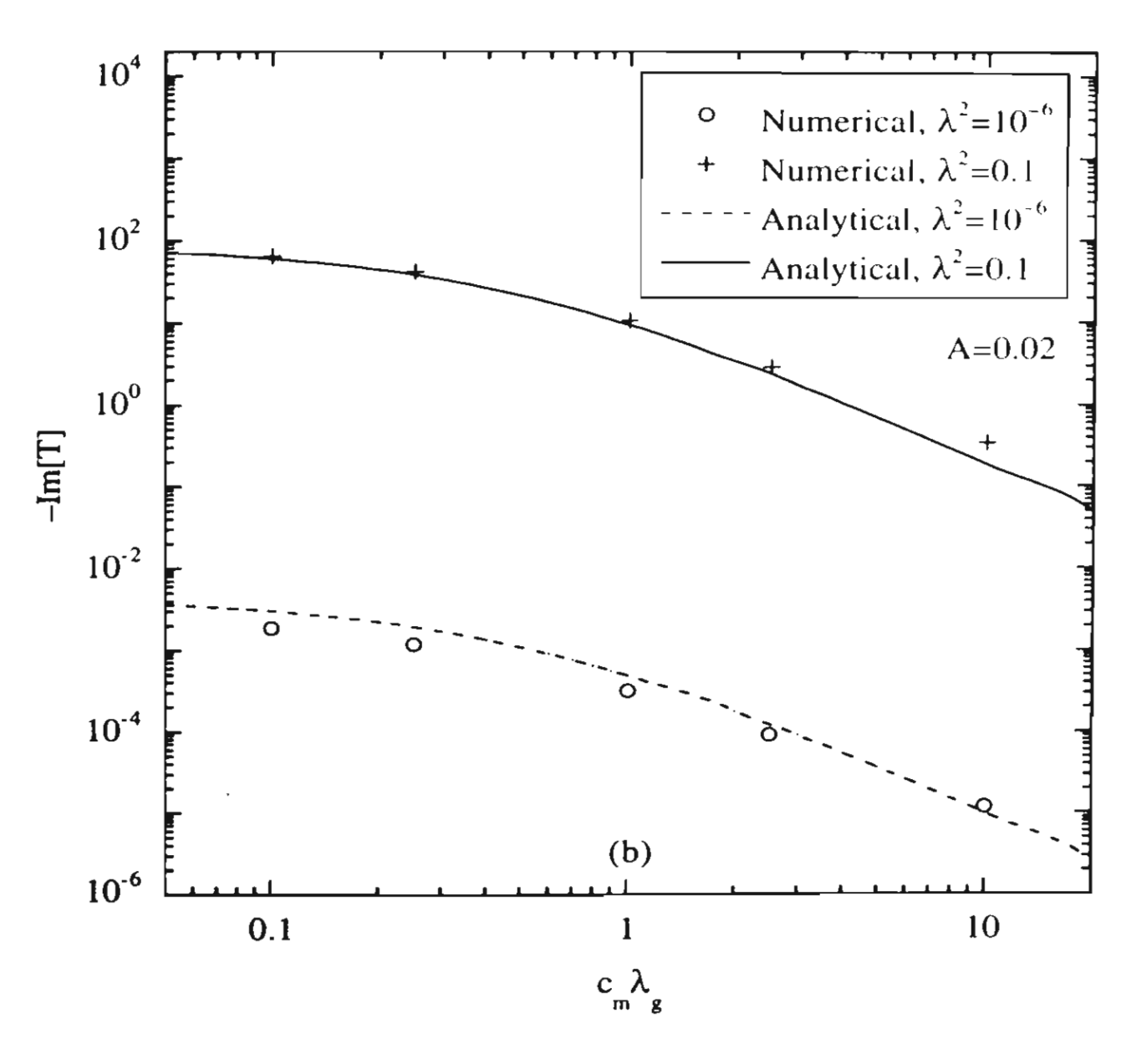


Figure 4(b). Tekasakul and Loyalka

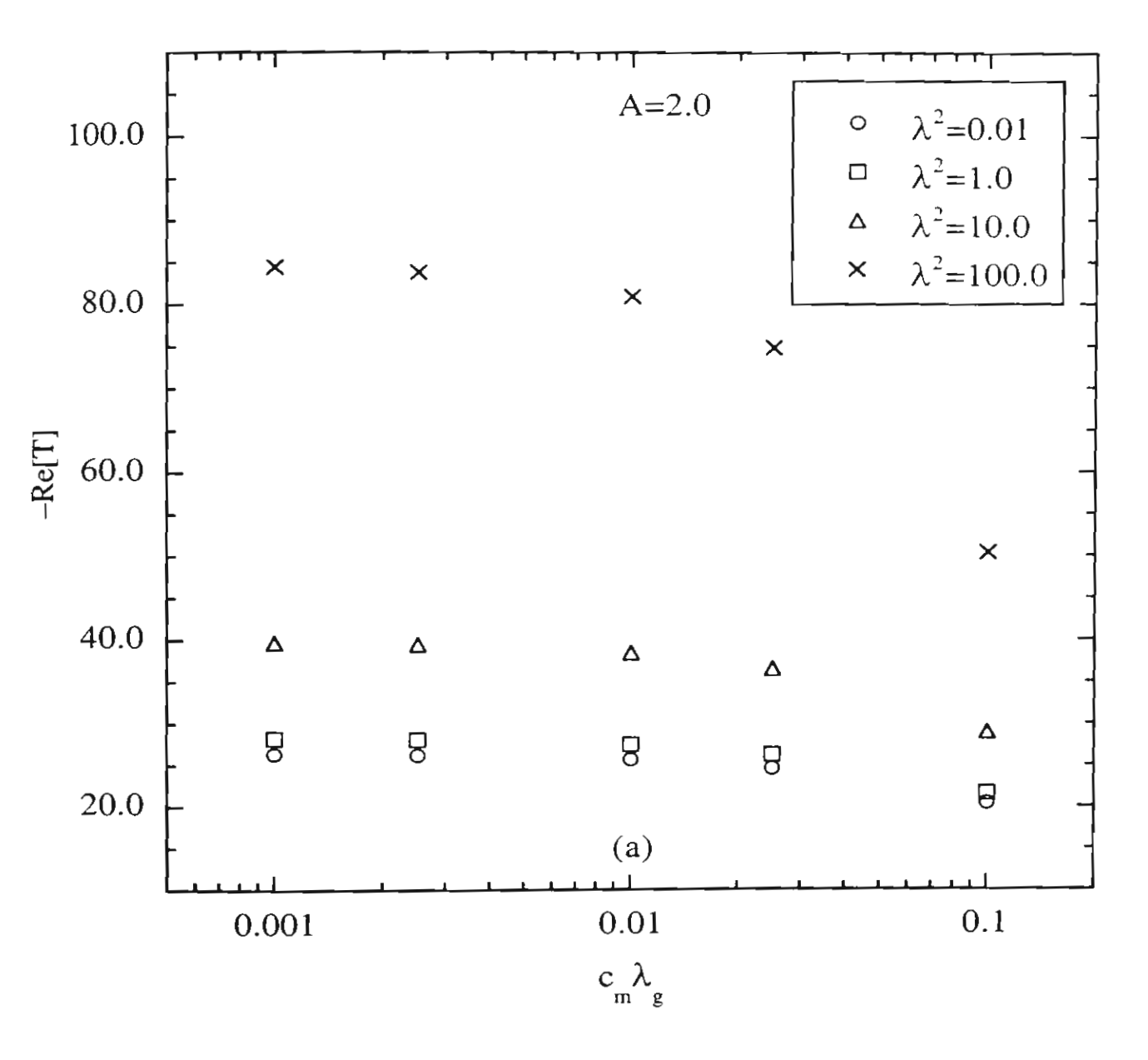


Figure 5(a). Tekasakul and Loyalka

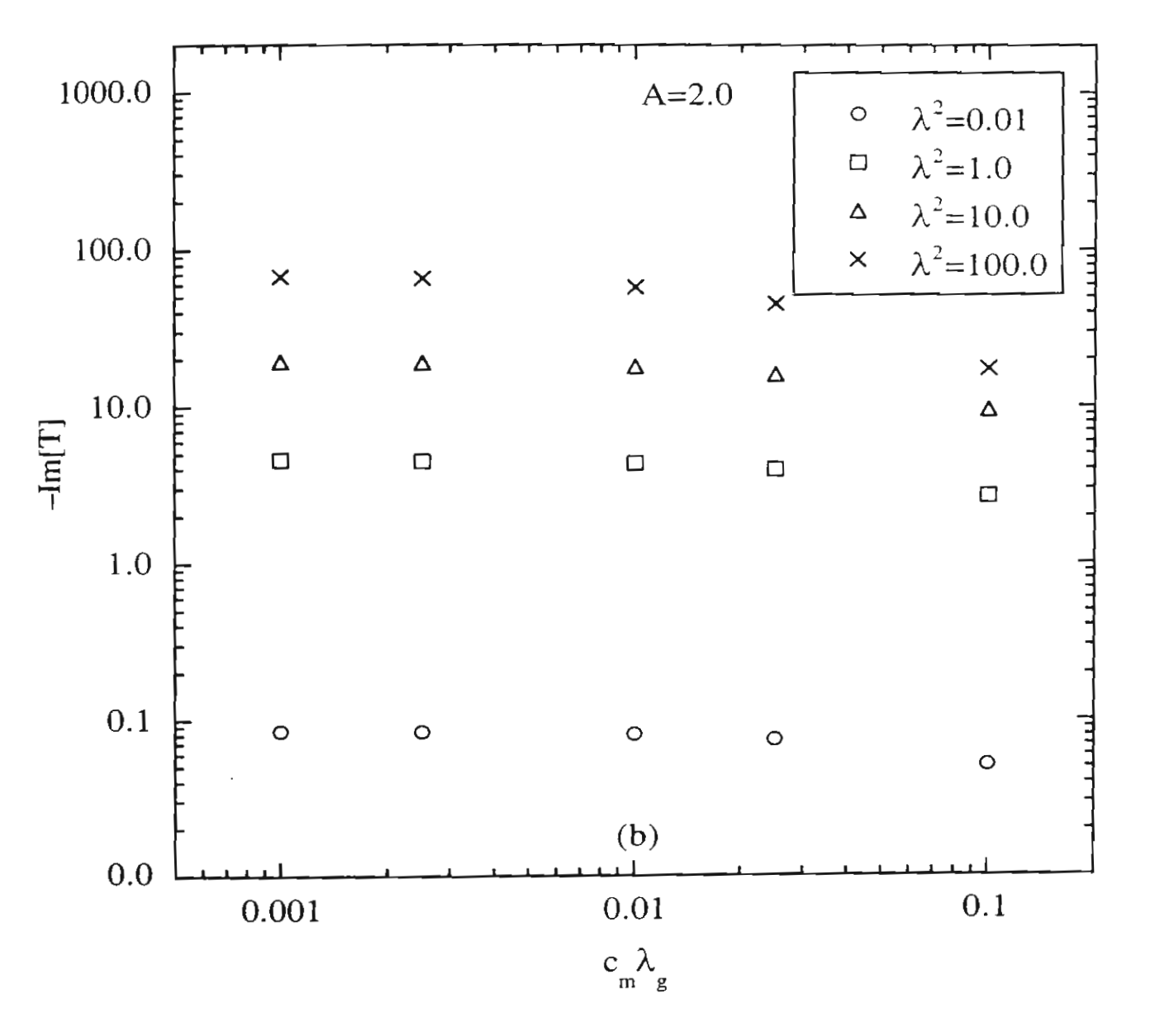


Figure 5(b). Tekasakul and Loyalka

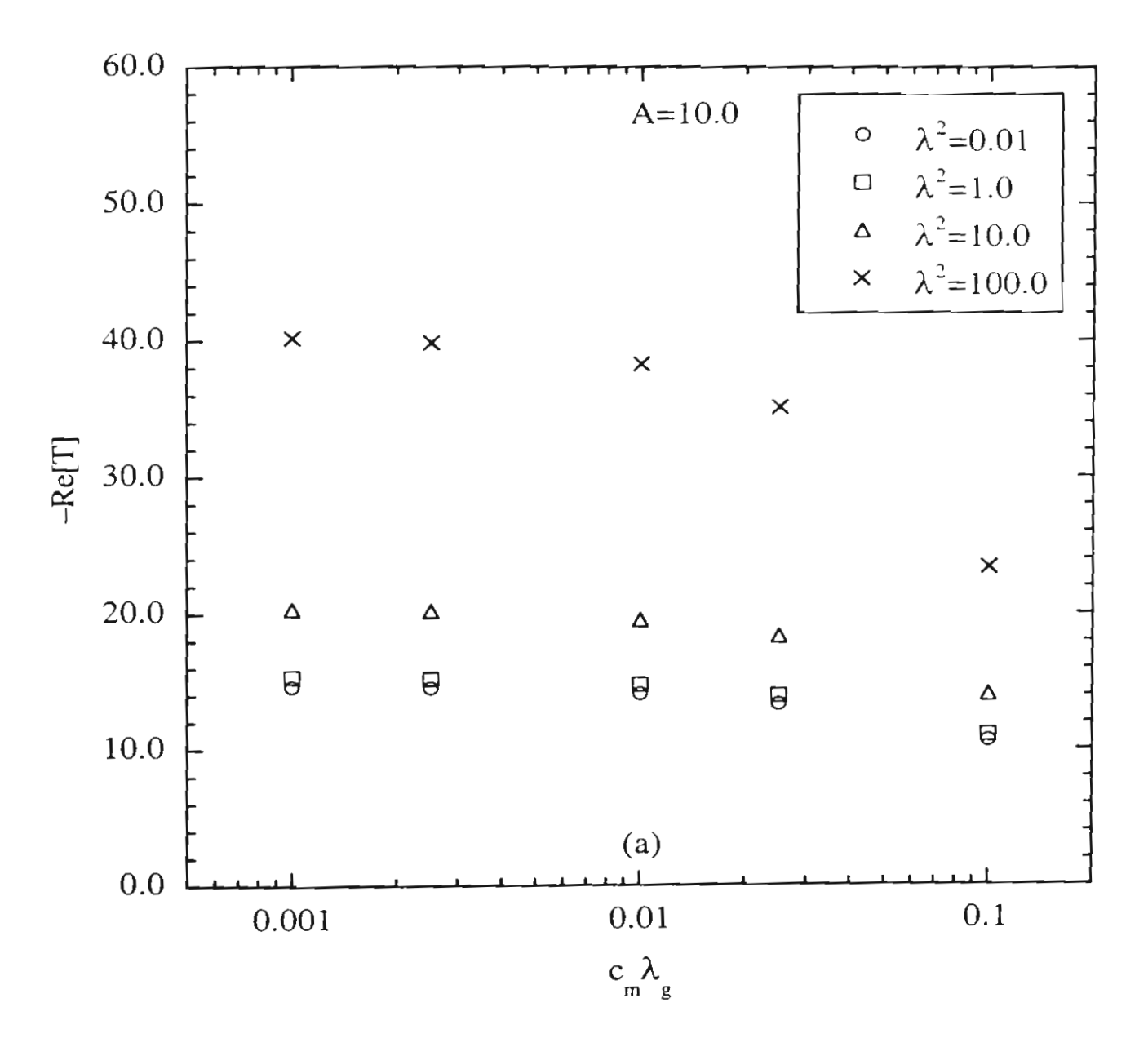


Figure 6(a). Tekasakul and Loyalka

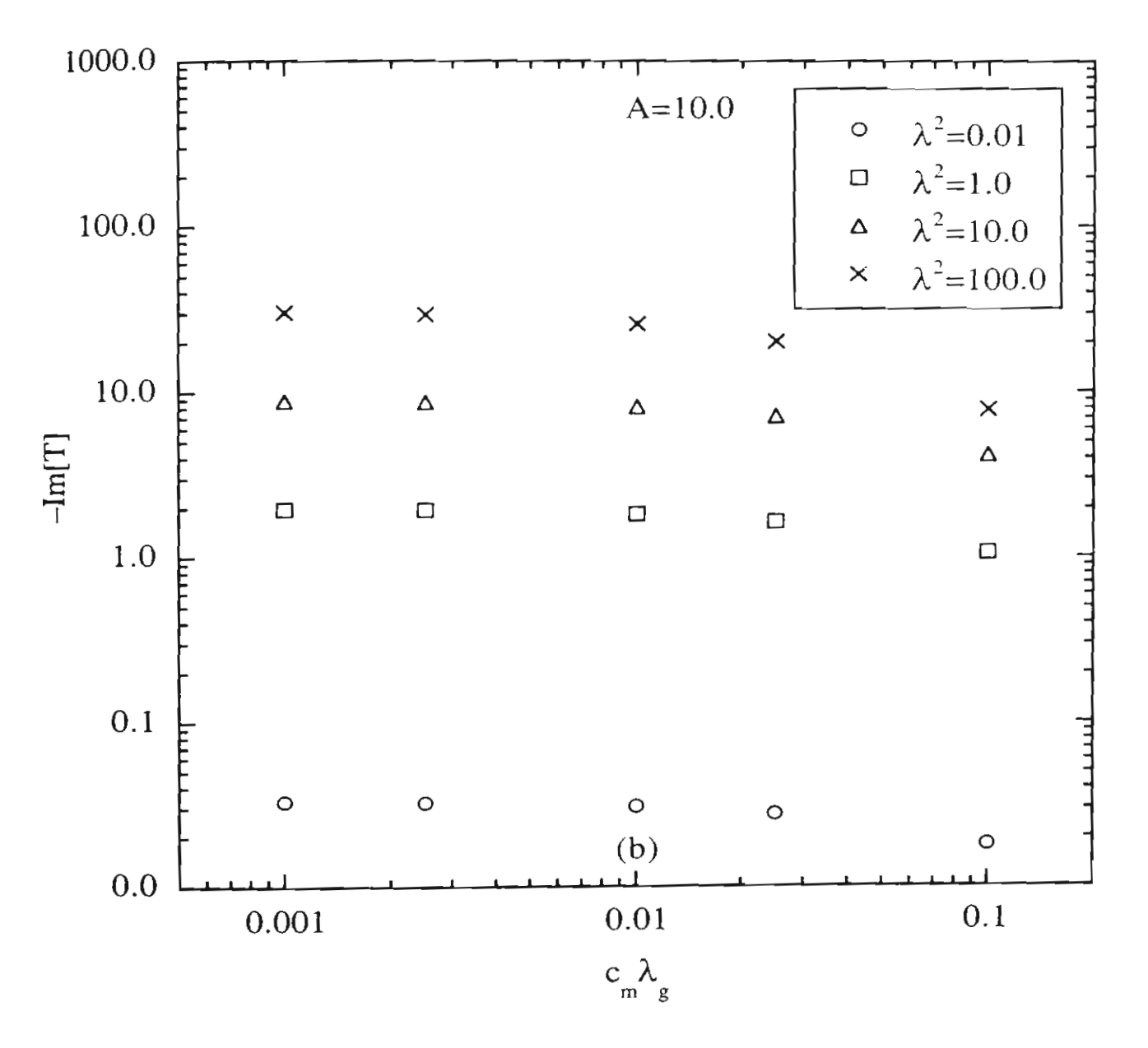


Figure 6(b). Tekasakul and Loyalka

Appendix D

Results: Rotatory Oscillations of Axi-Symmetric Bodies in

A Bounded Axi-Symmetric Viscous Flow with Slip: Numerical Solutions

for Sphere and Spheroids

Rotatory Oscillations of Axi-symmetric Bodies in a Bounded Axi-symmetric Viscous Flow with Slip: Numerical Solutions

Numerical Procedure: Two Bodies with Slip

From numerical procedure in Appendix A, the problem for two bodies can be fully written out in the following manner.

$$\left[g_{11}(\zeta_{1}) - 2\pi(c_{m}\lambda_{s})_{1}\right]\sigma_{1}(\zeta_{1}) + \int L_{11}(\zeta_{1}, \zeta_{1}')\left[\sigma_{1}(\zeta_{1}') - \sigma_{1}(\zeta_{1})\right]d\zeta_{1}'
+ \int L_{12}(\zeta_{1}, \zeta_{2}')\sigma_{2}(\zeta_{2}')d\zeta_{2}' = -k^{2}\Psi(\zeta_{1})$$
(1)

and

$$\left[g_{22}(\zeta_{2}) - 2\pi(c_{m}\lambda_{g})_{2}\right]\sigma_{2}(\zeta_{2}) + \int L_{22}(\zeta_{2}, \zeta_{2}')\left[\sigma_{2}(\zeta_{2}') - \sigma_{2}(\zeta_{2})\right]d\zeta_{2}'
+ \int L_{21}(\zeta_{2}, \zeta_{1}')\sigma_{1}(\zeta_{1}')d\zeta_{1}' = 0$$
(2)

where

$$g_{11}(\zeta_1) = \int L_{11}(\zeta_1, \zeta_1') d\zeta_1'$$
(3a)

$$g_{22}(\zeta_2) = \int L_{22}(\zeta_2, \zeta_2') d\zeta_2'$$
 (3b)

and

$$L_{11}(\zeta_{1},\zeta_{1}') = -f_{1}(\zeta_{1}')K_{11}(\zeta_{1},\zeta_{1}') + (c_{m}\lambda_{g})_{1}H(\zeta_{1},\zeta_{1}')$$
(4a)

$$L_{12}(\zeta_{1},\zeta_{2}') = -f_{2}(\zeta_{2}')K_{12}(\zeta_{1},\zeta_{2}') - (c_{m}\lambda_{s})_{2}H(\zeta_{1},\zeta_{2}')$$
(4b)

$$L_{21}(\zeta_{2},\zeta_{1}') = -f_{1}(\zeta_{1}')K_{21}(\zeta_{2},\zeta_{1}') + (c_{m}\lambda_{g})_{1}H(\zeta_{2},\zeta_{1}')$$
(4c)

$$L_{22}(\zeta_2, \zeta_2') = -f_2(\zeta_2') K_{22}(\zeta_2, \zeta_2') - (c_m \lambda_g)_2 H(\zeta_2, \zeta_2')$$
(4d)

Неге.

$$f_{i} = 1 + \frac{\left(c_{m}\lambda_{g}\right)_{i}}{\varpi'_{si}} \frac{\partial \varpi'_{si}}{\partial n'_{si}} \tag{5}$$

$$K = \frac{J_s'}{\cos(\phi)} \left[\int \psi(\mathbf{r}_s, \mathbf{r}_s') \cos(\phi_s') d\phi_s' \right]$$
 (6)

$$H = \frac{J_s'}{\cos(\phi)} \left[\int \frac{\partial \psi(\mathbf{r}_s, \mathbf{r}_s')}{\partial n_s'} \cos(\phi_s') d\phi_s' \right]$$
 (7)

and

$$\Psi = \frac{1}{\cos(\phi)} \left[\int \psi(\mathbf{r}_s, \mathbf{r}'_s) \varpi'_s \cos(\phi'_s) J'_s d\phi'_s d\zeta' \right]$$
(8)

The integrals in Eqs. (1) and (2) are thus converted to summations by the use of Gaussian quadratures and Eqs. (1) and (2) are then reduced to systems of linear algebraic equations by applying collocation at the nodal points of the quadrature. The integrals in Eqs. (3a) and (3b) are determined in the Cauchy principal value sense. The local stresses, $\sigma_1(\zeta)$ and $\sigma_2(\zeta)$, are determined at each nodal point and the torques on the inner and outer bodies are finally determined, respectively, from

$$T_{1} = -2\pi \int_{c} \varpi_{1}^{2} \sigma_{1}(\zeta) ds$$
 (5)

$$T_2 = -2\pi \int_{\mathcal{L}} \overline{\omega}_2^2 \ \sigma_2(\zeta) \, \mathrm{d} s \tag{6}$$

1. Determination of f

The radius ratio is defined as the ratio of the (equatorial) radius of the outer body to that of the inner body,

$$\alpha = \frac{a_2}{a_2} \tag{9}$$

a) Sphere

$$f_1 = 1 + \left(c_m \lambda_g\right)_1 \tag{10a}$$

$$f_2 = 1 - \left(c_m \lambda_s\right)_2 \alpha^{-1} \tag{11b}$$

b) Spheroids

$$z = c \lambda \zeta$$

$$\boldsymbol{\varpi} = c \left[\left(1 + \lambda^2 \right) \left(1 - \zeta^2 \right) \right]^{1/2}$$

$$c_1^2 = \begin{cases} 1 - A_1^{-2} & \text{Oblate spheroid} \\ A_1^{-2} - 1 & \text{Prolate spheroid} \end{cases}$$
 (12a)

$$c_2^2 = \begin{cases} \alpha^2 (1 - A_2^{-2}) & \text{Oblate spheroid} \\ \alpha^2 (A_2^{-2} - 1) & \text{Prolate spheroid} \end{cases}$$
 (12b)

$$\lambda_{01} = \begin{cases} \left(A_1^2 - 1\right)^{-1/2} & \text{Oblate spheroid} \\ \left(1 - A_1^2\right)^{-1/2} & \text{Prolate spheroid} \end{cases}$$
(13a)

$$\lambda_{02} = \begin{cases} \left(A_2^2 - 1\right)^{-1/2} & \text{Oblate spheroid} \\ \left(1 - A_2^2\right)^{-1/2} & \text{Prolate spheroid} \end{cases}$$
(13b)

Therefore,

$$f_{1} = 1 + \frac{\left(c_{m}\lambda_{g}\right)_{1}}{c_{1}} \cdot \frac{\lambda_{01}}{\left[\left(1 + \lambda_{01}^{2}\right)\left(\zeta_{1}^{2} + \lambda_{01}^{2}\right)\right]^{1/2}}$$
(14a)

and

$$f_2 = 1 - \frac{\left(c_m \lambda_g\right)_2}{c_2} \cdot \frac{\lambda_{02}}{\left[\left(1 + \lambda_{02}^2\right)\left(\zeta_2^2 + \lambda_{02}^2\right)\right]^{V^2}}$$
 (15b)

2. Determination of K (From Tekasakul, et al., 1998)

$$K(\zeta, \zeta') = \frac{J_s'}{\cos(\phi)} \int \psi(\mathbf{r}_s, \mathbf{r}_s') \cos(\phi') d\phi'$$

$$= K_L(\zeta, \zeta') + K_H(\zeta, \zeta')$$
(16)

where,

$$K_{L}(\zeta,\zeta') = \frac{J_{s}'}{\cos(\phi)} \int \frac{\cos(\phi')}{|\mathbf{r}_{s}' - \mathbf{r}_{s}|} d\phi' = \frac{2J_{s}'}{\sqrt{\varpi_{s} \varpi_{s}'}} Q_{1/2}(\gamma)$$
(17)

and

$$K_{H}(\zeta,\zeta') = \frac{J'_{s}}{\cos(\phi)} \int \frac{\exp(-ik|\mathbf{r}'_{s}-\mathbf{r}_{s}|)-1}{|\mathbf{r}'_{s}-\mathbf{r}_{s}|} \cos(\phi') d\phi'$$

$$= \frac{J'_{s}}{\cos(\phi)} \int_{0}^{2\pi} \frac{\exp(-ik[2\varpi_{s}\varpi'_{s}(\gamma-\cos(\phi-\phi'))]^{1/2})-1}{[2\varpi_{s}\varpi'_{s}(\gamma-\cos(\phi-\phi'))]^{1/2}} \cos(\phi') d\phi'$$
(18)

3. Determination of H (Tekasakul, et al., 1999.)

a) Sphere and spheroids

$$H_{i1}(\zeta_{1},\zeta_{1}') = -\frac{1}{\cos(\phi_{1})} \frac{\varpi_{s1}'}{A_{1}} \int_{0}^{2\pi} \left\{ (1+ikt) \exp(-ikt) \left[2\varpi_{s1}\varpi_{1}' \left(\gamma - \cos(\phi_{1} - \phi_{1}') \right) \right]^{-3/2} \right\}$$

$$\left[\left[z_{s1}' - z_{s1} \right] \frac{z_{s1}'}{\left[A_{1}^{-2} - z_{s1}'^{2} \right]^{1/2}} A_{1} + \varpi_{s1}' - \varpi_{s1} \cos(\phi_{1} - \phi_{1}') \right] \cos(\phi_{s1}') \right\} d\phi_{1}'$$

$$(19)$$

$$H_{12}(\zeta_{1},\zeta_{2}') = -\frac{1}{\cos(\phi_{1})} \frac{\varpi_{s1}'}{(A_{2}/\alpha)} \int_{0}^{2\pi} \left\{ (1+ik\ t) \exp(-ik\ t) \left[2\varpi_{s1}\varpi_{2}' \left(\gamma - \cos(\phi_{1} - \phi_{2}') \right) \right]^{-3/2} \right\}$$

$$\left[\left[z_{s2}' - z_{s1} \right] \frac{z_{s2}'}{\left[(\alpha/A_{2})^{2} - z_{s2}'^{2} \right]^{1/2}} A_{2} + \varpi_{s2}' - \varpi_{s1} \cos(\phi_{1} - \phi_{2}') \right] \cos(\phi_{s2}') \right\} d\phi_{1}'$$
(20)

$$H_{2i}(\zeta_{2},\zeta'_{1}) = -\frac{1}{\cos(\phi_{2})} \frac{\varpi'_{s1}}{A_{i}} \int_{0}^{2\pi} \left\{ (1+ikt) \exp(-ikt) \left[2\varpi_{s2}\varpi'_{1} \left(\gamma - \cos(\phi_{2} - \phi'_{1}) \right) \right]^{-3/2} \right\}$$

$$\left[\left[z'_{s1} - z_{s2} \right] \frac{z'_{s2}}{\left[A_{i}^{-2} - z'_{s1}^{2} \right]^{1/2}} A_{i} + \varpi'_{s2} - \varpi_{s2} \cos(\phi_{2} - \phi'_{1}) \right] \cos(\phi'_{s1}) d\phi'_{1}$$
(21)

$$H_{22}(\zeta_{2},\zeta_{2}') = -\frac{1}{\cos(\phi_{2})} \frac{\varpi_{s2}'}{(A_{2}/\alpha)} \int_{0}^{2\pi} \left\{ (1+ikt) \exp(-ikt) \left[2\varpi_{s2}\varpi_{2}' \left(\gamma - \cos(\phi_{2} - \phi_{2}') \right) \right]^{-3/2} \right\}$$

$$\left[\left[z_{s2}' - z_{s2} \right] \frac{z_{s2}'}{\left[(\alpha/A_{2})^{2} - z_{s2}'^{2} \right]^{1/2}} A_{2} + \varpi_{s2}' - \varpi_{s2} \cos(\phi_{2} - \phi_{2}') \right] \cos(\phi_{s2}') d\phi_{2}'$$
(22)

4. Determination of Ψ

From Tekasakul, et al., 1998., we have

$$\Psi(\zeta)\cos(\phi) = -\frac{4\pi}{k^2} \left(\varpi_s\cos(\phi)\right) - \int_{\substack{\text{inside} \\ \text{body}}} \frac{\exp(-i k |\mathbf{r}' - \mathbf{r}_s|)}{|\mathbf{r}' - \mathbf{r}_s|} \varpi'\cos(\phi') d\mathbf{r}'$$
 (23)

(a) Sphere

$$\Psi(\zeta)\cos(\phi) = \frac{2\pi \,\varpi_s \cos(\phi)}{k^2} \left\{ -2 + \left(1 + \frac{i}{k}\right) + \exp(-i\,2\,k) \left(1 - \frac{i}{k}\right) + \frac{i}{k} \left(1 + \frac{3}{k^2}\right) - \frac{\exp(-i\,2\,k)}{k^3} \left(3\,i - 6\,k - 5\,i\,k^2 + 2\,k^3\right) \right\}$$
(24)

(b) Oblate spheroid

$$\Psi(\zeta)\cos(\phi) = \frac{-4\pi}{k^{2}} \left[\varpi_{s}\cos(\phi)\right] - \frac{c^{3}}{2} \int_{0}^{\xi_{0}} d\xi' \int_{0}^{\pi} d\eta' \int_{0}^{2\pi} d\phi' \\
\times \left\{ \frac{\exp\left(-ik\left[2\varpi_{s}\varpi'_{s}\left(\gamma - \cos(\phi - \phi')\right)\right]^{1/2}\right)}{\left[2\varpi_{s}\varpi'_{s}\left(\gamma - \cos(\phi - \phi')\right)\right]^{1/2}} \\
\times \varpi'\cos(\phi')\left[\cosh(2\xi') + \cos(2\eta')\right]\cosh(\xi')\sin(\eta') \right\}$$
(25)

(c) Prolate spheroid

$$\Psi(\zeta)\cos(\phi) = \frac{-4\pi}{k^2} \left[\varpi_s \cos(\phi)\right] - \frac{c^3}{2} \int_0^{\xi_0} d\xi' \int_0^{\pi} d\eta' \int_0^{2\pi} d\phi' \\
\times \left\{ \frac{\exp\left(-ik\left[2\varpi_s \varpi_s' \left(\gamma - \cos(\phi - \phi')\right)\right]^{1/2}\right)}{\left[2\varpi_s \varpi_s' \left(\gamma - \cos(\phi - \phi')\right)\right]^{1/2}} \\
\times \varpi' \cos(\phi') \left[\cosh(2\xi') - \cos(2\eta')\right] \sinh(\xi') \sin(\eta') \right\}$$
(26)

Analytical Solutions

Analytical solution for torque on an oscillating inner sphere while the outer sphere is fixed was obtained by Shah (1971). He derived an expression of D(s) as

$$D(s) = \frac{8}{3} m s^{3/2} \left[\frac{1}{P_1 Q_1 + M_1 N_1} \left[N_1 K_{5/2} (\xi_0 \sqrt{s}) - P_1 I_{5/2} (\xi_0 \sqrt{s}) \right] \right]$$
 (27)

where

$$M_{1} = K_{3/2}(\xi_{0}\sqrt{s}) + (c_{m}\lambda_{g})_{1}\sqrt{s} K_{5/2}(\xi_{0}\sqrt{s})$$

$$N_{1} = I_{3/2}(\xi_{2}\sqrt{s}) + (c_{m}\lambda_{g})_{1}\sqrt{s} I_{5/2}(\xi_{2}\sqrt{s})$$

$$P_{1} = -K_{3/2}(\xi_{2}\sqrt{s}) + (c_{m}\lambda_{g})_{1}\sqrt{s} K_{5/2}(\xi_{2}\sqrt{s})$$

$$Q_{1} = I_{3/2}(\xi_{0}\sqrt{s}) - (c_{m}\lambda_{g})_{1}\sqrt{s} I_{5/2}(\xi_{0}\sqrt{s})$$

Here I and K are the modified Bessel function of the the first and the second kind, respectively, $\xi_0 = a_1/\delta$, and $\xi_2 = a_2/\delta$. Equation can be transformed into torque by using the following transformations:

$$s = -k^{2}$$

$$\xi_{0} = 1$$

$$\xi_{2} = \alpha = a_{2}/a_{1}$$

The torque on an inner sphere can then be determined from

$$T_{1} = D(-k^{2}) \frac{\pi}{mk^{2}}$$

$$= -\frac{8}{3} \pi (i k) \left[\frac{1}{P'_{1} Q'_{1} + M'_{1} N'_{1}} \left[N'_{1} K_{5/2}(i k) - P'_{1} I_{5/2}(i k) \right] \right]$$
(28)

where

$$M'_{1} = K_{3/2}(ik) + (c_{m}\lambda_{g})_{1}(ik)K_{5/2}(ik)$$

$$N'_{1} = I_{3/2}(ik\alpha) + (c_{m}\lambda_{g})_{1}(ik)I_{5/2}(ik\alpha)$$

$$P'_{1} = -K_{3/2}(ik\alpha) + (c_{m}\lambda_{g})_{1}(ik)K_{5/2}(ik\alpha)$$

$$Q'_{1} = I_{3/2}(ik) - (c_{m}\lambda_{g})_{1}(ik)I_{5/2}(ik)$$

Results: Sphere

Since the analytical solution for an oscillating sphere in a bounded sphere with slip boundary conditions can be obtained analytically (Shah, 1971), we first benchmark the accuracy of the numerical method against the analytical solutions for a sphere for values of $c_m \lambda_g$ ranging from 0.001 to 0.1 and values of λ^2 ranging from 0.01 to 100.0. In these calculations, 20 point Gaussian quadratures were used for $\lambda^2 \leq 10.0$ and 30 point quadratures were used for $\lambda^2 = 100.0$.

Numerical results for the real and imaginary parts of the torque on an inner sphere are given in Figs. 1(a) and 1(b), for $\alpha = a_2/a_1 = 2.0$, and in Figs 2(a) and 2(b) for $\alpha = 10.0$. In the first case where $\alpha = 2.0$, the spacing filled with fluid is of the same magnitude of the inner sphere, while in the second case where $\alpha = 10.0$, the spacing is comparatively large. Analytical values are also included for comparison. In general the agreement is very good with error well below 1%. Values of torques increase as the values of λ^2 increase as expected (Tekasakul, et al., 1998). The values of torques decrease as the slip term $c_m \lambda_s$ becomes greater. It is obvious that the effect of slip is significant for the range considered $(0.001 \le c_m \lambda_s \le 0.1)$ and becomes greater for an oscillation with higher frequency. When compared for the different values of α , the results show that for the low frequency ($\lambda^2 = 0.01$) as the spacing is widened, the torques are slightly reduced. As the frequency increases, the torques become almost identical. The case where $\alpha = 10.0$ can be considered as unbounded with error well below 1% when compared with the unbounded case previously obtained by Tekasakul and Loyalka (Appendix B).

The good agreement between the numerical and analytical values for the case of a sphere demonstrates accuracy of this method as it was proved in the case of the unbounded fluid. The errors are very small for small values of λ^2 and increase slightly only for the largest values of λ^2 . The errors at large values of λ^2 are due to the relative thinness of the oscillatory viscous boundary layer which requires a higher number of Gaussian quadrature points for accurate modeling.

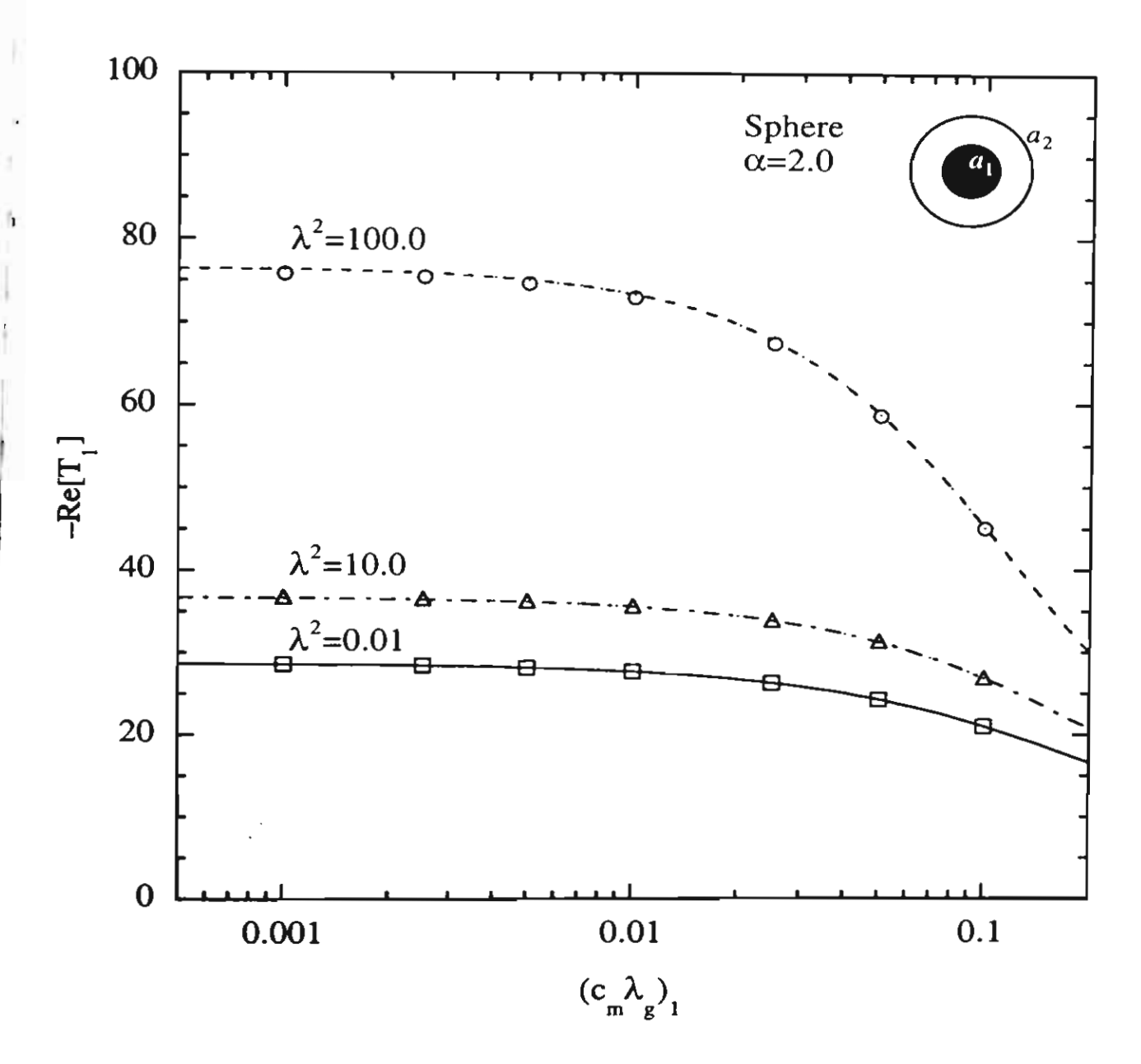


Figure 1(a) A comparison of the numerically determined torques on an inner sphere where the radius ratio $\alpha = a_2/a_1 = 2.0$ with the corresponding values determined analytically. Symbols indicate numerical results while various lines indicate corresponding analytical results: The real parts of the torques for $\lambda^2 = 0.01$ to 100.0. The number of Gaussian quadrature points used in the numerical calculations was 20 for $\lambda^2 = 0.01$ and $\lambda^2 = 10.0$, and 30 for $\lambda^2 = 100.0$.

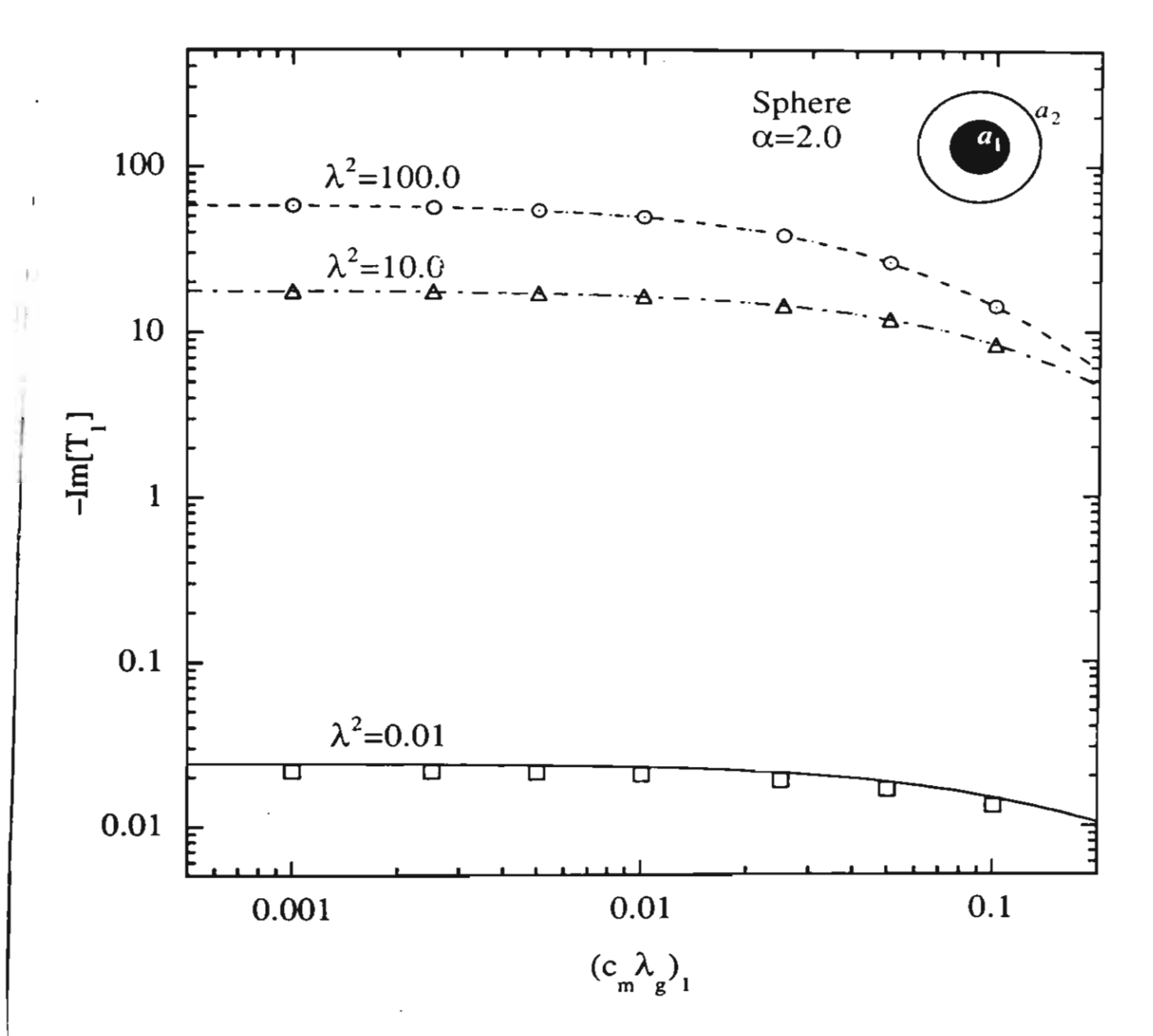


Figure 1(b) A comparison of the numerically determined torques on an inner sphere where the radius ratio $\alpha = a_2/a_1 = 2.0$ with the corresponding values determined analytically. Symbols indicate numerical results while various lines indicate corresponding analytical results: The imaginary parts of the torques for $\lambda^2 = 0.01$ to 100.0. The number of Gaussian quadrature points used in the numerical calculations was 20 for $\lambda^2 = 0.01$ and $\lambda^2 = 10.0$, and 30 for $\lambda^2 = 100.0$.

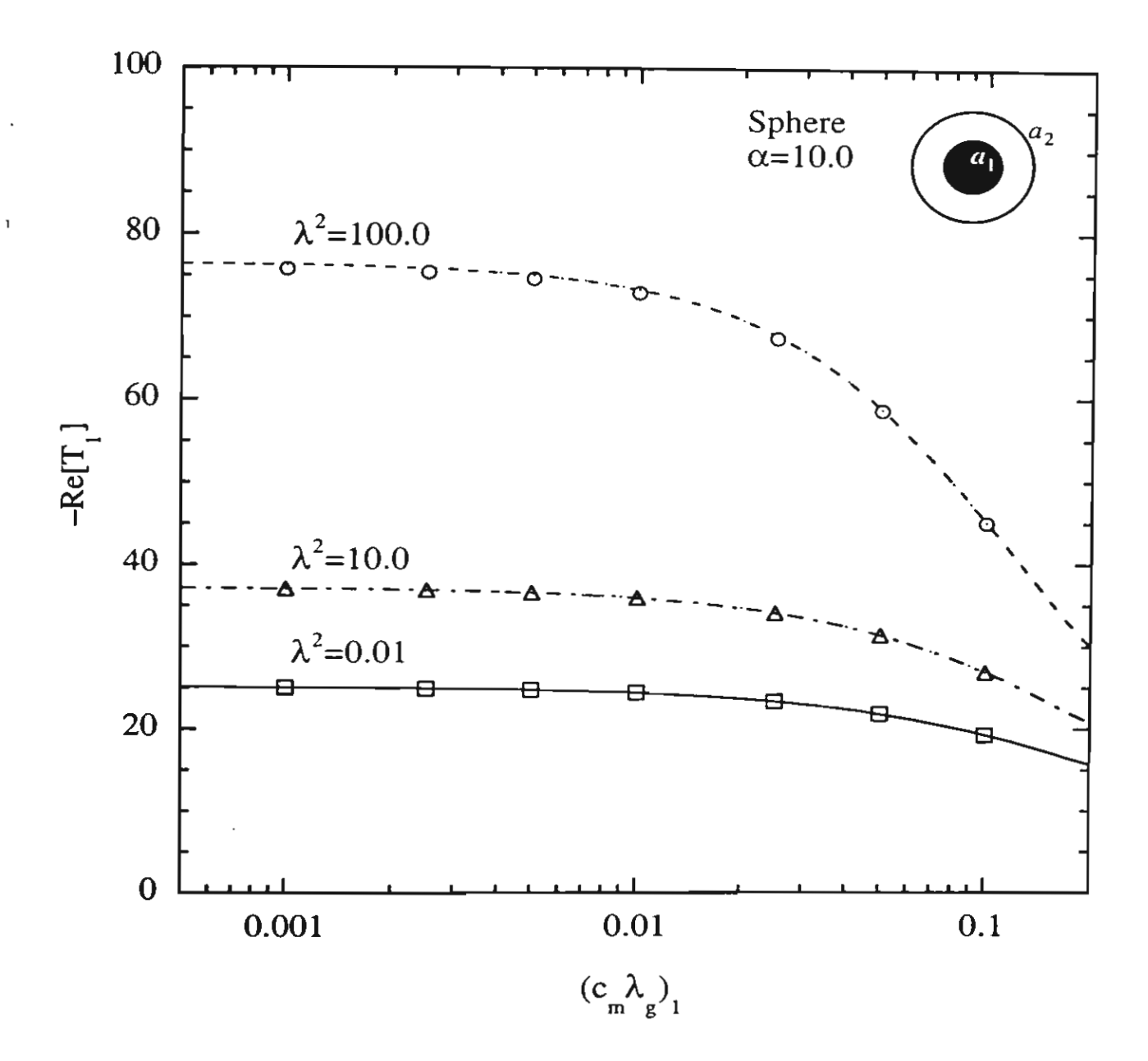


Figure 2(a) A comparison of the numerically determined torques on an inner sphere where the radius ratio $\alpha = a_2/a_1 = 10.0$ with the corresponding values determined analytically. Symbols indicate numerical results while various lines indicate corresponding analytical results: The real parts of the torques for $\lambda^2 = 0.01$ to 100.0. The number of Gaussian quadrature points used in the numerical calculations was 20 for $\lambda^2 = 0.01$ and $\lambda^2 = 10.0$, and 30 for $\lambda^2 = 100.0$.

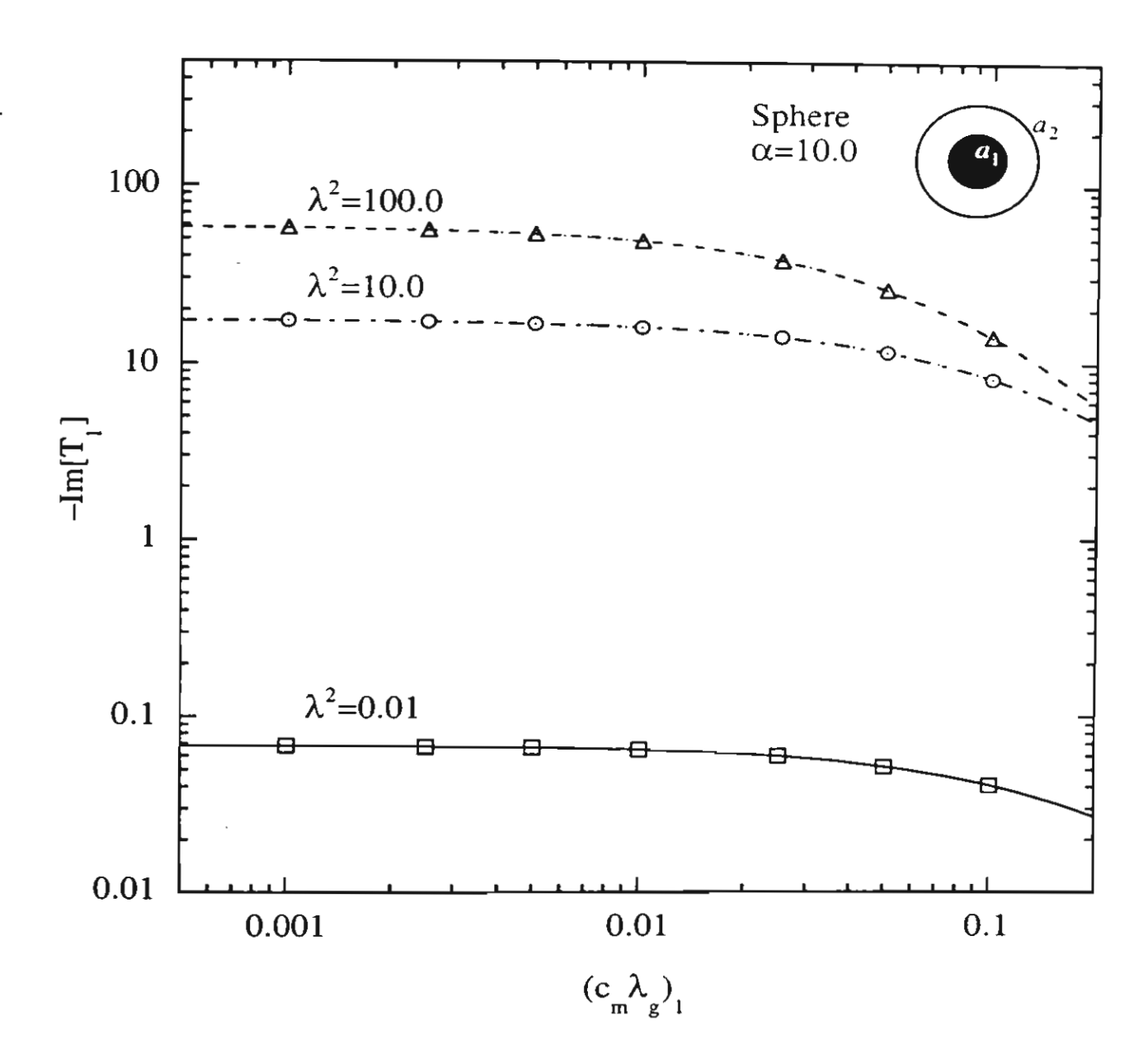


Figure 2(b) A comparison of the numerically determined torques on an inner sphere where the radius ratio $\alpha = a_2/a_1 = 10.0$ with the corresponding values determined analytically. Symbols indicate numerical results while various lines indicate corresponding analytical results: The imaginary parts of the torques for $\lambda^2 = 0.01$ to 100.0. The number of Gaussian quadrature points used in the numerical calculations was 20 for $\lambda^2 = 0.01$ and $\lambda^2 = 10.0$, and 30 for $\lambda^2 = 100.0$.

Results: Prolate Spheroid

Twenty-point Gaussian quadratures were used in the calculations for a prolate spheroid. Numerical results for the real and imaginary parts of the torque on an inner prolate spheroid with A=0.5 are given in Figs. 3(a) and 3(b) for $\alpha=a_2/a_1=2.0$, and in Figs 4(a) and 4(b) for $\alpha=10.0$. Results show identical effects of slip and oscillation frequency for the prolate spheroid as in the case of a sphere for the range considered $(0.001 \le c_m \lambda_g \le 0.1)$.

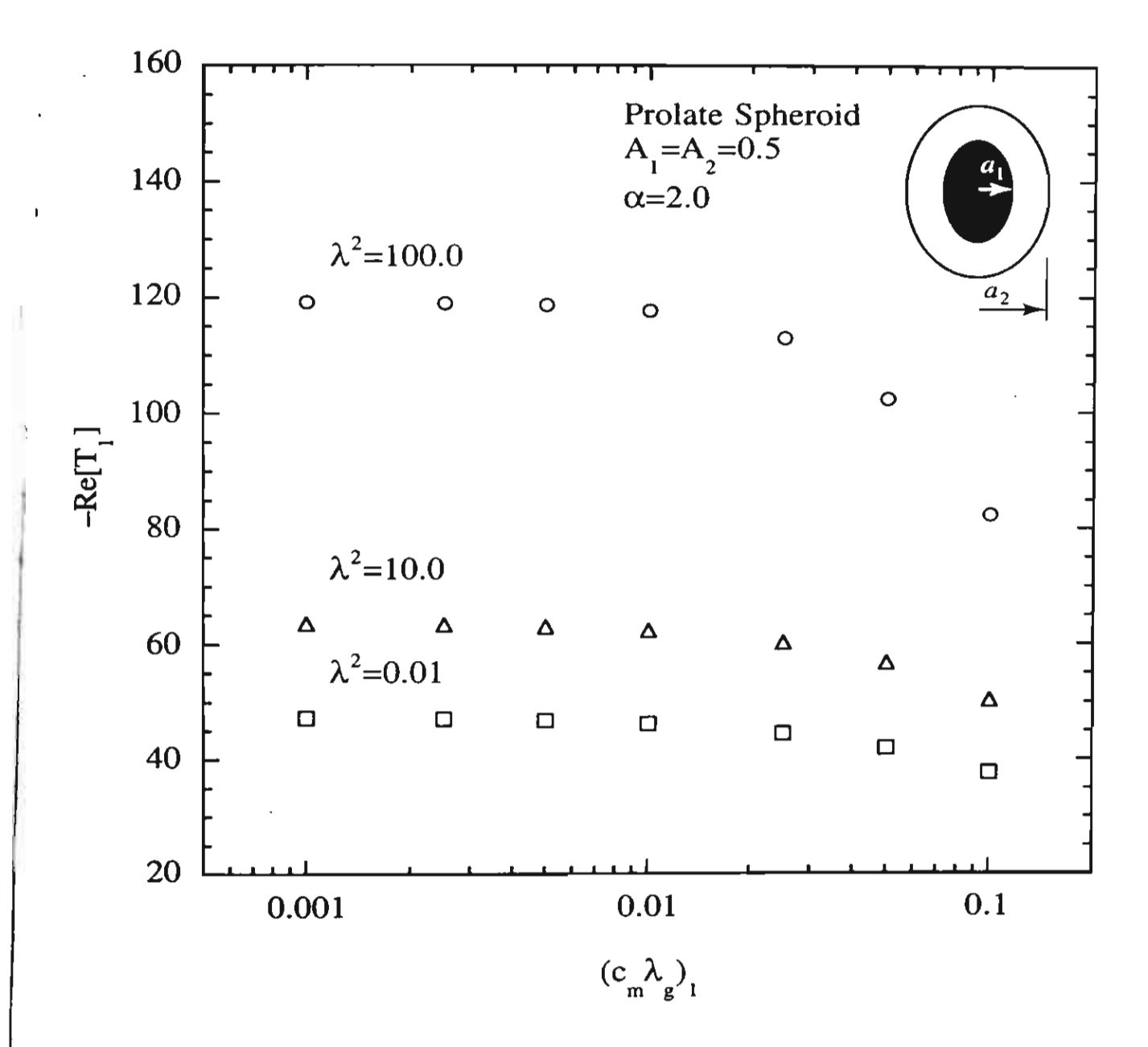


Figure 3(a) Numerical results for torques on an inner prolate spheroid. The aspect ratios of both the inner and outer spheroids are $A_1 = A_2 = 0.5$ while the equatorial radius ratio is $\alpha = a_2/a_1 = 2.0$. The real parts of the torques for $\lambda^2 = 0.01$ to 100.0. The number of Gaussian quadrature points used in the numerical calculations was 20.

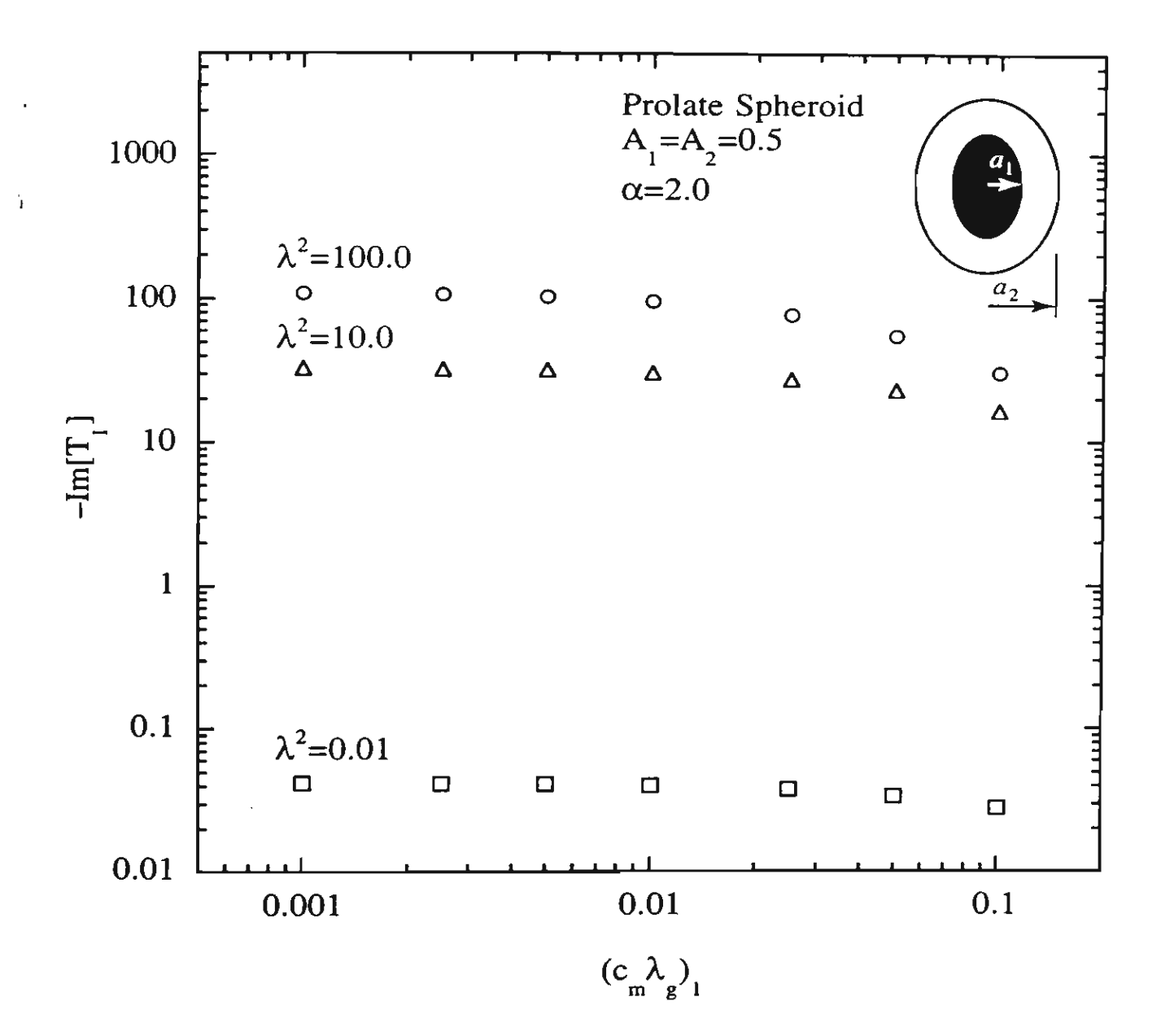


Figure 3(b) Numerical results for torques on an inner prolate spheroid. The aspect ratios of both the inner and outer spheroids are $A_1 = A_2 = 0.5$ while the equatorial radius ratio is $\alpha = a_2/a_1 = 2.0$. The imaginary parts of the torques for $\lambda^2 = 0.01$ to 100.0. The number of Gaussian quadrature points used in the numerical calculations was 20.

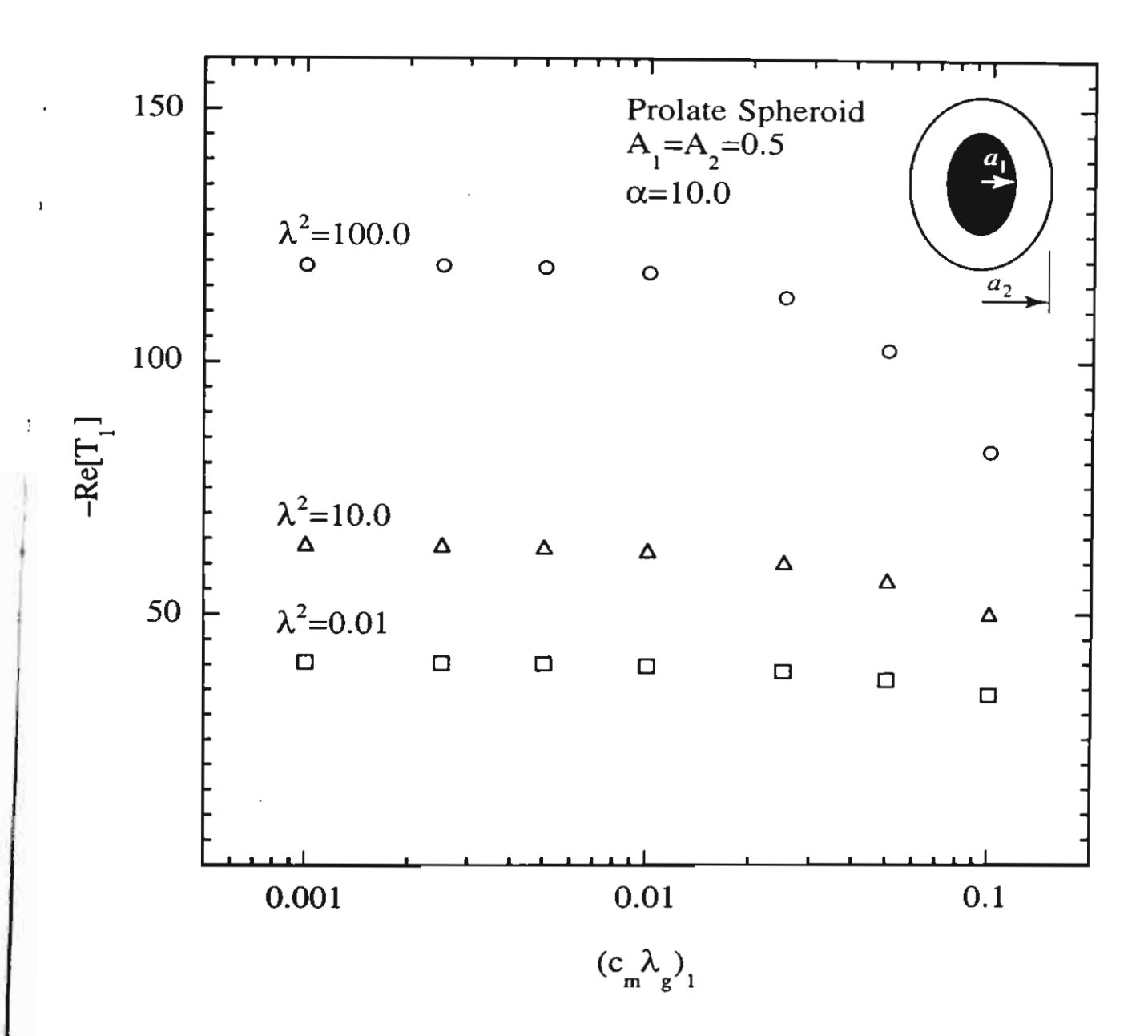


Figure 4(a) Numerical results for torques on an inner prolate spheroid. The aspect ratios of both the inner and outer spheroids are $A_1 = A_2 = 0.5$ while the equatorial radius ratio is $\alpha = a_2/a_1 = 10.0$. The real parts of the torques for $\lambda^2 = 0.01$ to 100.0. The number of Gaussian quadrature points used in the numerical calculations was 20.

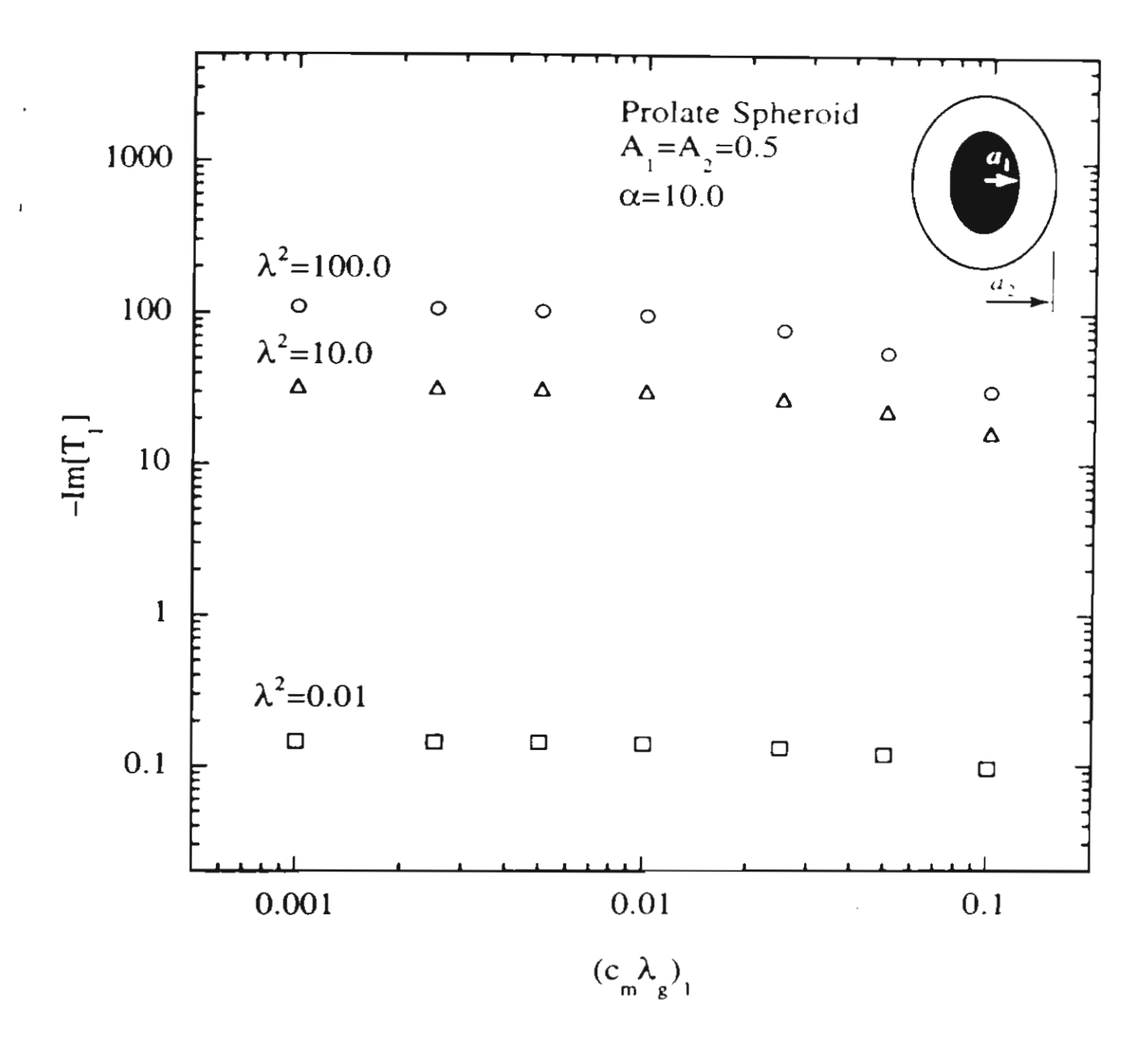


Figure 4(b) Numerical results for torques on an inner prolate spheroid. The aspect ratios of both the inner and outer spheroids are $A_1 = A_2 = 0.5$ while the equatorial radius ratio is $\alpha = a_2/a_1 = 10.0$. The imaginary parts of the torques for $\lambda^2 = 0.01$ to 100.0. The number of Gaussian quadrature points used in the numerical calculations was 20.

Results: Oblate Spheroid

Twenty-point Gaussian quadratures were also used in the calculations for an oblate spheroid. Numerical results for the real and imaginary parts of the torque on an inner oblate, spheroid with A=0.5 are given in Figs. 5(a) and 5(b) for $\alpha=a_2/a_1=2.0$, and in Figs 6(a) and 6(b) for $\alpha=10.0$. Results show identical effects of slip and oscillation frequency for the oblate spheroid as in the case of a sphere and a prolate spheroid for the range considered $(0.001 \le c_m \lambda_k \le 0.1)$.

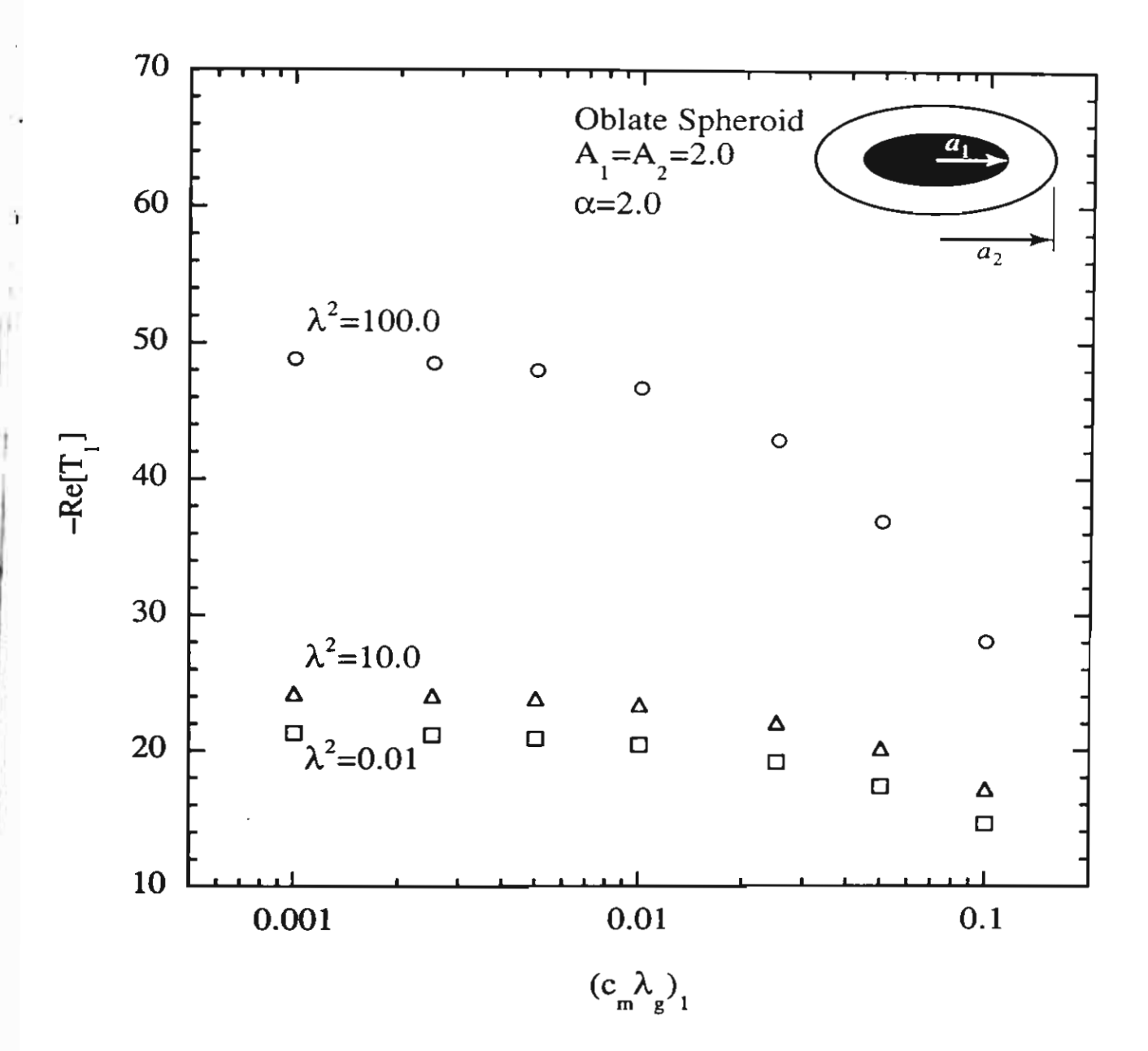


Figure 5(a) Numerical results for torques on an inner oblate spheroid. The aspect ratios of both the inner and outer spheroids are $A_1 = A_2 = 2.0$ while the equatorial radius ratio is $\alpha = a_2/a_1 = 2.0$. The real parts of the torques for $\lambda^2 = 0.01$ to 100.0. The number of Gaussian quadrature points used in the numerical calculations was 20.

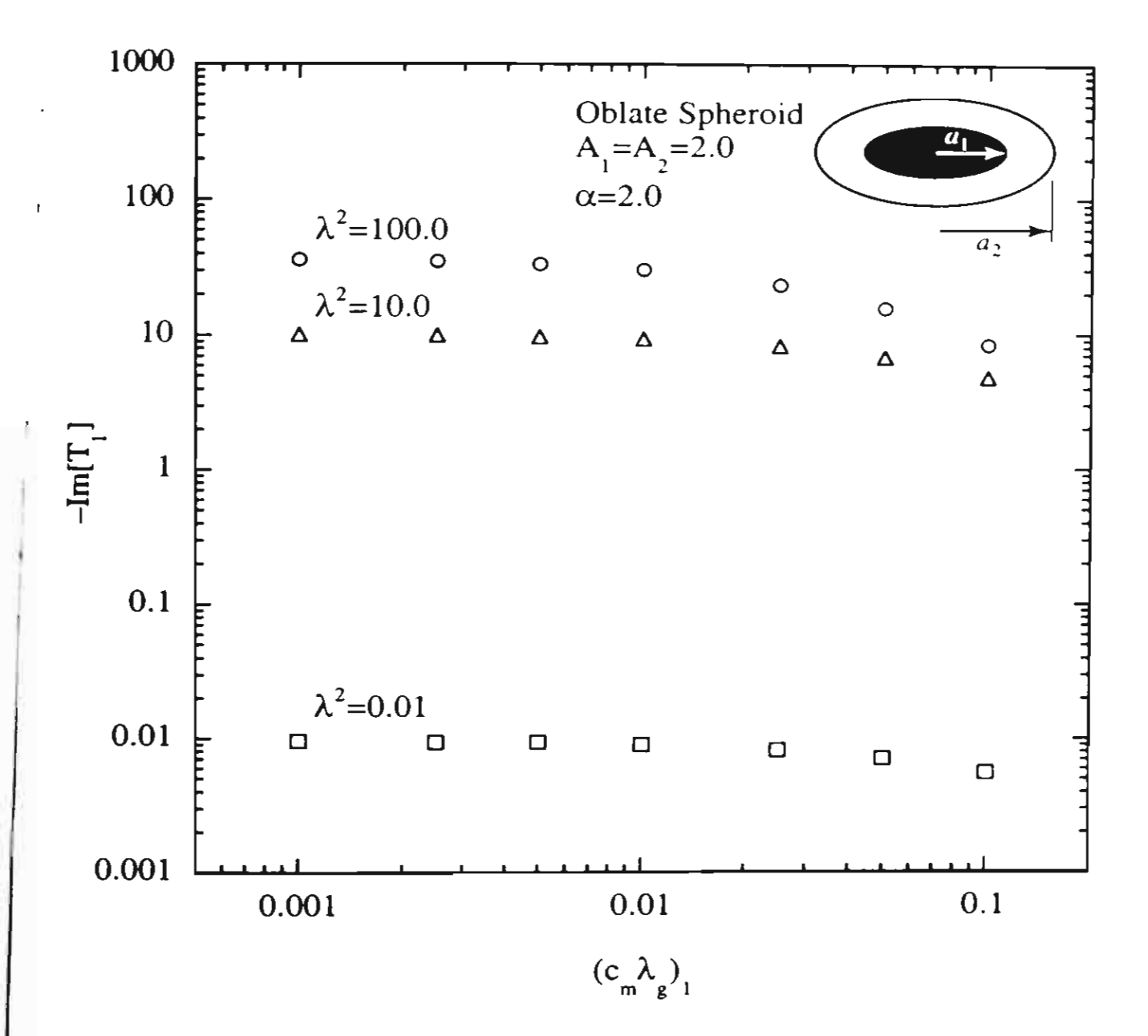


Figure 5(b) Numerical results for torques on an inner oblate spheroid. The aspect ratios of both the inner and outer spheroids are $A_1 = A_2 = 2.0$ while the equatorial radius ratio is $\alpha = a_2/a_1 = 2.0$. The imaginary parts of the torques for $\lambda^2 = 0.01$ to 100.0. The number of Gaussian quadrature points used in the numerical calculations was 20.

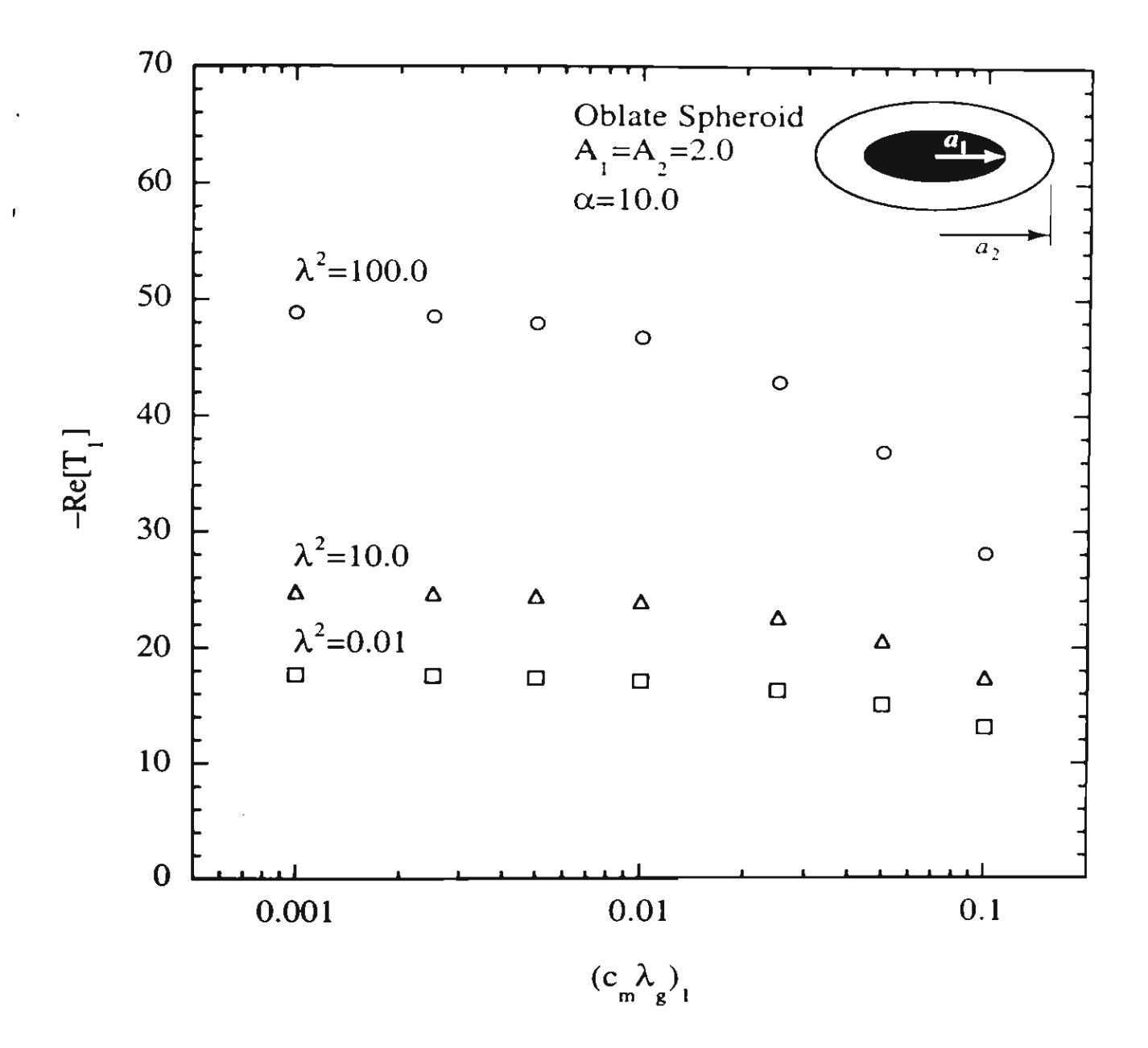


Figure 6(a) Numerical results for torques on an inner oblate spheroid. The aspect ratios of both the inner and outer spheroids are $A_1 = A_2 = 2.0$ while the equatorial radius ratio is $\alpha = a_1/a_1 = 10.0$. The real parts of the torques for $\lambda^2 = 0.01$ to 100.0. The number of Gaussian quadrature points used in the numerical calculations was 20.

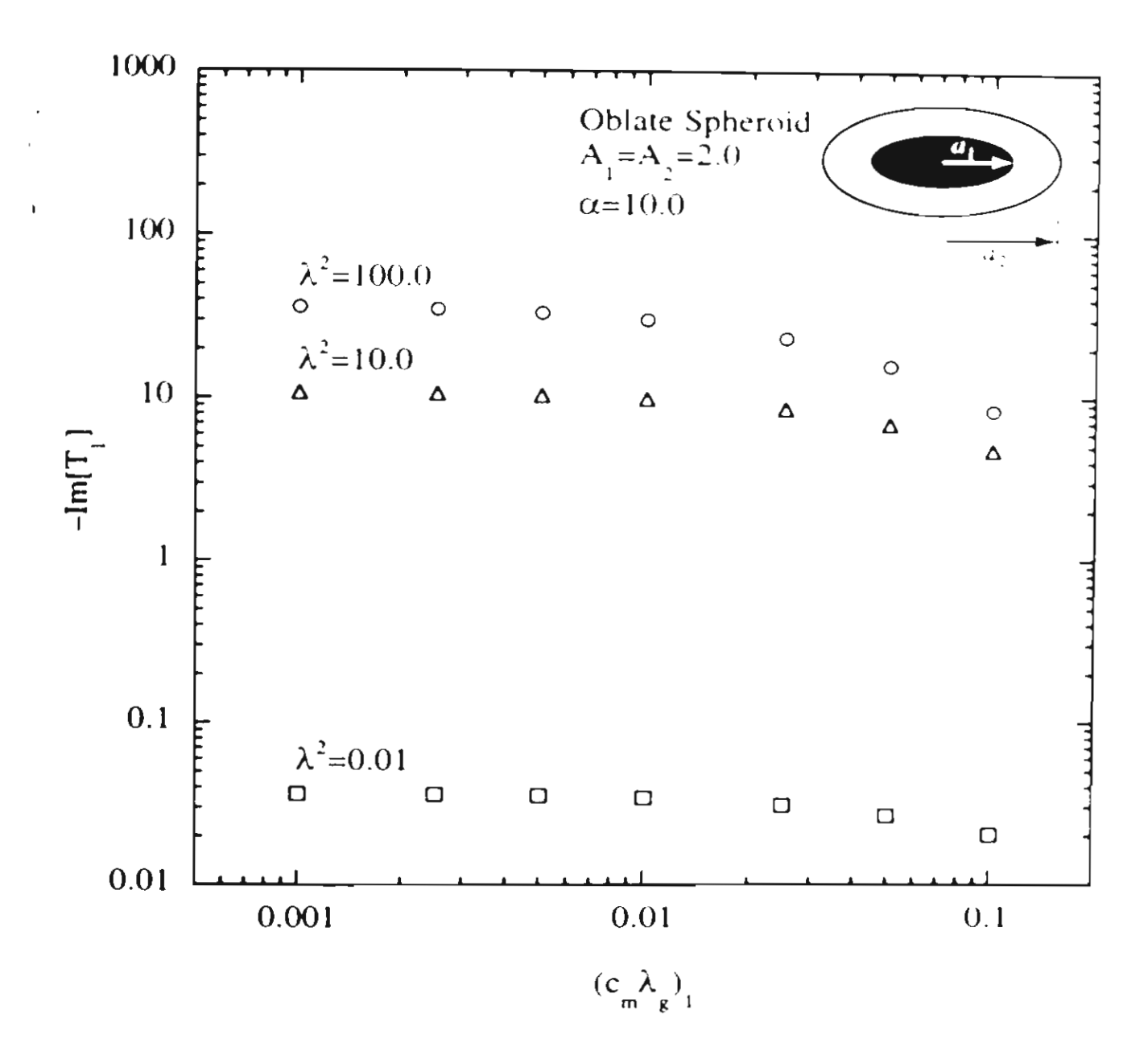


Figure 6(b) Numerical results for torques on an inner oblate spheroid. The aspect ratios of both the inner and outer spheroids are $A_1 = A_2 = 2.0$ while the equatorial radius ratio is $\alpha = a_2/a_1 = 10.0$. The imaginary parts of the torques for $\lambda^2 = 0.01$ to 100.0. The number of Gaussian quadrature points used in the numerical calculations was 20.

Appendix E

Manuscript: Evaporation from Non-Spherical Particles: The Equivalent-Volume
and Inscribed Sphere Approximations for Nearly Spherical Particles

Accepted for a Poster Presentation at the American Association for Aerosol Research
AAAR 2000 - Nineteenth Annual Conference, St. Louis, Missouri, U.S.A. on
November 9, 2000



he American Association for Aerosol Research

mper Woods Center, 1330 Kemper Meadow Dr., Cincinnati, OH 45240; (513)742-2227; FAX: (513)742-3355

May 3, 2000

A0002001

Sudarshan K. Lovalka

Univ of Missour/Columbia E1425C Eng

Columbia, MO, 65211

Dear Sudarshap K. Loyalka:

We would be honored if you will present your paper at the American Association for 10 Aerosol Research Annual Conference in St. Louis, MO, November 6 – 10, 2000.

Your submission, "Evaporation from Non-Spherical Particles: The Equivalent-Volume and Inscribed Sphere Approximations for Nearly Spherical Particles", has been accepted for a Poster presentation at the AAAR '00 Conference on Thursday, November 9, 2000 during the session time 12:30 pm - 3:00 pm.

Please famember to register prior to the conference by submitting the enclosed registration form to AAAR. Hotel information is contained on the next page.

If you are a presenting author, please read the following information for special instructions pertaining to Platform and Poster Presentations. (Please notify AAAR If you are a presenting author and cannot attend.) Follow the enclosed suggestions regarding your overheads and slides, and posters.

Poster Session Guidelines

Tuesday Evening Poster Session

Posters may be set up after 12:00 pm on Monday. Tuesday Evening Poster Session begins at 5:00 pm and ends at 7:00 pm. Posters May remain set up through 3:00 pm on Thursday.

Thursday Afternoon Poster Session

Posters may be set up after 12:00 pm on Monday, or after 12:00 pm on Wednesday. Thursday Afternoon Poster Session begins at 12:30 pm and ends at 3:00 pm.

raporation from non-spherical particles: The equivalent-volume and inscribed sphere approximations for nearly spherical particles

Running Title: Evaporation from non-spherical particles

(Accepted for a poster presentation at the American Association for Aerosol Research 2000 Imference on November 9, 2000 at St. Louis, U.S.A. and will be submitted for publication in the Journal of Aerosol Science)

P. Tekasakul¹ and S. K. Loyalka²

¹Department of Mechanical Engineering Faculty of Engineering Thammasat University, Rangsit Campus, Klong Luang, Pathum Thani 12121, Thailand (e-mail: tperapon@engr.tu.ac.th)

²Particulate Systems Research Center and Nuclear, Chemical, and Mechanical & Aerospace Engineering Departments, University of Missouri-Columbia, Columbia, MO 65211, USA (e-mail: loyalkas@missouri.edu)

Total # of Pages (including Figures and Tables): 18

Total # of Figures:

Total # of Tables: 2

Corresponding Author: P. Tekasakul Phone 66-2-564-6304 Ext. 3147

66-2-564-6303 Fax

Abstract – Two approximation methods for calculations of evaporation rate from nearly spherical particles situated in an infinite expanse of an absorbing gas without jump boundary conditions are proposed. The first method assumes a unit sphere inscribed in the particle while the second method employs the sphere of equivalent volume. Both approximations are proved to be accurate for spheroidal particles with aspect ratios between 0.8 and 1.2 by comparing the results with numerically calculated values from literature.

1. INTRODUCTION

The problem of evaporation or condensation of nonspherical particles has been of major interest for aerosol researchers. Recently, evaporation from nonspherical particles situated in an infinite expanse of an absorbing gas was numerically studied by Tekasakul et al. (1999). The results show excellent agreement with known solutions of a spherical particle with jump boundary conditions. For the problem of evaporation without jump boundary conditions, however, it would be very useful if simple approximate solutions can be obtained. Zhang and Stone (1998) used the equivalent-volume sphere approximations to study oscillatory motions of nearly spherical particles. Approximate analytical expressions for the hydrodynamic resistance and torque were obtained for translational and rotational oscillatory motions of nearly spherical particles, respectively. Results show good agreement with numerical values for prolate spheroids and oblate spheroids with aspect ratios close to one. This nearly spherical approximation can be modified to obtain approximate analytical expressions for evaporation rate from nearly spherical prolate and oblate spheroid particles. communications with Zhang and Stone (1997), the inscribed sphere approximation has been introduced. Tekasakul et al. (1998) has adopted this technique to derive approximate analytical expression for torques on prolate and oblate spheroids under rotational oscillatory motions and obtain good agreement with numerical results for the spheroids with aspect ratios in the range of 0.8 to 1.2. This method is also modifiable to evaporation problem.

In this paper we use both the inscribed sphere and equivalent-volume sphere approximations to calculate total evaporation rates from nearly spherical prolate and oblate spheroidal particles situated in an infinite expanse of an absorbing gas without jump. Values from both expressions are compared with numerically calculated values obtained by Tekasakul et al. (1999). Approximate analytical expression is also obtained for cylindrical particles using the equivalent-volume sphere approximation.

2. INSCRIBED SPHERE APPROXIMATION

In this method, a sphere of unit radius is assumed to be inscribed in the nearly spherical particle in which radius of the sphere is equal to the minimum cross-sectional radius of the nearly spherical particle, as seen in Fig. 1. This method has been suggested by Zhang and Stone (1997) for calculations of forces and torques on oscillating nearly spherical particles. The diffusion equations for the inscribed unit sphere (due to the particle) and the nearly spherical particle (due to the sphere) are, respectively,

$$\nabla \cdot \mathbf{J} - k^2 \phi = 0$$
 , $\phi = \phi_{p,s}$ on the surface of the particle, (1)

$$\nabla \cdot \tilde{\mathbf{J}} - k^2 \tilde{\phi} = 0$$
 , $\tilde{\phi} = \tilde{\phi}_{s,s}$ on the surface of the sphere, (2)

where, $\mathbf{J} = -\nabla \phi$ and $\tilde{\mathbf{J}} = -\nabla \tilde{\phi}$ are the dimensionless local current on the nearly spherical particle and inscribed unit sphere, respectively. Here ϕ and $\tilde{\phi}$ are the dimensionless vapor number density on the nearly spherical particle and inscribed unit sphere, respectively, and k is the inverse diffusion length defined as $k = (v \Sigma_a/D)^{1/2}$, where v is the molecular average thermal speed, Σ_a is the cross-section for vapor absorption by the gas and D is the diffusion coefficient of the vapor in the gas.

Applying reciprocal theorem to Eqs. (1) and (2), we have

$$(\nabla \cdot \mathbf{J})\tilde{\boldsymbol{\phi}} - (\nabla \cdot \tilde{\mathbf{J}})\boldsymbol{\phi} = 0.$$
 (3)

Let V represent the fluid volume surrounding the arbitrarily shaped particle, \tilde{V} be the fluid volume external to the sphere and $V_{dif} = \tilde{V} - V$. Integrating the above equation over the volume \tilde{V} enclosed by \tilde{S} , the surface of the inscribed unit sphere, and a distant surface S_{-} , and then applying the divergence theorem, leads to

$$\int_{\mathbf{v}+\mathbf{v}_{\mathbf{q}\mathbf{v}}} (\nabla \cdot \mathbf{J}) \tilde{\phi} \, dS + \int_{\tilde{S}} (\mathbf{n} \cdot \mathbf{J}) \phi \, dS = 0.$$
 (4)

Here **n** is the unit vector directing into the fluid volume (Fig. 1). The fluid volume is enclosed by S_p , the surface of the particle and S_m , and V_{dif} is enclosed by S_p and \tilde{S} . Again, applying the divergence theorem, we can write, for the evaporation problem,

$$-\int_{S_{\mathbf{q}}} (\mathbf{n} \cdot \mathbf{J}) \tilde{\boldsymbol{\phi}} \, dS + \int_{\tilde{S}} (\mathbf{n} \cdot \tilde{\mathbf{J}}) \boldsymbol{\phi} \, dS + \int_{V_{dd}} \nabla \cdot (\mathbf{J} \, \tilde{\boldsymbol{\phi}}) \, dV = 0.$$
 (5)

The surface of the nearly spherical body is described in the spherical coordinates as

$$r = 1 + \varepsilon f(\theta, \varphi), \tag{6}$$

where $\varepsilon \ll 1$ and $f(\theta, \varphi)$ is in the order of one and describes the detailed particle shape.

Now, let us consider Eq. (5) term by term. The density $\tilde{\phi}$ on S_p in the first integral can be written in a Taylor series about r=1

$$\left. \tilde{\phi} \right|_{r=1+\varepsilon f} = \tilde{\phi} \Big|_{r=1} + \varepsilon f \frac{\partial \tilde{\phi}}{\partial r} \Big|_{r=1} + O(\varepsilon^2). \tag{7}$$

Since the solution for the sphere gives

$$\left. \frac{\partial \tilde{\phi}}{\partial r} \right|_{r=1} = -(1+i\,k)\,\tilde{\phi}_{s,s} \ .$$

Therefore Eq. (7) becomes

$$\tilde{\phi}\Big|_{r=1+\varepsilon f} = \tilde{\phi}_{s,s} - \varepsilon f(1+ik)\tilde{\phi}_{s,s} + O(\varepsilon^2). \tag{8}$$

The term in the second integral is

$$\mathbf{n} \cdot \tilde{\mathbf{J}}\Big|_{r=1} = \mathbf{n} \cdot \left(-\mathbf{n} \frac{\partial \tilde{\phi}}{\partial r}\right)_{r=1}$$
$$= (1+ik) \tilde{\phi}_{s,s} . \tag{9}$$

The term in the last integral can be written as

$$\nabla \cdot \left(\mathbf{J} \, \tilde{\boldsymbol{\phi}} \right) = \, \tilde{\boldsymbol{\phi}} (\nabla \cdot \mathbf{J}) + \, \mathbf{J} \cdot \left(\nabla \tilde{\boldsymbol{\phi}} \, \right)$$

$$= \, k^2 \boldsymbol{\phi} \, \tilde{\boldsymbol{\phi}} - \, \mathbf{J} \cdot \tilde{\mathbf{J}}$$

$$\approx \, k^2 \boldsymbol{\phi}_{\rho,s} \, \tilde{\boldsymbol{\phi}}_{s,s} \,, \tag{10}$$

for the volume inside the nearly spherical body in which we assume $\phi = \phi_{p,s}$, $\tilde{\phi} = \tilde{\phi}_{s,s}$ and J = 0. Therefore, the integral becomes

$$\int_{V_{Af}} \nabla \cdot \left(\mathbf{J} \, \tilde{\boldsymbol{\phi}} \right) dV = \int_{V_{Af}} k^2 \phi_{\rho,s} \, \tilde{\phi}_{s,s} \, dV$$

$$= k^2 \phi_{\rho,s} \, \tilde{\phi}_{s,s} \int_{\tilde{s}} (r-1) dS + O(\varepsilon^2)$$

$$= k^2 \phi_{\rho,s} \, \tilde{\phi}_{s,s} \int_{\tilde{s}} \varepsilon \, f \, dS + O(\varepsilon^2). \tag{11}$$

Substituting Eqs. (8), (9) and (11) into Eq. (5), we obtain

$$-\int_{S_{\epsilon}} (\mathbf{n} \cdot \mathbf{J}) \left[\tilde{\boldsymbol{\phi}}_{s,s} - \varepsilon f (1+ik) \tilde{\boldsymbol{\phi}}_{s,s} \right] dS + \int_{\tilde{S}} (1+ik) \tilde{\boldsymbol{\phi}}_{s,s} dS + k^2 \phi_{\rho,s} \tilde{\boldsymbol{\phi}}_{s,s} \int_{\tilde{S}} \varepsilon f dS = 0,$$

Or

$$-\int_{S_{p}} (\mathbf{n} \cdot \mathbf{J}) dS + (1+ik) \int_{S_{p}} \varepsilon f(\mathbf{n} \cdot \mathbf{J}) dS = -(1+ik) \int_{\tilde{S}} dS - k^{2} \phi_{p,s} \int_{\tilde{S}} \varepsilon f dS.$$
 (12)

Since, in our problem, we have normalized $\phi_{p,s} = 1$ and $\tilde{\phi}_{s,s} = 1$, then

$$\int_{S} dS = 4\pi,$$

and

$$\int_{S_{p}} \varepsilon f(\mathbf{n} \cdot \mathbf{J}) dS \approx \int_{\tilde{S}} \varepsilon f(\mathbf{n} \cdot \tilde{\mathbf{J}}) dS$$
$$\approx (1 + ik) \int_{\tilde{S}} \varepsilon f dS.$$

Therefore the dimensionless total evaporation rate per unit surface area of the prolate spheroidal particle is

$$J_{\tau}/S = \int_{S_{\rho}} (\mathbf{n} \cdot \mathbf{J}) dS = 4\pi (1+ik) + k^{2} \int_{\tilde{S}} \varepsilon f dS + (1+ik)^{2} \int_{\tilde{S}} \varepsilon f dS$$
$$= 4\pi (1+ik) + \left[k^{2} + (1+ik)^{2}\right] \int_{\tilde{S}} \varepsilon f dS. \tag{13}$$

2.1 Prolate spheroid approximation

For a prolate spheroid, we have

$$\varepsilon f = r - 1 \approx \frac{1}{2} (1 - A^2) \cos^2 \theta.$$

We can write

$$\varepsilon = 1 - A$$
.

hence,

 $A=1-\varepsilon$,

and

$$1 - A^{2} = (1 - A)(1 + A)$$
$$= \varepsilon(2 - \varepsilon)$$
$$\approx 2\varepsilon$$
$$\approx 2(1 - A).$$

Therefore,

$$\varepsilon f \approx (1-A)\cos^2\theta.$$

Finally, we have

$$\int_{\bar{S}} \varepsilon f \, dS = (1 - A) \int_{\bar{S}} \cos^2 \theta \, dS$$

$$= (1 - A) \int_{0}^{2\pi\pi} \int_{0}^{\pi} \cos^2 \theta \sin \theta \, d\theta \, d\phi$$

$$= \frac{4\pi}{3} (1 - A), \qquad (14)$$

where A = a/b is the aspect ratio of the spheroid. Then the dimensionless total evaporation rate per unit surface area becomes

$$J_{T}/S = \int_{S_{\rho}} (\mathbf{n} \cdot \mathbf{J}) dS$$

$$= 4\pi (1 + ik) + \frac{4\pi}{3} (1 - A) [k^{2} + (1 + ik)^{2}]. \tag{15}$$

2.2 Oblate spheroid approximation

For an oblate spheroid, we have

$$\varepsilon f = r - 1 \approx \left(1 - \frac{1}{A}\right) \left[-1 + \frac{1}{2} \frac{1}{A} \left(1 + \frac{1}{A}\right) \sin^2 \theta\right].$$

We can write

$$\varepsilon=1-\frac{1}{A}\,,$$

hence,

$$\frac{1}{A}=1-\varepsilon\;,$$

and

$$1 + \frac{1}{A} = 2 - \varepsilon,$$

$$\frac{1}{A} \left(1 + \frac{1}{A} \right) = (1 - \varepsilon)(2 - \varepsilon)$$

$$\approx 2 - 3\varepsilon.$$

Therefore

The density bet-

participal is

$$\varepsilon f \approx \varepsilon \left[-1 + (2 - 3\varepsilon) \sin^2 \theta \right],$$

and

$$\int_{\bar{s}} \varepsilon f \, dS = \varepsilon \int_{\bar{s}} \left[-1 + (2 - 3\varepsilon) \sin^2 \theta \right] dS$$

$$= \varepsilon \int_{\bar{s}} \left[-1 + (2 - 3\varepsilon) \sin^2 \theta \right] \sin \theta \, d\theta \, d\phi$$

$$= \varepsilon \left[-4\pi + \frac{4\pi}{3} (2 - 3\varepsilon) \right]$$

$$\approx \varepsilon \left[-4\pi + \frac{8\pi}{3} \right]$$

$$\approx -\frac{4\pi}{3} \varepsilon$$

$$\approx -\frac{4\pi}{3} \left(1 - \frac{1}{A} \right). \tag{16}$$

The dimensionless total evaporation rate per unit surface area of the oblate spheroidal particle is then

$$J_{\tau}/S = \int_{S_{\rho}} (\mathbf{n} \cdot \mathbf{J}) dS$$

$$= 4\pi (1+ik) - \frac{4\pi}{3} \left(1 - \frac{1}{A}\right) \left[k^2 + (1+ik)^2\right]. \tag{17}$$

3. EQUIVALENT-VOLUME SPHERE APPROXIMATION

In this section, we assume the particle to be a sphere of equal volume. Figure 2 shows the geometry of the particle and its equivalent sphere. In this approach, the sphere center coincides with the center of mass of the nearly spherical particle. \tilde{S} and S_p represent the surfaces of the sphere and the nearly spherical particle, respectively. Portions of the nearly spherical particle that extend beyond the sphere are labeled V_i^- , i=1,...,N, where N is the number of bumps. These volume elements are enclosed by surfaces \tilde{S}_i^- and S_i^- . In the same manner, V_i^+ represents the volume elements of the sphere that extend beyond the nearly spherical particle and is enclosed by surfaces \tilde{S}_i^+ and S_i^+ . This method has been used by Zhang and Stone (1998) for calculations of forces and torques on oscillating nearly spherical particles. Using the above assumption of volume equivalent, Eq. (5) of the preceding section reduces to

$$-\int_{S_{\rho}} (\mathbf{n} \cdot \mathbf{J}) \tilde{\phi} \, dS + \int_{\tilde{S}} (\mathbf{n} \cdot \tilde{\mathbf{J}}) \phi \, dS = 0, \qquad (18)$$

or,

$$\int_{S_{*}} (\mathbf{n} \cdot \mathbf{J}) \tilde{\phi} \, dS = \int_{\tilde{S}} (\mathbf{n} \cdot \tilde{\mathbf{J}}) \phi \, dS.$$
 (19)

The density on the particle surface because of the sphere can be written as

$$\left. \vec{\phi} \right|_{r=1+\varepsilon f} = \begin{cases} \left. \vec{\phi}_{s,s} \right. & \text{over } S_i^+ \\ \left. \vec{\phi}_{s,s} + \varepsilon f \frac{\partial \vec{\phi}}{\partial r} \right|_{r=1} + O(\varepsilon^2) & \text{over } S_i^- \end{cases}, \tag{20}$$

since $\tilde{\phi}|_{r=1} = \tilde{\phi}_{s,s}$. The density on the sphere surface because of the sphere can be written as a regular perturbation expansion in ε :

$$\phi = \phi^{(0)} + \varepsilon \phi^{(1)} + O(\varepsilon^2). \tag{21}$$

A regular perturbation expansion about the boundary condition on the particle surface, as shown by Zhang and Stone (1998), leads to

$$\phi^{(1)}\Big|_{r=1} = -\varepsilon f \frac{\partial \phi^{(0)}}{\partial r}\Big|_{r=1}. \tag{22}$$

The density field evaluated on the surface \tilde{S} of the equivalent-volume sphere (due to the particle) is

$$\phi|_{\tilde{s}} = \begin{cases} \phi_{p,s} & \text{over } \tilde{S}_{i}^{-} \\ \phi_{p,s} - \varepsilon f \frac{\partial \phi^{(0)}}{\partial r}|_{\varepsilon=1} + O(\varepsilon^{2}) & \text{over } \tilde{S}_{i}^{+} \end{cases}$$
(23)

Substituting Eqs. (20) and (23) into Eq. (19), we obtain

$$\sum_{i=1}^{N} \int_{S_{i}^{-}} (\mathbf{n} \cdot \mathbf{J}) \tilde{\boldsymbol{\phi}}_{s,s} \, dS + \sum_{i=1}^{N} \int_{S_{i}^{-}} (\mathbf{n} \cdot \mathbf{J}) \left(\varepsilon f \frac{\partial \tilde{\boldsymbol{\phi}}}{\partial r} \Big|_{r=1} \right) dS + \sum_{i=1}^{N} \int_{S_{i}^{+}} (\mathbf{n} \cdot \mathbf{J}) \tilde{\boldsymbol{\phi}}_{s,s} \, dS$$

$$= \sum_{i=1}^{N} \int_{\tilde{S}_{i}^{-}} (\mathbf{n} \cdot \tilde{\mathbf{J}}) \boldsymbol{\phi}_{p,s} \, dS + \sum_{i=1}^{N} \int_{\tilde{S}_{i}^{+}} (\mathbf{n} \cdot \tilde{\mathbf{J}}) \boldsymbol{\phi}_{p,s} \, dS - \sum_{i=1}^{N} \int_{\tilde{S}_{i}^{+}} (\mathbf{n} \cdot \tilde{\mathbf{J}}) \left(\varepsilon f \frac{\partial \boldsymbol{\phi}^{(0)}}{\partial r} \Big|_{r=1} \right) dS + O(\varepsilon^{2}), \tag{24}$$

which can be written as

$$\int_{S_{\rho}} (\mathbf{n} \cdot \mathbf{J}) \tilde{\phi}_{s,s} \, dS = \int_{\tilde{\mathbf{S}}} (\mathbf{n} \cdot \tilde{\mathbf{J}}) \phi_{\rho,s} \, dS$$

$$- \left\{ \sum_{i=1}^{N} \int_{S_{i}^{r}} (\mathbf{n} \cdot \mathbf{J}) \left(\varepsilon f \frac{\partial \tilde{\phi}}{\partial r} \Big|_{r=1} \right) dS + \sum_{i=1}^{N} \int_{\tilde{S}_{i}^{r}} (\mathbf{n} \cdot \tilde{\mathbf{J}}) \left(\varepsilon f \frac{\partial \phi^{(0)}}{\partial r} \Big|_{r=1} \right) dS \right\} + O(\varepsilon^{2}). \tag{25}$$

Normalizing $\tilde{\phi}_{s,s} = 1$ and $\phi_{p,s} = 1$, and approximating $S_i^- = \tilde{S}_i^-$ with the error of $O(\varepsilon^2)$, the above equation reduces to

$$\int_{S_{p}} (\mathbf{n} \cdot \mathbf{J}) \tilde{\boldsymbol{\phi}}_{s,s} \, dS = \int_{\tilde{\mathbf{J}}} (\mathbf{n} \cdot \tilde{\mathbf{J}}) \boldsymbol{\phi}_{p,s} \, dS - \int_{\tilde{\mathbf{J}}} (\mathbf{n} \cdot \tilde{\mathbf{J}}) \left(\varepsilon f \frac{\partial \tilde{\boldsymbol{\phi}}}{\partial r} \Big|_{r=1} \right) dS + O(\varepsilon^{2}),$$

Of Since the ognivate

$$J_{T} = \vec{J}_{T} - \int_{\vec{S}} \left(\mathbf{n} \cdot \tilde{\mathbf{J}} \right) \left(\varepsilon f \frac{\partial \tilde{\phi}}{\partial r} \bigg|_{r=1} \right) dS + O(\varepsilon^{2}).$$

Applying Eq. (9) to the above equation, we have

$$J_{T} = \tilde{J}_{T} + \varepsilon \left(\frac{\partial \tilde{\phi}}{\partial r} \bigg|_{r=1} \right)^{2} \int_{\tilde{S}} f \, dS + O(\varepsilon^{2}). \tag{26}$$

Because of volume equivalency, we have $\int_{\frac{3}{2}} f \, dS = 0$ (Zhang and Stone, 1998), Eq. (26) then

reduces to a cylinder with high meaner has

$$J_{\tau} = \tilde{J}_{\tau} + O(\varepsilon^2), \tag{27}$$

which means that the total evaporation rate on the nearly spherical particle can be approximated by the total evaporation rate on a sphere of equal volume with the error of $O(\varepsilon^2)$. This applies for particle of arbitrary shapes.

4. RESULTS AND DISCUSSIONS

Results of the dimensionless evaporation rate per unit surface area from spheroidal particles are given in Table 1 for the particles with aspect ratios ranging from 0.5 to 2.0, and the dimensionless absorption parameter (λ^2) ranging from 0.0 to 10^{-3} . Here, the dimensionless absorption parameter is defined as $\lambda^2 = -k^2$. Values obtained from both the equivalent-volume sphere and the inscribed sphere methods are presented in comparison with values obtained numerically by Tekasakul, et al. (1999). The values obtained from the equivalent-volume sphere and inscribed sphere agree very well with the numerically calculated values for the particles with aspect ratios between 0.8 to 1.2 which represent nearly spherical spheroidal particles. The equivalent-volume sphere method yields slightly better results with the agreement of 0.5% for A = 0.8 to 1.1 while the results using the inscribed sphere method agree within 1.5% of the numerical results. For particles that depart significantly from spherical shape, the agreement becomes poorer as seen from the values for A = 0.5 and 2.0 with an exception for the results obtained from the inscribed sphere method for A = 2.0.

Since the equivalent-volume method works well with spheroids and since the calculations are simple, we have calculated the dimensionless evaporation rate per unit surface area for cylindrical particles using this method. The results are shown in Table 2 together with corresponding numerical results. It can be seen that, for a cylindrical particle, the method fails even for A = 0.9 to 1.1. This is because the surface of a cylindrical particle is not continuously defined as in the case of sphere or spheroids. Even for the cylindrical particle with aspect ratio of 1.0, it differs significantly from a sphere, while the spheroid with aspect ratio of one is simply a sphere. However, the results for A = 2.0 is surprisingly good (1%). This could be because the cylinder with high aspect ratio (thin disk) behaves as a thin oblate spheroid.

5. CONCLUSIONS

Results for nearly spherical spheroidal particles using both the equivalent-volume sphere and inscribed sphere methods have shown excellent agreement with numerical results, though the results for cylindrical particles do not yield the same accuracy. This indicates that the approximations can be used for calculations for evaporation rate from nearly spherical particles without performing lengthy numerical procedure. However, these approximations are limited to the case in which jump boundary condition is absent. If the jump plays significant role, numerical technique suggested by Tekasakul *et al.* (1999) is necessary. The numerical technique based on Green's function is applicable for arbitrary axi-symmetric particles.

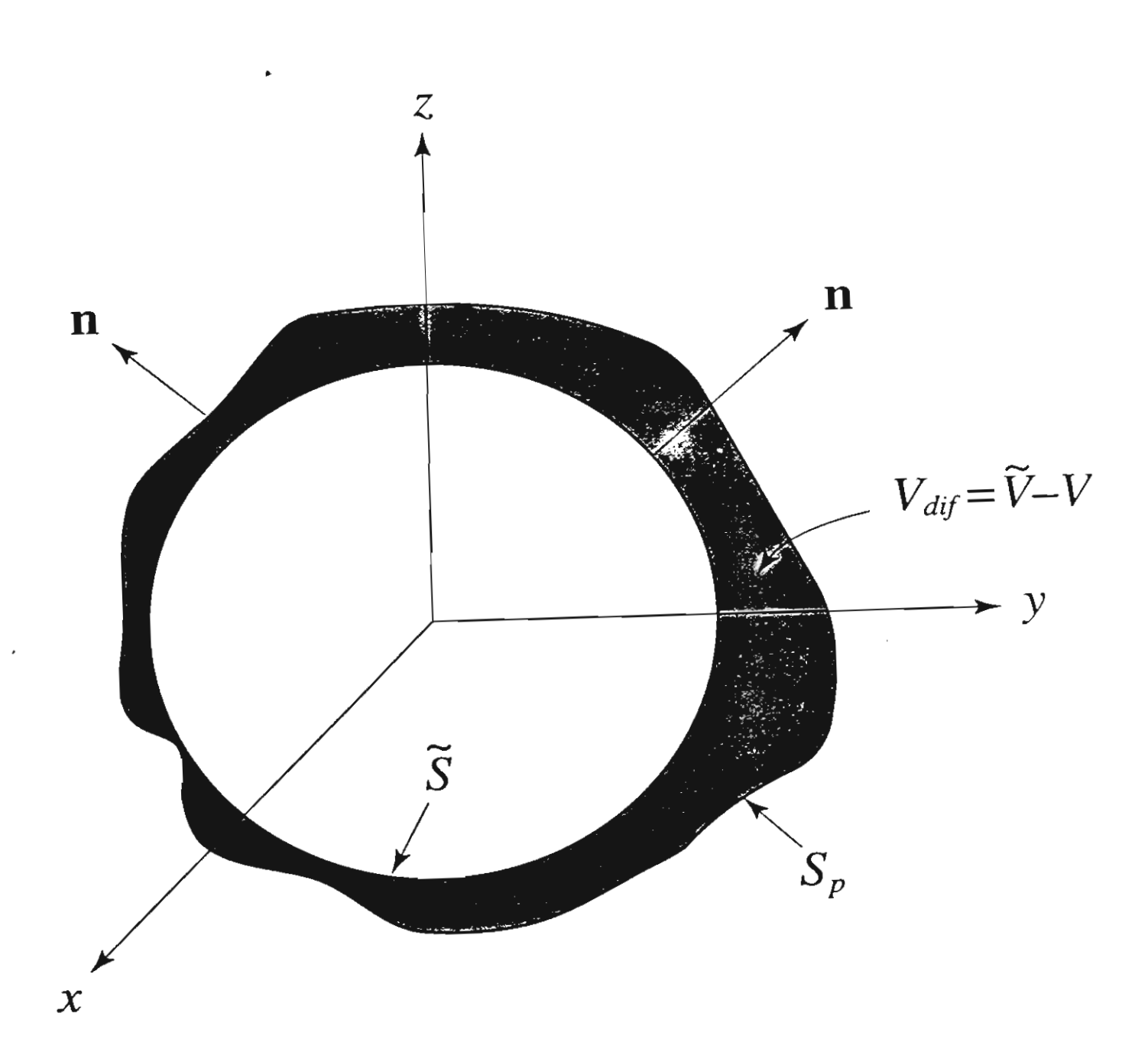
Acknowledgements – This research was carried out with the financial support from the Thailand Research Fund (TRF) through grant PDF/32/2541.

REFERENCES

- Tekasakul, P., Tompson, R. V. and Loyalka, S. K. (1998) Rotatory oscillations of arbitrary axi-symmetric bodies in an axi-symmetric viscous flow: Numerical solutions. *Phys. Fluids A* 10, pp. 2797-2818.
- Tekasakul, P., Tompson, R. V. and Loyalka, S. K. (1999) Evaporation from a nonspherical aerosol particle situated in an absorbing gas. J. Aerosol Sci. 30, pp. 139-156.
- Zhang, W and Stone, H. A. (1997) Private communications.
- Zhang, W and Stone, H. A. (1998) Oscillatory motions of circular disks and nearly spherical particles in viscous flows. *J. Fluid Mech.* 367, pp. 329-358.

Figure Captions

- Fig. 1. Geometry for a unit sphere inscribed in the particle.
- Fig. 2. Geometry for an equivalent-volume sphere.



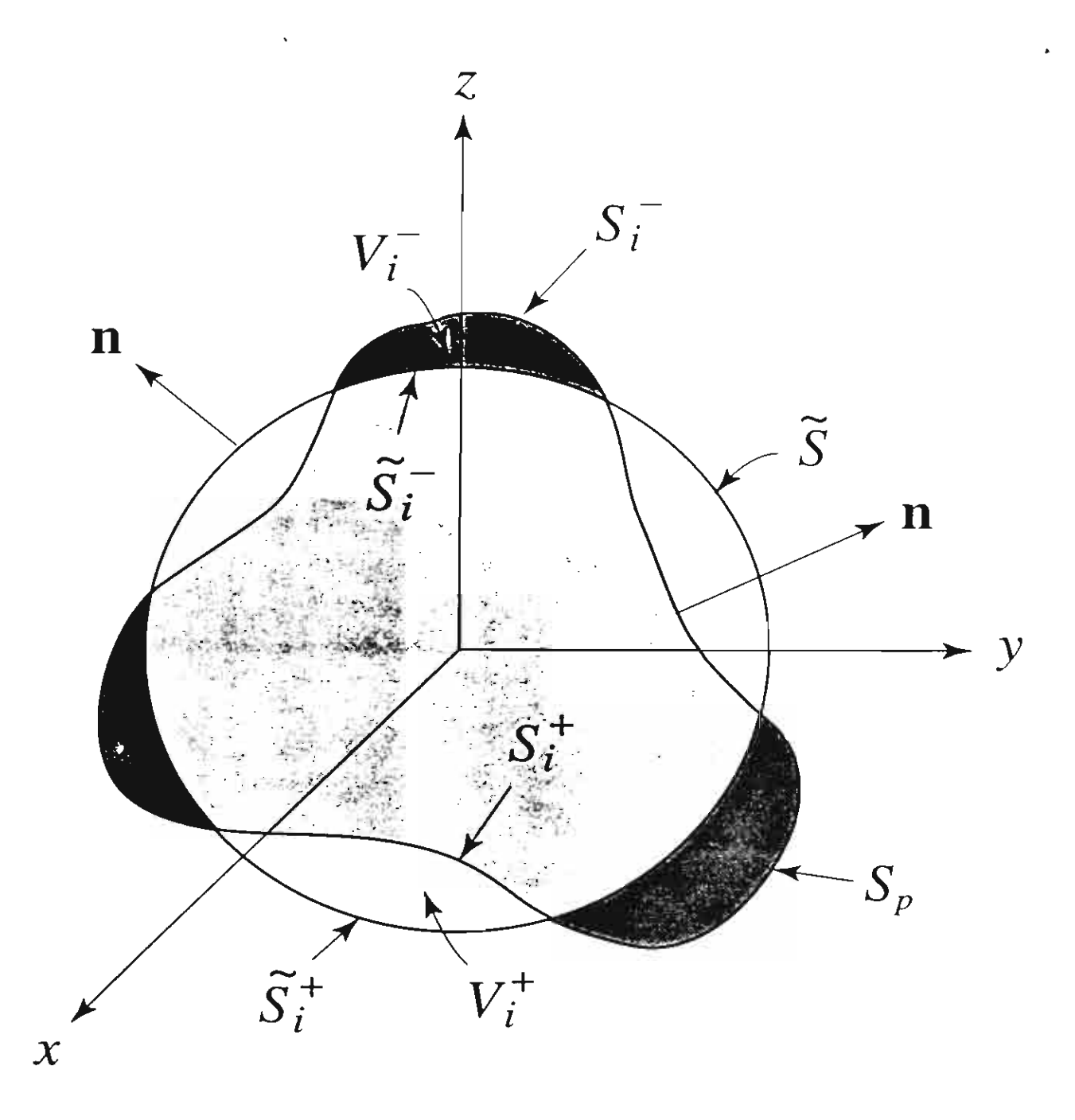


Table 1. Comparison of the dimensionless evaporation rate per unit surface area from spheroidal particles, using numerical, volume-equivalent sphere, and inscribed sphere methods.

	-		J_{τ}/S	
Α	λ^2	Numerical	Equivalent-volume sphere	Inscribed sphere
0.5	0.0	0.7695	0.7371	0.6826
	10-9	0.7695	0.7372	0.6826
	10^{-7}	0.7698	0.7374	0.6828
	10-5	0.7727	0.7401	0.6850
	10 ⁻³	0.8019	0.7665	0.7072
0.8	0.0	0.9246	0.9204	0.9114
	10-9	0.9246	0.9205	0.9115
	10 ⁻⁷	0.9249	0.9208	0.9117
	10-5	0.9277	0.9236	0.9145
	10^{-3}	0.9566	0.9518	0.9421
0.9	0.0	0.9646	0.9636	0.9614
	10-9	0.9646	0.9636	0.9614
	10-7	0.9649	0.9639	0.9617
	10 ⁻⁵	0.9677	0.9668	0.9645
	10 ⁻³	0.9965	0.9952	0.9928
1.1	0.0	1.0314	1.0306	1.0316
	10-9	1.0315	1.0306	1.0316
	10^{-7}	1.0318	1.0309	1.0319
	10-5	1.0346	1.0338	1.0345
	10 ⁻³	1.0634	1.0622	1.0604
1.2	0.0	1.0594	1.0562	1.0601
	10-9	1.0594	1.0563	1.0601
	10 ⁻⁷	1.0597	1.0566	1.0603
	10-5	1.0625	1.0594	1.0627
	10-3	1.0913	1.0877	1.0864
2.0	0.0	1.1984	1.1502	1.2076
	10-9	1.1984	1.1502	1.2076
	10 ⁻⁷	1.1987	1.1504	1.2077
	10-5	1.2015	1.1530	1.2091
	10 ⁻³	1.2300	1.1790	1.2228

Table 2. Comparison of the dimensionless evaporation rate per unit surface area from cylindrical particles, using numerical, and volume-equivalent sphere methods.

		J_{τ}/S		
<i>A</i>	λ²	Numerical	Equivalent-volume sphere	
0.5	0.0	0.6292	0.7631	
	10 ⁻⁹	0.6292	0.7632	
	10^{-7}	0.6295	0.7634	
	10 ⁻⁵	0.6323	0.7659	
	10^{-3}	0.6609	0.7908	
0.8	0.0	0.7391	0.8700	
	10 ⁻⁹	0.7391	0.8700	
	10^{-7}	0.7394	0.8702	
	10-5	0.7421	0.8727	
	10^{-3}	0.7697	0.8969	
0.9	0.0	0.7681	0.8915	
	10-9	0.7681	0.8915	
	10^{-7}	0.7684	0.8918	
	10-5	0.7711	0.8942	
	10^{-3}	0.7985	0.9180	
1.1	0.0	0.8181	0.9221	
	10-9	0.8181	0.9221	
	10 ⁻⁷	0.8184	0.9223	
	10 ⁻⁵	0.8211	0.9246	
	10^{-3}	0.8482	0.9477	
1.2	0.0	0.8398	0.9327	
	10-9	0.8399	0.9327	
	10 ⁻⁷	0.8401	0.9330	
	10 ⁻⁵	0.8428	0.9352	
	10 ⁻³	0.8699	0.9579	
2.0	0.0	0.9639	0.9615	
	10-9	0.9639	0.9615	
	10 ⁻⁷	0.9641	0.9617	
	10 ⁻⁵	0.9668	0.9637	
	10 ⁻³	0.9935	0.9834	